# *In vitro* and *In vivo* Study of Effects of Andrographolide on Hepatocarcinogenesis

**LAU Ven Gie Vengie**

**A Thesis Submitted in Partial Fulfillment**

**of the Requirements for the Degree of**

**Master of Philosophy**

**in**

**Biochemistry**


**September 2006**


香港中文大學
圖書館系統
02 SEP 2008
UNIVERSITY
LIBRARY SYSTEM
THE CHINESE UNIVERSITY OF HONG KONG

Thesis/Assessment Committee

Professor J. Wang (Chair)
Professor W.S. Ho (Thesis Supervisor)
Professor T.B. Ng (Committee Member)
Professor N. Li (External Examiner)

I declare that the thesis here submitted is original except for source material explicitly acknowledged. I also acknowledge that I am aware of University policy and regulations on honesty in academic work, and of the disciplinary guidelines and procedures applicable to breaches of such policy and regulations, as contained in the website http://www.cuhk.edu.hk/policy/academichonesty/

Signature

SEPT 11, 2006

Date

LAU VEN GIE

Name

04975780

Student ID

# Acknowledgements

I would like to express my gratitude to my supervisor, Prof. John Wing Shing Ho, for his valuable input to my research project and thesis. He has enlightened and encouraged me throughout my M.Phil program.

I would also like to extend my gratitude to Prof. W. Y. Chan and his members in the Department of Anatomy of CUHK; special thanks to Peggy Yip, who provided a lot of assistance and guidance in the histological and immunohistochemical techniques.

I am grateful to those who have helped me through my research study, especially all my labmates in Rm. 612A of MMW in the Department of Biochemistry. Their patience and guidance have been a great support to my study over the past two years.

Special thanks to the members of my thesis committee, Prof. T.B. Ng, Prof. J. Wang and Prof. N. Li.

Finally, I would like to give thanks to my parents and boyfriend for their love and support throughout the years.

# Abstract

Andrographolide (AND), a bicyclic diterpenoid lactone, is one of the major components of the herb *Andrographis Paniculata* and has been shown to possess a wide range of pharmacological properties. The present study is to understand the biological activity of AND. *In vitro* study, treatments of HepG2, Clone 9 and WRL 68 cell lines with AND were performed in a time-course study. Results showed that AND inhibited the growth of the cell lines. Cell cycle analysis demonstrated that AND-treated HepG2 cells were blocked in the $G_0$-$G_1$ phase of cell cycle, and DNA fragmentation was observed. Microarray analysis indicated the changes in the gene expressions that are associated with cell cycle control and apoptosis.

*In vivo* study of effects of AND on tumor development in the promotion and progression stages were investigated in a 28- and 56-week study, respectively using Spraque Dawley (SD) rats. Health conditions of the AND-treated group (10mg/kg; once daily), positive control group (DEN-$CCl_4$ treated) and negative control group were monitored. After treatment, AST and ALT assays were performed to study the effect of the active component on liver. Western blots were performed to detect the protein expressions of PCNA, Bax, Bcl-2, p21, Mdm2, total and wild-type p53. mRNA expression levels of *p53* and *Mdm2* were also investigated. Haemotoxylin and Eosin (H&E) staining and immunostaining of GST-P of the liver sections of rats were performed to study the responses of hepatocytes.

The results showed that AST and ALT levels were reduced in the AND-treated group in both promotion and progression experiments. The protein expression of PCNA

was found to decrease, indicating a reduction of liver cell proliferation in the treatment group. Also, the over expression of wild-type p53 activated the expressions of Bax and p21 but inactivated the expression of Bcl-2. The regulator of p53, Mdm2, was also found to decrease. The overall regulation of these proteins showed the effects of AND on the apoptotic event in liver cells. At the transcriptional level, the mRNA expressions of *p53* and *Mdm2* were also found to reduce with treatment of AND. The results demonstrated that the increase in total p53 protein was due to the increase in wild-type p53 in the AND-treated group. Histological examinations revealed that the basic hexagonal structure was restored and the immunostaining of the liver section showed reduction in GST-P foci after treatment with AND. These findings showed that AND has pharmacological activity in cancer cells. The over-expression of genes associated with cell differentiation showed the potential therapeutic benefits of AND in treatment of cancer.

# 論文摘要

穿心蓮內酯，一種二環的雙萜化合物內酯，是草藥穿心蓮的主要成分之一，並且已經被證實有廣泛的藥理性質。該研究旨在了解穿心蓮內酯的生物活性。細胞時序實驗中，在人類肝癌細胞系(HepG2)、人類正常肝細胞系(WRL-68) 和大鼠正常肝細胞系(Clone 9) 時序的研究中，表明穿心蓮內酯抑制了該三種細胞系的生長。細胞週期分析證明，穿心蓮內酯能阻滯 HepG2 細胞週期中的$G_0$-$G_1$期。我們也發現了穿心蓮內酯處理後的DNA的片段化。微陣列分析了與細胞週期控制和細胞凋亡有關基因的調節情況。

在動物實驗中，我們用SD大鼠來進行穿心蓮內酯對抑制腫瘤發展兩個階段的影響。穿心蓮內酯服用組(10毫克/公斤/天)、陽性對照組(DEN-$CCl_4$處理)和陰性對照組的健康情況會被檢測。AST和ALT酶的化驗被用來研究該活性成分對肝臟的效果。PCNA、Bax、Bcl-2、p21、Mdm2、總p53和原始類型p53的蛋白質表達通過Western Blot來測定。p53和Mdm2的mRNA表達水平也被檢測了。Haemotoxylin 和 Eosin (H&E) 染色和胎盤型穀胱苷肽硫轉移酶(GST-P)的免疫組織化學染色被用來研究肝細胞的反應。結果顯示，穿心蓮服用組AST和ALT酶的水平在兩個肝癌發展階段皆明顯降低。減少的PCNA的蛋白質表達顯示了服用組的肝細胞增殖降低。同時，上升的原始類型p53表達使得Bcl-2的表達受阻，且激發了Bax 和 p21的蛋白質表達。p53的調節基因Mdm2的蛋白質表達也被發現有所減少。在基因轉譯層面，穿心蓮內酯的處理也會令p53和Mdm2的mRNA表達減少。結果證明了總p53蛋白質

表達的增加是因爲穿心蓮內酯提高了原始類型p53的緣故。從組織學角度的檢測顯示，肝細胞的基本六角形結構被恢復，並且胎盤型穀胱苷肽硫轉移酶(GST-p)陽性病竈的面積也減少。這些結果證實穿心蓮內酯對肝癌細胞有藥物療效。提升的細胞增殖相關基因表達也顯示了穿心蓮內酯的潛在藥用療效。

# Table of Contents

# List of Figures

# List of Tables

MATERIALS AND METHODS

# List of Abbreviations

| | |
|---|---|
| ABC | Avidin-biotin complex |
| ALT | Alanine aminotransferase |
| AND | Andrographolide |
| AP | Andrographis panciculata |
| APS | Ammonium persulfate |
| AST | Aspartate aminotransferase |
| $CCl_4$ | Carbon tetrachloride |
| DEN | Diethylnitrosamine |
| DEPC | Diethylpyrocarbonate |
| DTT | Dithiothreitol |
| EAF | Enzyme-altered foci |
| EB | Ethidium bromide |
| GST-P | Glutathione S-transferase Placental type |
| HCC | Hepatocellular carcinoma |
| H&E | Hematoxylin & Eosin |
| HRP | Horseradish peroxidase |
| I.P. | Intraperitoneal |
| MOPS | Morpholinopropane sulphonic acid |
| NR | Neutral red |
| PBS | Phosphate buffered saline |
| PCNA | Proliferating cell nuclear antigen |
| PCR | Polymerase chain reaction |
| PI | Propidium idodide |
| PMSF | Phenylmethylsulphonylfluoride |
| SD | Sprague Dawley |
| SDS-PAGE | Sodium dodecyl sulfate-polyacrylamide gel electrophoresis |
| TBE | Tris borate EDTA |
| TBST | Tris buffered saline with Tween |
| TEMED | N,N,N,N-tetramethyl ethylene diamine |
| TE | Tris EDTA |
| WT | Wild-type |

## Introduction I -- *Hepatocellular Carcinoma*

Hepatocellular carcinoma (HCC, also called hepatoma or liver cancer) is a primary malignancy that arises from hepatocytes, the major cell type of the liver. It is the fifth most common cancer and causes one million deaths annually worldwide (1). It is especially prevalent in parts of Asia (China, Hong Kong, Taiwan, Korea and Japan) and sub-Saharan Africa (Mozambique and South Africa). However, a recent study indicate that the frequency of HCC in the U.S. overall is rising as well (2).

### Risk factors

HCC is considered a multistage disease whose occurrence is caused by the interaction between genetic and environmental factors. Chronic hepatitis virus (HBV and HCV) infections, dietary aflatoxin B1 (AFB1) ingestion, diabetes, chronic alcohol abuse and cirrhosis associated with genetic liver diseases are the most prevalent risk factors for HCC overall (3). Among them, chronic infection with HBV or HCV is the most frequent underlying cause of HCC. Recent study revealed that HBV infection accounts for as much as 80% of the tumors in HCC in developing countries (4). Besides that, a higher incidence of HCC has been shown in certain genetic defects such as porphyria, α-1 antitrypsin deficiency, and Wilson disease (5). Certain carcinogenic chemicals, including arsenic and anabolic steroids are also identified as risk factors of liver cancer.

Usually, HCC arises from an adenomatous hyperplasia in an already diseased liver and progresses from a well-differentiated stage to less-differentiated forms (6). Ordinary HCCs formed by progression show highly increased cellular proliferation,

neovascularization, production of basic fibroblast growth factor, and aneuploidy in some tumors (7). Corresponding to its malignant progression, HCCs also show loss of heterozygosity for multiple chromosomes (8).

**Stages in chemical carcinogenesis**

The molecular mechanisms behind HCC malignancies are complex. It has been proposed that inflammation of the liver may lead to aberrant cell death or the deviant stimulation of mitosis, resulting in an accumulation of molecular and cellular events necessary for oncogenic hepatocyte cell transformation (9). The process of hepatocarcinogenesis can be distinguished into three different stages: initiation, promotion and progression.

*1. Initiation*

The first stage in carcinogenesis is tumor initiation which results from irreversible genetic change. For mutations to accumulate, they must arise in cells that proliferate and survive the lifetime of the organism. A chemical carcinogen causes a genetic alteration or error by the modification of the molecular structure of DNA that leads to a mutation during DNA synthesis. Most often, DNA mutation is brought about by formation of an adduct between the chemical carcinogen or one of its functional groups and a nucleotide in DNA. There is a positive correlation between the number of carcinogen-DNA adducts and the number of tumors that develop in animal models. Therefore, tumors can hardly be detected in tissues that do not form these carcinogen-DNA adducts. The formation of these adducts is considered to be a necessary, but not sufficient, prerequisite for tumor initiation (10). The cellular responses to DNA adducts may result in repair of the damage,

cell death by apoptosis, or continued cell proliferation. However, if these DNA errors are not repaired before cell replication, cells with modified DNA sequence will result.

Histological sections of grossly normal liver from an animal treated with a carcinogen just a few weeks earlier revealed the presence of discrete areas of aberrant enzyme activity (11). These 'islands' are generally referred to as enzyme-altered foci (EAF) which display many phenotypic alterations such as increase in glucose-6-phosphate dehydrogenase. These EAF are believed to be the earliest identifiable progeny of initiated cells that have the potential to progress to hepatocellular carcinomas (12).

Carcinogenic initiators can be divided into two types: direct acting and indirect acting initiators. Direct acting initiators are often alkylating or acetylating agents such as cyclophosphamide and aflatoxin B1 which have weak initiator activity. Indirect initiators are also called "procarcinogens" and they are the most common type of initiators. These initiators require metabolic conversion through the P450 systems to exert their toxic effects. Examples include polycyclic aromatic hydrocarbons (PAH) like epoxides found in smoked foods and nitrosamines like diethylnitrosamine (DEN) in pickled foods.

*2. Promotion*

The second stage in carcinogenesis is promotion which comprises a reversible process involving multiple applications of a promoting agent. This agent induces cellular proliferation and selective clonal expansion of the preneoplastic cells. Since the accumulation rate of mutations is proportional to the rate of cell division, clonal expansion of initiated cells produces a larger population of cells that are at risk of further genetic changes and malignant conversion. Tumor promoters generally are non-mutagenic and non-carcinogenic alone. These agents can mediate their biological effects without further

metabolic transformation. They are characterized by their ability to reduce the latency period for tumor formation after exposure of a tissue to a tumor initiator or to increase the frequency of tumors formed in that tissue. Moreover, they can induce the formation of a tumor in conjunction with a dose of an initiation that is too low to be carcinogenic alone (12).

Many tumor promoters can be found in the environment. An example is croton oil which is isolated from *Croton tiglium* seeds. It has been widely used as a promoter in skin carcinogenesis. Its most potent constituent, 12-tetradecanoylphorbol-13-acetate, activates protein kinase C which in turn causes phosphorylation of many substances and stimulates a cascade of epigenetic changes that can lead to cell growth (13). Another example will be carbon tetrachloride, $CCl_4$, a solvent that was used in the past as cleaning fluid and industrially in the synthesis of refrigeration fluid and propellants for aerosol cans (14). The major effect of exposure to $CCl_4$ in humans and animals is hepatotoxicity, which is detectable by biochemical alterations such as elevated levels in enzymatic activities in the liver or histological examination such as destruction of intracellular organelles and necrosis of central hepatocytes. The toxic effects of $CCl_4$ are related to its metabolism by cytochrome P-450 oxygenases, CYP 2E1. This enzyme metabolizes $CCl_4$ and generates a reactive metabolite called trimethyl chloride radial. This reactive radial covalently binds to DNA in the liver and causes lipid peroxidation products in animals by intraperitoneal injection. In addition, there is evidence that $CCl_4$ can also cause cancer by a nongenotoxic mechanism involving cellular regeneration. The increase in cell proliferation could result in either the replication of unrepaired DNA damage or the induction of more errors during

the replication process. Both of which can produce mutations that result in promoted growth of initiated preneoplastic cells.

The contribution of tumor promotion to the process of carcinogenesis is the expansion of a population of initiated cells. Repeated administration of a promoter may transform a preneoplastic cell into one that expresses the malignant phenotype. Conversion of a fraction of these cells to malignancy could be accelerated with the increase in the rate of cell division, a process that may mediate the activation of proto-oncogenes and inactivation of tumor-suppressor genes (15).

*3. Progression*

This stage of hepatocarcinogenesis comprises the expression of the malignant phenotype and the tendency of already malignant cells to acquire more aggressive characteristics with time, one of which is the metastasis of neoplastic cells. In this process, there are secretions of proteases from malignant cells that allow invasion beyond the EAF. The most prominent characteristic of malignant phenotype is the propensity for genomic instability and uncontrolled cell growth (16). This process again involves the activation of proto-oncogenes and the functional loss of tumor-suppressor genes to cause further genetic changes. The mutated or over-expressed products of the oncogenes stimulate mitosis even though normal growth factors like PDGF (platelet-derived growth factor) are absent. Tumor-suppressor genes are those that inhibit mitosis. Mutated or deleted tumor suppressor genes such as *p53* will result in uncontrollable cell division. There are also genes that enable tumor cells to separate from the primary tumor and migrate to other parts of the body. There can be mutations in the metastasis genes whose products normally keep cells adhering to one another. An example is the E-cadherin genes that hold

epithelial cells together. Mutations can also occur in genes whose products normally keep the cells adhering to their substrate, such as the integrin genes. Elevated expression of the genes that encode proteases can break down the extracellular material which holds the cells in place (17).

**Treatment of hepatocarcinoma**

The various treatment options are dictated by the stage of HCC and also the overall condition of the patient. Most common therapies for HCC include chemotherapy, trans-arterial chemoembolization (TACE), radiofrequency ablation (RFA), percutaneous ethanol injection, liver resection and liver transplantation.

*1. Chemotherapy – hepatic arterial infusion (HAI)*

Chemotherapy for the treatment of hepatic metastases has evolved from a systemic-only regimen to a liver-directed regimen. Since HCC tumor cells get blood exclusively from the hepatic artery, chemotherapy agents are specifically delivered through an implanted subcutaneous constant-flow pump directly to the tumor. At present, the most commonly infused chemotherapy agent in the treatment of hepatic metastases is fluorodeoxyuridine (FUDR). It is a pyrimidine antagonist related to 5-fluorouracil (5-FU) that has shown activity against hepatic colorectal metastases (18).

The rationale of HAI chemotherapy is based on three concepts. First, hepatic metastases greater than 3 mm in size derive their blood supply from the hepatic artery and not the portal vein (19). Second, a 4-fold increase in the concentration of chemotherapeutic agent can be achieved in the liver when drug is delivered through the hepatic artery instead of being systematically infused (20). Third, certain chemotherapy

agents such as FUDR can be completely extracted during the first pass through the liver, allowing for large doses to be given via the hepatic artery with minimal systemic effects (19). However, there are also some common complications related to this treatment. Chemical cholecystitis and peptic ulceration or perforation have been reported due to malperfusion. In some cases, sclerosing cholangitis and cirrhosis have been developed with the FUDR-based chemotherapy. Nausea, vomiting and diarrhea are the common complications of floxuridine- or 5-FU-based HAI chemotherapy (21).

*2. Trans-arterial chemoembolization (TACE)*

This technique is the standard approach in selected patients with unresectable HCC. It also takes advantage of the fact that HCC is a very vascular tumor and gets its blood supply from branches of hepatic artery. This procedure is similar to intra-arterial infusion of chemotherapy. First, a very high concentration of chemotherapy is delivered directly into the tumor, without exposing the drug systemically. Second, an additional step of blocking (embolizing) the blood flow to the tumor deprives it of oxygen and nutrients, and traps the drug at the tumor site to enable them to be more effective. The embolization is achieved with different types of compounds such as gelfoam or gelatin sponge. Therefore, TACE has the advantages of exposing the tumor to high concentrations of chemotherapy and confining the agents locally.

TACE has been shown to be effective in decreasing the size of the tumor in two-thirds of HCC treated. It can also be used in combination with other therapies such as radiation and tumor ablation. However, there is always a risk that embolization material can lodge in the wrong place and deprive normal tissue of its blood supply. Further, they can be used only in patients with unresectable intermediate HCC and relatively preserved

liver function because the procedure can lead to liver failure and eventually death in individuals with poor liver function.

*3. Radiofrequency ablation (RFA)*

Radiofrequency ablation is being increasingly performed worldwide. Currently, it is predominantly performed for treatment of hepatic tumors that are not amenable to resection. The most common tumors treated by RFA are HCC and colorectal metastases. Results of long-term survival rates of individuals treated by this procedure have recently become available. These studies show that the most important determinant for achieving complete ablation is the size of the tumor. In general, technically successful ablation is possible in 90% of tumors that are less than 2.5 cm in diameter, in approximately 70% to 90% of tumors with 2.5- to 3.5-cm diameter, in 50% to 70% of tumors with 3.5 to 5.0 cm in diameter, and less than 50% of tumors with greater than 5.0 cm in diameter (22-24). Tumor type is also reported to affect the outcome with better success in treating HCC. Studies have also shown that tumor histology directly affects the success rate with well-differentiated HCC having better results of ablation than infiltrating lesions (22, 24).

This procedure is performed laparoscopically (through small holes in the abdomen) or during open exploration of the abdomen. In some instances, the procedure can be done without opening the abdomen by using ultrasound for visual guidance. In RFA, heat is generated locally by a high frequency, alternating current that flows from the electrodes. A probe is inserted into the center of the tumor and the non-insulated electrodes, which are shaped like prongs, are projected into the tumor. The local heat generated melts the tissue (coagulative necrosis) that is adjacent to the probe. The probe is left in place for about 10 to 15 minutes. The whole procedure is monitored visually by ultrasound scanning.

*4. Percutaneous ethanol injection (PEI)*

Pure alcohol is injected into the tumor through a very thin needle with the help of ultrasound or CT visual guidance. Alcohol induces tumor destruction by dehydrating tumor cells and thereby denaturing the structure of cellular proteins. It may take up to five or six sessions of injections to completely destroy the tumor. The ideal patient for alcohol injection should have fewer than three HCC tumors, each of which should be less than 3 cm in diameter, should have distinct margins and fibrous encapsulation and should not be near the surface of the liver. Moreover, patients with HCC undergoing PEI should have no signs of chronic liver failure such as jaundice (25).

The most common side effect of alcohol injection is leakage of alcohol onto the surface of the liver and into the abdominal cavity, thereby causing pain and fever. It is important that the location of the tumor relative to the adjacent blood vessels and bile ducts is clearly identified. The reason for that is to avoid injuring them during the procedure and causing bleeding, bile duct inflammation, or bile leakage (25).

*5. Liver resection*

The goal of liver resection is to completely remove the tumor and the appropriate surrounding liver tissue without leaving any tumor behind. This option is limited to patients with one or two small (3 cm or less) tumors and excellent liver function, ideally without associated cirrhosis. When a portion of a normal liver is removed, the remaining liver can regenerate to the original size within one to two weeks. A cirrhotic liver, however, cannot grow back. Therefore, before resection is performed for HCC, the non-tumor portion of the liver should be biopsied to determine whether there is an associated cirrhosis. The biggest concern about resection is that the patient may develop post-

operational liver failure, which can occur if the remaining portion of the liver is inadequate to provide the necessary support for life.

*6. Liver transplantation*

This is the ultimate treatment for patients with end-stage (advanced) liver disease of various types (e.g., chronic hepatitis B and C, alcoholic cirrhosis, primary biliary cirrhosis, and sclerosing cholangitis). Survival rates for these patients without HCC are 90% at one year, 80% at three years, and 75% at five years. Moreover, liver transplantation is the best option for patients with HCC in which a single lesion is less than 5 cm in diameter. If more than one lesion is present, all lesions should also be less than 3 cm in diameter (26). Successful transplantation also requires patients to have no evidence of vascular invasion or metastatic disease (27).

The most frequently encountered problem to liver transplantation is the availability of the donor. Although the absolute number of donors has increased over the past decade, it has been overwhelmed by the number of potential recipients listed for transplantation. Due to this rapidly escalating discrepancy between demand and supply for donor organs, most patients with end-stage HCC cannot be offered the opportunity for liver transplantation. Therefore, patients to be considered for transplantation must be very carefully selected.

## Introduction II -- *Molecular mechanisms: oncogenes and tumor-suppressor genes*

Multiple genetic alterations including the activation of oncogenes and inactivation of tumor suppressor genes are required for malignancy in human cancers and are correlated with increased stages of carcinogenesis and further tumor progression. An oncogene is a gene that when mutated or expressed at abnormally-high levels contributes to converting a normal cell into a tumor cell, possibly resulting in cancer. A proto-oncogene or oncogene precursor is a normal gene that can become an oncogene, either after mutation or increased expression. The proto-oncogenes that have been identified so far have many different functions in the cell. Many of them code for proteins that help to regulate cell growth and differentiation, and they are often involved in signal transduction and execution of mitogenic signals. Mutations in these genes distort the function of the associated proteins, resulting in abnormal growth and differentiation. Oncogenic versions of the *ras* genes were first identified in human tumors in 1982. It was an important oncogene because the three human *ras* genes represent the most frequently mutated oncogenes in human cancers. Since then, much research effort has been made to identify the function of *ras* both in normal and neoplastic cells (28). Another most commonly overexpressed oncogene in human cancers is the *myc* gene. Mutations in the *myc* gene have been found in many different cancers, including Burkitt's lymphoma, B-cell leukemia, and lung cancer (29).

Tumor suppressor genes are genes that reduce the probability of a cell in a multicellular organism to turn into a tumor cell. A mutation or deletion of such a gene

will therefore increase the probability of the formation of a tumor. Unlike oncogenes, tumor suppressor genes usually require that both alleles that code for a particular gene must be affected before the effect is manifested. However, there are also cases where mutations in only one allele will cause an effect, such as *p53*. If a person inherits only one functional copy of the *p53* gene from their parents, they are predisposed to cancer and usually develop several independent tumors in a variety of tissues in early adulthood (30). This condition is rare, and is known as Li-Fraumeni syndrome. However, mutations in *p53* are found in most tumor types, and so contribute to the complex network of molecular events leading to tumor formation (30).

**Cell cycle control**

Tumor-suppressor genes act primarily through their influence on the cell cycle. The life cycle of a dividing cell can be described by a four-phase cell cycle composed of M phase, $G_1$ phase, S phase, and $G_2$ phase. M phase is the phase of mitosis, when the cell physically divides. $G_1$ phase is the first gap phase or growth phase, which occurs immediately after mitosis. During $G_1$ the cell is synthesizing proteins and growing to achieve the size that a normal cell has before splitting in two during mitosis. S phase is a phase of DNA synthesis or replication in preparation for cell division. The $G_2$ phase is characterized by DNA repair of errors that have been introduced during DNA replication, and by preparation for the coming mitosis. Cells that rest for extended periods between divisions (such as liver cells) have temporarily or permanently exited the cell cycle by going into the $G_0$ phase at the end of the $G_1$ phase.

**p53 mutation in HCC**

The *p53* gene has been mapped to chromosome 17. Mutation in *p53* gene has been shown to be clinically significant in causing liver cirrhosis and hepatocellular carcinoma (31). A specific missense mutation (AGG to AGT transversion; Arg to Ser) in the p53 gene at codon 249 has been reported in over 50% of HCC tumors and in paired blood samples from hepatitis B virus-endemic areas with high dietary aflatoxin intake (32). This exon 7 mutation is detected in individuals that come from different places including China (33), Nigeria (34), Guinea in West Africa (35), Egypt (36) and Thailand (37).

**Normal functions of p53 and its target genes**

This prominent tumor suppressor gene encodes a protein called p53. This protein is the central part of a major defensive pathway against neoplastic transformation. Loss of p53 function leads to tumorigenesis, and at least half of all human tumors examined display *p53* gene mutations (38). The p53 tumor suppressor protein plays multiple roles in cells. It is a nuclear transcription factor that is responsible for cell cycle regulation, preventing inappropriate movement of G1 cells into S phase. Expression of high levels of wild-type (but not mutant) p53 in response to DNA damage and other forms of cellular stress leads to cell cycle arrest or apoptosis. Cells lacking p53 are shown to be genetically unstable and thus more prone to tumors (39).

*1. p21(Waf1/Cip1/Sdi1)*

Unlike other cell-cycle proteins, p53 is expressed at low levels in normal cells because it is extremely unstable and rapidly degraded (40). Under stressful situations, such as ultraviolet, p53 binds to specific DNA sequences and activate expression of

certain genes. The most important protein relative to cell-cycle control whose transcription is activated by p53 is the cyclin-kinase inhibitor (CKI) p21 (Waf1/Cip1/Sdi1). This protein contains conserved cyclin and cdk-binding domains near the amino terminus of the molecule (41). These sequences allow p21 to bind almost all of cyclin-dependent kinase (CDK) complexes such as Cdk1-, Cdk2-, Cdk4-, and Cdk6-cyclin complexes that function at major transition points in the cell cycle. Binding of these cyclin complexes is essential for cell cycle progression in mediating both G1 and G2/M arrests (42). While this binding leads to an inhibition of the activity of the cyclin/cdk complex, the C-terminal region of p21 is also able to directly inhibit DNA replication. It binds tightly to and blocking the action of the DNA polymerase processivity factor PCNA (proliferating cell nuclear antigen), which is a DNA-tracking protein required for rapid and processive replication of DNA by the polymerase $\delta$ and $\varepsilon$ (43).

*2. PCNA*

The proliferating cell nuclear antigen (PCNA) is a 36 kD protein which is highly conserved between species. It functions as a co-factor for DNA polymerase $\delta$ and $\varepsilon$ in S phase of the cell cycle and also during DNA synthesis associated with DNA damage repair mechanisms. It has been suggested that expression of high levels of PCNA protein correlates with organ metastasis and vascular invasion. Therefore, detection of high levels of PCNA is suggested to be a significant marker of clinical malignancy and a factor for prognostic implication in various cancers such as lymphomas (44), skin cancer (45), laryngeal cancer (46) and breast cancers (47).

*3. Bcl-2 and Bax: the Bcl-2 family*

When signals of survival factors such as cell stress and injury are received, p53 activates the expression of genes that lead to apoptosis (48). The known transcriptional targets for p53 in promoting this programmed cell death include various pro-apoptotic and anti-apoptotic Bcl-2 members (49). Bcl-2 is the prototype for a family of mammalian genes and their proteins. They govern mitochondrial membrane permeabilisation (MMP) and can be either pro-apoptotic such as Puma, Noxa, Bak and Bax or anti-apoptotic such as Bcl-2, Bcl-xL and Bcl-w (50). Mitochondrial permeability is, therefore, determined by the balance between the pro-apoptotic proteins like Bax and their anti-apoptotic cousins like Bcl-2. The activity of these proteins is positively or negatively regulated by BH3-only members, the Bcl-2 family members that contain a single Bcl-2 homology-3 domain. These BH3-only members act as the terminal effectors of distinct signaling pathways. When the net dominance of the pro-apoptotic proteins is produced, the mitochondria will be permeabilized and will release pro-apoptotic factors. One such factor, cytochrome *c*, acts together with the cell-death adaptor Apaf-1 to trigger the activation of caspase-9, a cysteine protease that initiates a downstream proteolytic cascade that also involves caspase-3 and caspase-7. Once activated, caspases cleave proteins that are important for cell and genome integrity.

*Bcl-2* is a proto-oncogene located on chromosome 18 (51). This gene was discovered as the translocated locus in B-cell leukemia. In the majority of follicular lymphomas, a translocation involving chromosomes 14 and 18 is observed (52). This t(14;18) translocation places the *bcl-2* gene close to the immunoglobulin heavy chain gene located on chromosome 14 (53). The heavy chain gene enhancer is very active in B cells and it increases the rate of transcription of the *bcl-2* gene. Its product is a 26-kD

integral membrane protein called Bcl-2. This protein is normally located in the membranes of the endoplasmic reticulum (ER), nuclear envelope, and in the other membranes of the mitochondria.

After receiving certain apoptotic stimuli, Bcl-2 directly or indirectly prevents the release of cytochrome c from mitochondria by inhibiting the actions of caspases (54). Evidence showed that an increased level of the Bcl-2 protects cells from apoptosis triggered by different stimuli (55) and enhances resistance to chemotherapeutic agents (56).

The *Bax* gene encodes a 21 kD protein which belongs to one of the pro-apoptotic members of the Bcl-2 family. It is assumed to exert at least part of its apoptosis-inducing function by facilitating mitochondrial permeability transition pore opening, a process that is supposedly antagonized by the anti-apoptotic members Bcl-2 and Bcl-xL by the ability to form heterodimers (57). Its gene expression is regulated by p53 through a DNA-binding response element located within the *Bax* promoter (58). However, this regulation of *Bax* expression by wild-type p53 was demonstrated to be cell type specific. In the mouse, *Bax* expression following ionizing radiation was seen in the prostate, thymus, spleen, small intestine, and lung, as well as sympathetic, Purkinje, and olfactory cortical neurons. In the kidney, heart, liver, and brain, however, no p53-dependent regulation of *Bax* could be observed (59). In addition, several tumor-derived p53 mutants have been identified that are capable of activating transcription through the promoter of the *p21* gene but not through the *Bax* promoter (60). It suggests that a failure in the ability of p53 to transactivate the *Bax* gene may play an important role in tumor formation.

Bax has been reported to be an integral membrane protein associated with organelles or bound to organelles by a soluble protein found in the cytosol. Confocal

microscopy revealed that GFP-Bax was distributed diffusely throughout the cytosol. Upon induction of apoptosis, however, Bax moved intracellularly and redistributed itself to organelles to promote cell death (61).

*4. Mdm2*

Wild-type p53 is a key regulator that controls cell growth by functioning as a transactivator of gene expression. The control of the expression of this protein is, therefore, essential for normal growth and development. It has been reported that p53 is regulated at the level of transcription, translation, change in conformation and covalent and non-covalent modifications (62).

p53 has been reported to undergo degradation directed by Mdm2 through an ubiquitin-dependent pathway (63). Mdm2 is a 90-kD oncoprotein that negatively regulates the activity of p53. It functions as a p53-specific E3 ubiquitin ligase in vitro, and the ubiquitinated p53 is degraded on 26S proteasomes (64). Furthermore, it recognizes the N-terminal activation domain of the p53 transcription factor and blocks the ability of p53 to associate with factors involved in gene transcription. The mdm2 shuttling between the nucleus and the cytoplasm is essential for mdm2 activity to target p53 for degradation (65). The negative regulation of p53 functions by mdm2 is important as shown in a study that inactivation of mdm2 by gene disruption was lethal for early mice embryos. However, lethality of the mice was rescued by the simultaneous disruption of the *p53* gene (66).

Importantly, mdm2 itself is the product of a p53-inducible gene. p53 binds the *mdm2* P2 promoter and transcriptionally up-regulates *mdm2* expression. An increase in Mdm2 causes a decrease in p53 activity, which subsequently results in a decreased Mdm2 to constitutive levels. Mdm2 can also ubiquitinate itself and induce its own degradation.

Thus, an autoregulatory feedback loop has been established between p53 and Mdm2, in which p53 induces expression of its own antagonist (67).

The mdm2 protein also has p53-independent functions. Evidence has shown that mdm2 interacted directly with p21 both in vitro and in vivo with the binding region in amino acids 180-298 of the mdm2 protein (68). It was suggested that mdm2 was also a negative regulator of p21.

## Introduction III -- *Evaluation of the effects of hepatocarcinogenesis*

### GST-P

Glutathione S-transferases (GSTs) are dimeric multifunctional and multigene family proteins. They are versatile enzymes and participate in nucleophilic attact of the sulfur atom of glutathione on electrophilic centers of xenobiotic compounds. Of all classes of GST ($\alpha$, $\mu$, $\pi$, $\sigma$, $\theta$), GST-pi, a 24-KDa GST isoform, has significance in diagnosis of cancers. Placental GST-P, the only GST of the pi class in rats, is normally absent in rat hepatocytes. It becomes specifically induced at an early stage of chemical hepatocarcinogenesis (69). It is then expressed constitutively and is present at high levels in preneoplastic hepatocytes and HCCs. Therefore, it appears to be a valuable marker for HCC in rat.

In addition, GST-pi was also shown to be higher in other tumors. In an immunohistochemistry retrospective study, it was demonstrated that GST-pi expression could be a marker for astrocytomas tumoral progression (70). In another study it was suggested that neoplastic processes increase the expression of placental isozyme of GST-pi and also affect metabolic pathway involved in bile acid synthesis. Thus placental form of GST-P as new marker enzyme for preneoplastic hepatocytes, but it is not found that human placental form, GST-pi to be possible tumor marker for various human tissues except liver (71).

### ALT & AST

The enzyme alanine aminotransferase is widely reported in a variety of tissue

sources. The major source of ALT is of hepatic origin and has led to the application of ALT determination to the study of hepatic diseases. Elevated serum levels are found in hepatitis, cirrhosis, and obstructive jaundice. ALT determinations via ultraviolet methods were first developed in 1956 by Wroblewski and LaDue (72). The method was based on the oxidation of NADH by lactate dehydrogenase (LDH) in the reactions below:

$$\text{L-Alanine} + \alpha\text{-ketoglutarate} \xrightarrow{\text{ALT}} \text{Pyruvate} + \text{L-Glutamate}$$

$$\text{Pyruvate} + \text{NADH} + \text{H}^{-} \xrightarrow{\text{LDH}} \text{L-Lactate} + \text{NAD}^{-} + \text{H}_2\text{O}$$

Aspartate Transminase (AST) is one of several enzymes that catalyze the exchange of amino and oxo groups between α-amino acids and α-oxo acids. It is widely distributed throughout body tissues with significant amounts in heart and liver. Lesser amounts are found in skeletal muscles, kidneys, pancreas, spleen, lungs and brain. Injury to these tissues results in release of AST enzyme to the general circulation. An increase in serum AST is also found with hepatitis, liver necrosis, cirrhosis and liver metastasis. The enzyme reaction is as follows:

$$\text{L-Aspartate} + \text{2-Oxoglutarate} \xrightarrow{\text{AST}} \text{Oxalacetate} + \text{L-Glutamate}$$

$$\text{Oxalacetate} + \text{NADH} + \text{H}^{-} \xrightarrow{\text{MDH}} \text{L-Maltate} + \text{NAD}^{-} + \text{H}_2\text{O}$$

## Introduction IV – *Traditional Chinese Medicine (TCM)*

Traditional Chinese Medicine (TCM) is an integral part of Chinese culture. It has made many contributions to the aspect of herbal medicine and has become widely accepted as an alternative therapy to treat different diseases. Today, both of TCM and western medicine are being used in providing medical and health services worldwide. TCM is recognized for its effectiveness in enhancing energy, lowering recurrence in some cancers and offsetting side effects that caused by chemical treatment of cancer in conventional treatment.

### Andrographis Paniculata

Andrographis Paniculata (AP) is a traditional Chinese herbal drug for the treatment of various diseases. It belongs to a plant family called Acanthaceae and is commonly called "the King of bitters" or Chuan Xin Lian in Chinese. Andrographis Paniculata grows abundantly in southeastern Asia like India, Pakistan and Indonesia. It, however, is mostly cultivated in China, Thailand, the East and West Indies. The aerial parts of the plant (leaves and stems) are used in combination with other herbs to treat diseases such as GI tract and upper respiratory infections, fever, herpes, sore throat, and a variety of other chronic and infectious diseases. However, there is not much research on the TCM until recent years. Since then, this plant has been extensively studied and early study has confirmed that Andrographis Paniculata possesses a broad range of pharmacological properties (73-75).

The extraction of the active phytochemicals from the leaves of this plant reveals that one of the major components, andrographolide, is medicinally active. This primary medicinal component of Andrographis is a diterpene lactone, which has the structure of 20 carbon atoms arranged as four isoprene units (Fig. 1). The cyclic ester lactone in the compound is believed to be the major active part that possesses the medicinal effects. Other medicinal components like deoxyandrographolide, -19β-D-glucoside, neo-andrographolide, 14-deoxy-11,12-didehydroandrographolide (andrographolide D), homoandrographolide, andrographan, andrographon, andrographosterin, and stigmasterol have also been isolated from this plant.

In recent years, the pharmacological effects, safety, efficacy and mechanisms of action of andrographolide have been described. Previous study indicated that andrographolide was widely distributed throughout the body when orally administered to rats. Its half life is short, of approximately 6 hrs, and the compound is metabolized and excreted in urine and bile (76). Other studies suggested that andrographolide possesses the medicinal properties such as anti-inflammatory, antibacterial, antipyretic, immune enhancer, anticancer, and in particularly hepatoprotective (77-79).

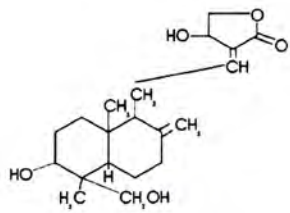


Fig 1. Andrographis Paniculata (on the left), and its active component, andrographolide (on the right).

**Pharmacological properties of andrographolide**

In a recent study by Iruretagoyena et al. (2006), andrographolide was shown to be able to interfere with NF-κB activation in mouse MLE-12 cells. NF-κB is a transcription factor that is known to play a central role in immune and inflammatory responses. By interfering with this activation, dendritic cells (DCs) that were treated with andrographolide failed to mature in response to LPS and to activate antigen-specific T cells *in vitro* (80).

Its anti-inflammatory mechanism was evaluated in another study. Andrographolide was able to inhibit Complement 5a (C5a) -induced chemotatic migration of macrophages. It significantly attenuated C5a-stimulated phosphorylation of ERK ½, and of its upstream activator, MAP kinase-ERK kinase (MEK ½). Inhibition of cell migration was also observed in response to macrophage inflammatory protein-1α (MIP-1α) (81). Qin LH et al. (2006) investigated the effect of andrographolide on the production of TNF- α and IL-12 (Interleukin-12), the two major inflammatory mediators secreted by macrophages, in murine peritoneal macrophages. The results revealed that andrographolide significantly reduced TNF- α and IL-12a and IL-12b at mRNA level, and decreased the production of TNF- α and IL-12p70 proteins in a concentration-dependent manner. The mechanism of the inhibition of LPS-induced production of TNF- α was found to be due to the suppression of the ERK1/2 signaling pathway (82).

Andrographolide has also been shown to be a remedy for fever, pain reduction and disorders of the intestinal tract (83). There was a reduction in rectal body temperature of rats for 30, 100, and 300 mg of andrographolide/kg of body weight. While the analgesic activity of andrographolide was weak compared to aspirin, the anti-pyretic activity was

comparable to that of aspirin. It was found that 300 mg/kg body weight of andrographolide was as effective as the same amount of aspirin, in fact, the AP extract was found to possess antiulcerogenic activity. It reduced the development of ulcers by 31%, while the standard ulcer drug, cimetidine had an 85.43% reduction rate. Thus, andrographolide caused a significant decrease in total stomach acidity and acid stomach juice secretion, without the cost and side effects associated with ulcer therapy (83).

Furthermore, the crude extract and isolates of Andrographis Paniculata, andrographolide, showed viricidal activity against herpes simplex virus 1 (HSV-1) (73).

The anti-cancer property of the compound was suggested and confirmed by a most recent study on breast cancer cells. In cell cycle studies, andrographolide effectively inhibited the growth of breast cancer cells by blocking the cell cycle at G0/G1 phase. The effect was similar to Lovastatin, which was the positive control in this study. This inhibition was due to its interaction with some cell cycle proteins, like p27 & CDK4. In vivo studies showed that cell cycle inhibitor p27 was increased upon treatment of andrographolide, which subsequently led to a decrease in CDK4. An early study demonstrated that andrographolide had potent cell differentiation inducing activity on mouse leukemia cells and thus causing maturation of cancer cells (84).

Andrographolide was also shown to be hepatoprotective (85). Pretreatment of mice with andrographolide for three consecutive days produced significant decrease in malondialdehyde formation, reduced glutathione (GSH) depletion and enzymatic leakage of glutamic-pyruvate transaminase (GPT). Other diterpenes extracted from AP also showed a comparable hepatoprotective effect with silymarin in terms of the formation of the degradation products of lipid peroxidation and release of GPT in the serum.

Andrographolide also showed a significant increase in the percent viability on the *ex vivo* preparation of isolated rat hepatocytes against paracetamol-induced toxicity. It was found to be more potent than the standard hepatoprotective agent, silymarin (79).

## Introduction V -- *Aim of the project*

Although the beneficial effects of andrographolide have been reported in the previous studies, its biological in the liver has yet to be elucidated. Therefore, the purpose of my present study is to investigate the effects of andrographolide on liver through *in vitro* and *in vivo* studies.

## Materials & Methods -- *In vitro*

In this part of the experiment, the biological activity of andrographolide in liver cancer cell line was investigated. Neutral red assay, cell cycle analysis, DNA fragmentation, and cDNA microarray were employed to study the effects of the active component on HepG2 cells.

## Chapter 1: Effects of andrographolide on cell viability and cell cycle

*Neutral red assay, flow cytometry & DNA fragmentation*

*1.1 Materials & Solutions*

| | |
|---|---|
| Trypsin-EDTA (1X), Dulbecco's Modified Eagle Medium (DMEM), RPMI Medium 1640, PSN Antibiotic mixture | Invitrogen (Ca., USA) |
| Fetal Bovine Serum (FBS) | Biosera (UK) |
| Sodium chloride (NaCl), potassium chloride (KCl), sodium dodecyl sulfate (SDS), agarose, proteinase K, bromophenol blue | USB (Cleveland, USA) |
| Sodium phosphate ($NaH_2PO_4$), potassium ($KH_2PO_4$), neutral red (NR), sodium bicarbonate ($NaHCO_3$), propidium iodide (PI), ethylenediaminetetraacetic acid (EDTA), xylene cyanole, ethidium bromide (EB) | Sigma Chemicals (St. Louis, USA) |
| Andrographolide (AND) 98% | Sigma-Aldrich (USA) |
| Dimethylsulfoxide (DMSO ) | Fisher Scientific (USA) |
| DNA ladder (GeneRuler) | Fermentas (Ont. Canada) |

| | |
|---|---|
| RNase A | Amersham (USA) |
| Steritop-GP 500 ml (0.22 μm), millex-GP (0.22 μm) | Millpore (Ma., USA) |
| 75 $cm^2$ culture flask, 96-well microplate | Iwaki (Tokyo, Japan) |
| 60 mm culture dish | Corning (USA) |
| Flow cytometer | Beckman Coulter (USA) |

*1.2 Preparation of solutions*

RPMI: The medium was prepared by dissolving one pack of RPMI medium and 2.0 g of $NaHCO_3$ in 895 ml of $dH_2O$. After the powder was completely dissolved, the solution was adjusted to pH 7.2. The solution was sterilized in the culture hood by filtering through a Steritop membrane with pore sizes of 0.22 μm. Fetal bovine serum (100 ml) and PSN antibiotic mixture (2 ml) were added to the filtered solution and the completed medium was stored at 4°C. All containers for cell culture use were sterilized.

DMEM: The medium was prepared by dissolving one pack of DMEM medium and 3.7 g of $NaHCO_3$ in 895 ml of $dH_2O$. After pH was adjusted to 7.2, membrane filtration was performed in the culture hood. Before use, 100 ml of FBS and 2 ml of PSN antibiotic mixture were added to the filtered solution and the completed medium was stored at 4°C. The containers for cell culture use were sterilized.

10 X Phosphate-buffered saline (PBS): The solution contained 80 g of NaCl, 2 g of KCl, 14.4 g of $NaH_2PO_4$, and 2.4 g of $KH_2PO_4$ in 900 ml of $dH_2O$. The pH of the solution was adjusted to 7.4, and the volume was made up to 1000 ml with $dH_2O$.

1 X PBS: It was made by diluting 100 ml of 10 X PBS with 900 ml of $dH_2O$. This solution was autoclaved for cell culture use.

Andrographolide (AND) stock solution (20mM): It was made by dissolving 7.6 mg of AND in 1.08 ml of DMSO. Different concentrations of AND were prepared by diluting the stock solution with culture medium.

NR solution: The solution was made by dissolving 1 g of NR in 200 ml of 1 X PBS, followed by membrane filtration using Millex GP with pore size of 0.22 μm.

Lysis buffer: It contained 200 mM Tris-HCl, pH 8.3, 100 mM EDTA and 1% SDS

Proteinase K solution (10 mg/ml): The solution was made by dissolving 5 mg of proteinase K in 0.5 ml of $dH_2O$.

6 X DNA loading dye: It was made up of 93.6 μl of glycerol, 3 μl of 0.5 M EDTA (pH 8.0), 0.3 mg of bromophenol blue, 0.3 mg of xylene cyanole and $dH_2O$ to a final volume of 250 μl.

10 X Tris-Borate-EDTA (TBE) buffer: The buffer was prepared by dissolving 108 g of Tris base, 55 g of Boric acid and 9.3 g of $Na_4EDTA$ in 1000 ml of distilled water.

Ethidium bromide (EB): It was prepared by dissolving 50 mg of EB in 100 ml of $dH_2O$.

*1.3 Procedures*

**1.3.1 Seeding cells into culture flask (performed inside culture hood)**

Cells stored in liquid nitrogen were thawed in a 37°C water bath, along with 1 X PBS and completed medium. Cells were transferred to a new tube and were centrifuged at 1,000 rpm for 3 min. The supernatant was discarded and the cell pellet was washed twice with PBS by centrifugation at 1,000 rpm for 3 min. The supernatant was discarded and 1

ml of the completed medium was added to resuspend cells. After that, cells were transferred to a new 75 $cm^2$ culture flask with 12 to 15 ml of warm medium. The flask was stored in a 37°C incubator supplied with 5% $CO_2$.

### 1.3.2 Subculturing technique (performed inside culture hood)

The medium was discarded from the 75 $cm^2$ culture flask and cells were rinsed with warm PBS twice to remove any trace of serum. Trypsin-EDTA (1 ml) was added to the flask and incubated at 37°C. After a few minutes, four milliliters of completed medium were added to stop the activity of trypsin. The cells were transferred to a new tube and spinned at 1,000 rpm for 3 min. The supernatant was discarded and the cell pellet was resuspended in warm medium. Cells were washed again by centrifugation at 1000 rpm for 3 min, and were resuspended in 1 ml medium. Subsequently, 2 µl of cells was added to 18 µl of dye and the mixture was placed onto a hematometer for cell counting. Approximately 0.5 ml of 1 x $10^6$ cells was seeded in a new 75 $cm^2$ culture flask with 12 ml of fresh medium. The culture flask was put inside a 37°C incubator with 5% $CO_2$.

### 1.3.3 Neutral red assay (cell viability test for HepG2, WRL 68 & Clone 9 cells)

The inhibitory effect of AND on cell viability was measured by neutral red assay. HepG2, the human liver cancer cells, were thawed from stock using RPMI medium. After several subcultures, 100 µl of 1 x $10^4$ cells was seeded onto 96-well plates and allowed to be pre-treated for 24 hrs. After that, attached cells were incubated with 100 µl of 1% DMSO as the control or different concentrations of AND. The plates were incubated at

various time periods: 24, 48 and 72 hrs. After treatment, the culture medium was removed and cells were washed with 200 µl of non-sterilized PBS twice. Then, neutral red solution (50 µl) was added to all the wells except the blank. The plates were wrapped in aluminum foil and incubated for 1 hr at 37°C. After that, wells were washed with 200 µl of PBS twice and the plates were inverted and allowed to dry in a 65°C oven. To each well of the plates, 100 µl of 1% SDS was added. The plates were shaken for 2 min and placed in a microplate reader to measure the absorbance at 540 nm. The cell viability (%) was plotted against the concentration of AND and the $IC_{50}$, the concentration of the agent that reduced the cell viability by 50%, was recorded.

The same procedure was applied to human normal liver embryo cells, WRL 68, and rat normal liver cells, Clone 9, except that the culture medium was DMEM for these two cell lines.

### 1.3.4 DNA purification of HepG2 cells

Apoptotic cells were detected by DNA fragmentation. Approximately 1 x $10^6$ HepG2 cells were seeded onto a 60 mm culture dish and incubated with 1% DMSO or different concentrations of AND (12.5, 20, 25 and 50 µM). After 72 hrs, cells were harvested and washed with PBS by centrifugation at 1,000 for 3 min. The cell pellet was resuspended in 400 µl of lysis buffer in a 1.5 ml microtube with gentle vortexing. When no cell debris was left, 20 µl of 10 mg/ml of proteinase K was added to each tube and the lysed cells were incubated at 37°C for 3 hrs. After samples were cooled to room temperature, 150 µl of saturated NaCl solution was added and the contents were mixed by vigorous shaking. The tubes were then centrifuged at 7,000 rpm for 15 min at room

temperature. The supernatant containing DNA was poured to a new tube, and 1 ml of cold ethanol was added. After the tube was inverted several times, it was centrifuged at 14,000 rpm at 4°C for 20 min. Samples were washed once with 70% EtOH and the DNA pellet was allowed to air dry for 15 to 20 min. TE buffer (20 to 50 µl) containing 0.2 mg/ml of RNase A was added to each DNA pellet. The samples were incubated at 37°C for 90 min. About 2 µl of the DNA solution was added to 998 µl of TE buffer and concentration was measured using UV spectrophotometry (Beckman, DU 650) with $OD_{260}$.

### 1.3.5 DNA gel electrophoresis

DNA gel electrophoresis was performed to detect DNA fragmentation. DNA gel containing 1.5% (w/v) agarose and 0.5 X TBE was boiled to completely dissolve the agarose. The gel solution was mixed thoroughly and 5 µg/mL of EB was added when the solution had cooled down to room temperature. Then the solution was poured into a gel casting mould for solidification. After the concentration of each sample was adjusted to 625 µg/ml, 10 µl of DNA samples were mixed with 2 µl of 6 X DNA loading dye and the mixture was loaded into the wells. The gel was run at 60 V for 45 min in 0.5 X TBE buffer. Electrophoresis was completed when the bromophenol blue had migrated down 2/3 of the length of the gel. The DNA bands were visualized under UV illuminator (UVP) and photographed for record.

### 1.3.6 Flow cytometry (cell cycle analysis)

The nuclear DNA content was measured by using propidium iodide (PI) staining and fluorescence-activated cell sorting (FACS) analysis. HepG2 cells were counted and

approximately 1 x $10^6$ cells were seeded onto a 60 mm culture dish and cells were pre-incubated for 24 hrs. After incubation with 1% DMSO or 12.5, 20 and 25 uM of AND for 24 and 48 hrs, floating cells in the spent medium and adherent cells were collected by combining the spent medium and trypsin-treated samples. Cells were harvested by centrifugation at 1,000 rpm for 3 min. The medium was discarded and the cell pellet was washed once with 1 ml PBS by centrifugation. The cell pellet was resuspended with 0.1 ml PBS and fixed in 1 ml of ice-cold 70% ethanol. The cell suspension was allowed to store overnight at 4°C. After fixing, cells were washed once with 1 ml PBS by centrifugation at 1,000 for 3 min at room temperature and resuspended in 1 ml PBS containing 8 µg/ml of RNase A and 40 µg/ml of PI. Samples were then incubated at 37°C for 15 to 30 min and DNA content was analyzed using a FACScan flow cytometer.

The total number of cells counted was set to 10,000. The DNA profile was represented in 1D plot (histogram), where the x-axis is the channel number and y-axis the number of events. After the profiles were obtained, the data was analyzed using FCS Express (Version 2) software by De Novo Company. The histograms showing the DNA profiles of the control and AND-treated groups were compared and the number of cells suspending in Sub $G_1$, $G_0/G_1$, S and $G_2/M$ phases were counted.

## Chapter 2: Effects of andrographolide on gene expressions

*mRNA extraction from cells and cDNA microarray*

*2.1 Materials & Solutions*

| | |
|---|---|
| Agarose, diethyl pyrocarbonate (DEPC), MOPS, | USB |

| | |
|---|---|
| Chloroform, EDTA, isopropanol, formaldehyde, tris, deionized formamide, ethidium bromide (EB) | Sigma |
| Trizol reagent | Gibco BRL |
| Ethanol (EtOH) | BDH |

| | |
|---|---|
| Oligo GEArray Human Toxicology & Drug metabolism microarray membrane (OHS-401), ArrayGrade cRNA cleanup kit, TrueLabelling-AMP 2.0, Oligo GEArray Reagent Kit | SuperArray, Bio-Gene Tech. |
| Biotin-16-UTP | Roche Applied Science |

*2.2 Preparation of solutions*

Diethyl pyrocarbonate (DEPC)-treated water: DEPC was added to autoclaved nano-pure water to make a final concentration of 0.1% by volume. It was stirred overnight and autoclaved before use.

1 X TE buffer: It contained 10 mM Tris-HCl and 1 mM EDTA. The pH was adjusted to 8.0 with HCl.

10 X MOPS: It was prepared by dissolving 83.72 g of MOPS in 450 ml of DEPC-treated $dH_2O$, and pH was adjusted to 7.0. Then 8.203 g of NaOAc and 3.722 g of EDTA were added to the solution. A final volume of 500 ml was made up with DEPC-$dH_2O$.

RNA sample buffer: It contained 10 ml of deionized formamide, 3.5 ml of 12.3 formaldehyde, 1 ml of 10 X MOPS buffer and 1 ml of DEPC-treated water and stored at -20°C.

6 X RNA loading dye: It was made up of 10 mM of EDTA (pH 8.0), 50% (v/v) glycerol, 0.25% bromophenol blue (w/v) filter-sterilized and stored at -20°C.

*2.3 Procedures:*

**2.3.1 Cell treatments**

HepG2 cells (5 x $10^6$) were seeded in a culture flask for 24 hrs in a 37°C incubator. After incubation, cells were treated with 1% DMSO or 16 uM of AND for 48 hrs. The medium was discarded and cells were trypsinized and washed with PBS twice by centrifugation at 1,000 rpm for 3 min.

**2.3.2 mRNA extraction from cell**

a) Cell lysis: 0.5 ml of Trizol reagent was added to the cell pellet, vortexed and stored at room temperature for 10 to 15 min. It was then centrifuged at 12,000 g for 10 min at 4°C. The supernatant was transferred to a new tube.
b) RNA Extraction: 0.1 ml of chloroform was added to the supernatant, and mixed vigorously. The sample was stored at room temperature for 10 to 15 min. It was then centrifuged at 12,000 g for 15 min at 4°C.
c) RNA Precipitation: the aqueous layer, which contained RNA, was transferred into a new tube. Isopropanol (0.25 ml) was added and stored at room temperature for 10 min. The sample was centrifuged at 12,000 g for 15 min at 4°C.

d) RNA Wash: the RNA pellet was mixed with 0.5 ml of 75% ethanol. It was then centrifuged at 7,500 g for 5 min at 4°C.

e) Solubilization: ethanol was discarded and the RNA pellet was allowed to air dry for 15 to 30 min. It was dissolved in 50 µl of DEPC-treated $dH_2O$ and incubated at 55 to 60°C for 10 min.

f) Storage: It was kept at -20°C for temporary storage or at -70°C for a long term storage.

### 2.3.3 Determination of total RNA yield and quality yield

The RNA sample was diluted in 1:500 with 1 X TE buffer. The yield of total RNA was obtained by UV spectrophotometry (Beckman, DU 650) at wavelength 260 nm, using 1 X TE buffer as blank. The amount of total RNA was calculated by the formula that 1 $A_{260}$ unit has 40 µg/ml of single stranded RNA. The result was divided by 2 as the dilution factor. The quality of RNA was assessed by the ratio of $A_{260}/A_{280}$. The integrity of the RNA was determined by formaldehyde agarose gel electrophoresis. The ratio of 28S and 18S ribosomal RNAs was close to 2:1 after EB staining.

### 2.3.4 RNA formaldehyde agarose gel eletrophoresis

The agarose gel was prepared by dissolving 0.3 g of agarose in 14.4 ml of DEPC-treated water. The solution was heated in a microwave to completely dissolve the agarose. When the mixture was cooled down for a few minutes, formaldehyde and 1 X MOPS were added to the gel solution. It was mixed thoroughly, and was poured into the gel casting mould for solidification.

Table 2.3.4 Protocol for formaldehyde agarose gel

| | |
|---|---|
| Agarose | 0.3 g or 1.5% (w/v) |
| DEPC-treated water | 14.4 ml |
| 1 X MOPS | 2 ml |
| Formaldehyde | 3.6 ml |

The RNA sample for gel electrophoresis was prepared by mixing 2 to 3 μg of RNA with 10 μl of RNA sample buffer, 1 μl of RNA loading dye and DEPC-treated water to make a final volume of 20 μl. The mixture was heated to 65°C for 10 min, and allowed to cool to room temperature before loaded into the gel.

After samples had been loaded into the wells, the gel was run in 1 X MOPS buffer at 120 V for 20 min or until the bromophenol blue dye had migrated down 2/3 of the length of the gel. The gel was stained with 5 ug/ml of EB for 30 min and then destained with three rinses of DEPC-treated water. The RNA bands were examined under UV illuminator (UVP) and it was photographed for record.

**2.3.5 cDNA synthesis**

Table 2.3.5 cDNA SuperArray kit components

| **Tube** | **Contents** |
|---|---|
| G1 | TrueLabeling Primer |
| R1 | RNase Inhibitor |
| G2 | cDNA Synthesis Enzyme Mix |

| | |
|---|---|
| G3 | 5 X cDNA Synthesis Buffer |
| $H_2O$ | RNase-free $H_2O$ |
| G24 | 2.5 X RNA Polymerase Buffer |
| G25 | RNA Polymerase Enzyme |
| Spin columns | |
| Elution Tubes | |
| GEAhyb. Hybridization solution | |
| Solution Q | |
| 5X buffer F | |
| AP-SA | |
| Buffer G | |
| CDP-Star chemiluminescent substrate | |

The components in G1, G3, $H_2O$, and G24 were thawed, mixed and collected at the bottom of the tube with a brief spin in a microcentrifuge.

a) Preparation of the annealing mixture

In a sterile PCR tube, 3.0 µg of total RNA (extracted in section 2.3.2), 1.0 µl of G1 and RNase-free $H_2O$ were added to make a final volume of 10 µl. The contents were mixed well followed by a brief centrifugation to collect the mixture at the bottom of the tube. Samples were incubated at 70°C for 10 min, then centrifuged briefly and placed on ice.

b) Preparation of the cDNA synthesis master mix

| cDNA synthesis master mix | Per reaction |
|---|---|
| RNase-free $H_2O$ | 4 µl |
| 5 X cDNA Synthesis Buffer (G3) | 4 µl |
| RNase Inhibitor (RI) | 1 µl |
| cDNA Synthesis Enzyme Mix (G2) | 1 µl |
| Final volume | 10 µl |

The components were combined in the order listed above, and mixed well with pipetting up and down two to three times followed by brief centrifugation to collect the mixture at the bottom of the tube. The cDNA synthesis master mix was then placed on ice.

c) cDNA Synthesis reaction: To each tube containing 10 µl of annealing mixture, 10 µl of cDNA synthesis master mix was added. The components were mixed well and then centrifuged briefly. Each reaction tube was incubated at 42°C for 50 min followed by 75°C for 5 min then cooled to 37°C.

### 2.3.6 cRNA synthesis, labeling and amplification

a) Preparation of the amplification master mix

| Amplification master mix | Per reaction |
|---|---|
| 2.5 X RNA Polymerase Buffer (G24) | 16 µl |
| Biotin-UTP | 2 µl |
| RNA Polymerase Enzyme (G25) | 2 µl |

| | |
|---|---|
| Final volume | 20 µl |

The above components were well mixed with pipetting up and down two to three times followed by brief centrifugation.

b) cRNA Synthesis reaction: To each tube containing 20 µl of cDNA synthesis reaction, 20 µl of amplification master mix was added. The components were mixed gently and centrifuged briefly. Then the reaction tubes were incubated overnight at 37°C.

**2.3.7 cRNA purification**

a) Binding cRNA to the Spin Column: A spin column was set up in a collection tube for each sample. RNase-free $H_2O$ (60 µl) was added to each cRNA synthesis reaction tube for a final volume of 100 µl. The entire reaction mixture was transferred to one 1.5-ml RNase-free tube. Lysis & binding buffer (G6) (350 µl) was added to each of the reaction mixture. The contents were mixed well with gentle pipetting for two to three times. Then 350 µl of room temperature ACS-Grade 100% ethanol was added and contents were mixed well with gently pipetting. Each sample was loaded to the center of its own spin column and centrifuged for around 30 sec at 8,000 x g. The column was removed from the tube and the flow-through was discarded.

b) Washing the spin column: To each spin column, 600 µl of washing buffer (G17 with ethanol) was applied. The column was centrifuged for about 30 sec at 8,000 x g. The column was removed and the flow-through was discarded. The column was placed back into the collection tube. Then 200 µl of washing buffer (G17 with ethanol) was

applied to each spin column, and the column was centrifuged for 3 min at 11,000 x g.

c) Eluting the cRNA from the spin column: Each spin column was transferred to a fresh elution tube. To the center of each spin column, 50 µl of room temperature RNase-free 10 mM Tris buffer pH 8.0 (G26) was added. The spin column was incubated at room temperature for 2 min, followed by centrifugation for 1 min at 8000 x g. After the entire volume of buffer passed through the filter, the purified cRNA was stored on ice.

d) cRNA quality assessment: The quality of cRNA was assessed by UV spectrophotometry as described previously.

### 2.3.8 Oligo GEArray hybridization

a) Pre-hybridization: To pre-wet the array membrane, roughly 5 ml of deionized water was added to the hybridization tube. The cap was screwed on hand-tight and the tube was allowed to sit inverted for 5 min. The GEAhyb Hybridization solution was warmed to 60°C and the bottle was inverted several times to allow complete dissolution of the buffer components. The deionized water was discarded from the hybridization tube and 2 ml of pre-warmed GEAhyb hybridization solution was added. The tube was briefly vortexed and placed in the hybridization cylinder. After checking that the warm hybridization tubes and cylinders were sealed hand-tight, the tubes were pre-hybridized in the hybridization oven at 60°C for 2 hours with continuous but slow agitation at 5 to 10 rpm.

b) Hybridization: At least 2 µg of biotin-labeled cRNA target was added to 0.75 ml of pre-warmed GEAhyb hybridization solution and mixed well. Then the pre-

hybridization solution was discarded from the hybridization tube and the target hybridization mix containing the labeled cRNA target was added to the tube. Hybridization was continued overnight at 60°C with slow agitation at 5 to 10 rpm.

c) Preparation of wash solutions: Wash solution 1 (2 X SSC, 1% SDS) was prepared by mixing 10 ml of 20 X SSC with 5 ml of 20% SDS and 85 ml of $dH_2O$. Wash solution 2 (0.1 X SSC, 0.5% SDS) was prepared by mixing 0.5 ml of 20 X SSC with 2.5 ml of 20% SDS and 97 ml of $dH_2O$. Both wash solutions 1 and 2 were warmed to 60°C before use. The preparations of 20 X SSC and 20% SDS were as follows:

| 20 X SSC (pH 7.0) | |
|---|---|
| Sodium Chloride (NaCl) | 2.63 g |
| Sodium citrate dihydrate | 1.323 g |
| Distilled water | 10 ml |
| 20% SDS | |
| Sodium dodecyl sulfate (SDS) | 200 g |
| Distilled water | 1 L |

d) Washing: The target hybridization mix was transferred to a clean microcentrifuge tube and 5 ml of wash solution 1 was added to the hybridization tube. The tube was placed back into the hybridization oven and the membrane was washed at 60°C with faster agitation at 20 to 30 rpm for 15 min. The wash solution was discarded and 5 ml of wash solution 2 was added. The membrane was washed for 15 min at 60°C with 20 to 30 agitations. The wash solution was immediately discarded and the cap was placed

back on the hybridization tube to prevent membrane from drying. The tube was allowed to cool to room temperature.

### 2.3.9 Chemiluminescent detection

a) Blocking the Oligo GEArray: GEAblocking solution Q (2 ml) was added to the hybridization tube and vortexed briefly. The tube was incubated for 40 min with continuous agitation at 20 to 30 rpm.

b) Preparation of solutions

   i) 1 X Buffer F: 5 X Buffer F was diluted five-fold with $dH_2O$.

   ii) Dilute AP-SA Buffer: AP-SA was diluted in 1:8,000 with 1 X Buffer F. For 8 Oligo GEArrays, 2 µl of AP-SA was added into 16 ml of 1 X Buffer F.

c) Binding of alkaline phosphate-conjugated streptavidin (AP): After GEAblocking solution Q was discarded from the tube, 2 ml of diluted AP-SA buffer was added and incubated for exactly 10 min with continuous but gentle agitation (5-10 rpm).

d) Washing: The membrane was washed four times with 4 ml 1 X Buffer F for 5 min with gentle agitation. The tube was well vortexed after each addition of fresh 1X Buffer F.

e) Rinsing: After the last wash was discarded, 3 ml of Buffer G was added and the tube was inverted three times. The buffer was discarded and the procedure was repeated twice.

f) Detection: After rinsing, 1.0 ml CDP-Star chemiluminescent substrate was applied to the hybridization tube. The tubes were rotated in room temperature hybridization oven for 3 to 5 min.

g) Image acquisition: After the CDP-Star incubation, the GEArray was ready for image acquisition. To remove excess CDP-Star solution, one corner of the array membrane was held by forceps and the opposite membrane corner was in contact with a piece of clean, absorbent paper. The membrane was placed between two plastic transparencies and image was acquired on a Super RX film (Fuji).

h) Microarrays: After obtaining exposures, the damp membrane was returned back to its original plastic disposable hybridization tube. The cap was placed hand-tight and stored at -20°C.

**2.3.10 Data analysis**

Image, data and statistical analysis were performed with GEArray® Expression Analysis Suite Package. After logging into the site, http://geasuite.superarray.com/, project name was created and Array image was uploaded to each project. Images were optimized and adjusted to the crop frame in the Image Setting Workplace. Then workplace was switched to Grid/Readout where circles on the grid were aligned to the spots on the image. When the position and size of the spots were adjusted, readout was built and saved. Once readouts were available for all arrays, analysis was done to Arrays in two groups and gene names and their expressions were listed. A Scatter plot was obtained from all Arrays in one group and fold changes in gene expression between groups were calculated.

## Materials & Methods -- *In vivo*

Andrographolide is believed to have pharmacological activity. In this part of the experiment, the effect of andrographolide on hepatocarcinoma in rats was investigated through ALT & AST assays, hematoxylin & eosin staining, immunohistochemical staining of GST-P, RNA expressions of *p53* & *mdm2* and western blot analysis of p53, mdm2, PCNA, Bax, Bcl-2 and p21.

## Chapter 3. Effects of andrographolide on hepatocarcinogenesis in rats

*Animal Treatment, liver perfusion, AST/ALT Assays & Stainings*

*3.1 Materials & Solutions*

| Chemicals & Reagents | Purchasers |
|---|---|
| ALT/SGPT (UV-Rate) & AST/SGOT (UV-Rate) Kits for detection of alanine and aspartate transferases respectively | Stanbio Laboratory (Texas, USA) |
| Diethylnitrosamine (DEN), hydrogen peroxide (30%), diaminobenzidine (DAB), formaldehyde 36% | Sigma Chemicals (St. Louis, USA) |
| Anti-GST-P polyclonal antibody (rabbit) | Medical & Biological Laboratories |
| Biotinylated goat anti-rabbit IgG and avidinbiotin-peroxidase complex (ABC Staining System) | Santa Cruz Biotechnology (Ca., USA) |
| Superfrost / plus microscope slide (25 x 75 x 1.0 mm), DMSO (Dimethylsulfoxide) | Fisher Scientific (Pittsburgh, USA) |

| | |
|---|---|
| Glass microscope slide (25.4 x 76.2 x 1.2 mm) | Sail Brand (Shanghai) |
| Ethanol 100% | BDH (England) |
| Carbon tetrachloride ($CCl_4$) | Merck (Germany) |
| Tris, sodium dodecyl sulfate (SDS), citric acid (trisodium dehydrate) | USB (Cleveland, USA) |
| Andrographolide (AND) 98% | Sigma-Aldrich (USA) |
| Corn Oil | Vecorn (USA) |

*3.2 Preparation of Solutions*

DEN solution (200 mg/ml): DEN solution for the initiation of rat HCC was prepared by diluting 2.52 ml of DEN to 12 ml with DMSO.

$CCl_4$ solution: It was prepared by mixing $CCl_4$ with corn oil in 1:1 ratio.

Andrographolide (10 mg/ml) solution: It was prepared by dissolving 500 mg of AND in 50 ml of corn oil.

Tris-sucrose buffer (pH 7.4): The buffer used for liver perfusion was prepared by dissolving 95.6 g of sucrose and 6.06 g of Tris in 900 ml of $dH_2O$. The pH was adjusted to be 7.4 with HCl and volume was made up to 1000 ml with $dH_2O$. The solution was then stored at 4°C.

Formaldehyde solution (10%): Formaldehyde buffer for the liver section fixation was prepared by mixing 10 ml of 36% formaldehyde with 26 ml of $dH_2O$ to make 36 ml of formaldehyde solution.

1% hydrogen peroxide ($H_2O_2$): The solution was freshly prepared by diluting 3 ml of 30%

hydrogen peroxide with $dH_2O$ to make a final volume of 300 ml.

Citric acid buffer (pH 6.0): It was prepared by dissolving 0.63 g of citric acid with 300 ml of $dH_2O$. The pH was adjusted to 6.0 with sodium hydroxide (NaOH).

Diluted normal serum (NS): The solution was prepared by diluting 150 µl of NS from ABC staining kit in 10 ml of 1 X PBS.

Diluted anti-GST-P antibody (1:10): This primary antibody was diluted in 1:10 ratio by adding 0.5 ml of anti-GST-P antibody to 4.5 ml of diluted NS.

Diluted Biotinylated goat anti-rabbit IgG (1:200): It was prepared by diluting 25 µl of antibody in 4.975 ml of diluted NS.

Diluted avidinbiotin-peroxidase complex (ABC): It was prepared by mixing 100 µl of A and B from ABC staining kit in 4.8 ml of 1X PBS.

DAB solution: It was freshly prepared by dissolving 15 mg of DAB in 150 ml of PBS, with 8 µl of 30% $H_2O_2$ added before use.

*3.3 Procedures*

**3.3.1 Animal treatment**

Male Spraque Dawley rats (80-90 g of body weight) were obtained from Laboratory Animal Services Center of The Chinese University of Hong Kong (Hong Kong SAR, The People's Republic of China). They were divided into three groups (Negative control, Positive control and Treatment) and housed in three different cages in animal room maintained with a 12 hr light-dark cycle (06:00-18:00) at constant temperature and humidity of 55 ± 5%. They were given unlimited rodent diet (Supastok Autoclavable Rodent Diet, Ridley Agripoducts, Australia) and water *ad libitum*. Rats were observed

during the acclimatizing week and were then used for different treatments according to the protocols described below.

Table 3.3.1 Treatment of rats for the promotion & progression stages of hepatocarcinogenesis

| | i.p. injection of toxicant/ vehicle (once a week) | Oral treatment (once a day) |
|---|---|---|
| Negative Control | DMSO + Corn Oil | Corn Oil |
| Positive Control | DEN + $CCl_4$ | Corn Oil |
| AND-treated | DEN + $CCl_4$ | Andrographolide (10 mg/kg) |

**Table 3.3.1** The treatment of rats in two stages of hepatocarcinogenesis. Rats were divided into three groups: negative, positive and AND-treated. The negative control group received i.p. injection of the vehicle, DMSO, and oral treatment of corn oil. The positive control and AND-treated groups received i.p. injection of a tumor initiator, DEN, for the first two weeks and then a tumor promoter, $CCl_4$, for the rest of the weeks. Rats in the positive control group were given corn oil once daily whereas those in the AND-treated group were given 10 mg/kg of AND.

### 3.3.2 Promotion (Experiment 1):

This experiment was designed to study the effect of AND at the promotion stage of rat hepatocarinogenesis. Fifteen Sprague Dawley rats were equally divided into negative control, positive control and AND-treated groups. The negative control group received weekly intraperitoneal injection of DMSO (1 ml/kg of body wt) for the first two weeks, followed by a 5-day period of fasting for the next two weeks. Corn oil (1 ml/kg of body wt) was then administered intraperitoneally for the rest of the weeks. On the other hand,

both the positive control and AND-treated groups received DEN (200 mg/kg body wt) for the first two weeks and then two 5-day periods of fasting. Between two weeks' of fasting, two days of *ad libitum* feeding were applied to allow maximum fasting experience with minimal fatalities. After the fasting periods, $CCl_4$ was administered intraperitoneally for the rest of the weeks. From the 5$^{th}$ week onwards, both the negative and positive controls received oral treatment of corn oil once a day. AND (10 mg/kg of body weight) was administered orally to the treatment group once daily. At the end of the experiment, which lasted for 28 weeks, all rats were weighed and then killed by nitrogen gas. Blood samples were collected. The liver samples were perfused with cold Tris-sucrose buffer and then removed, washed and weighed. Liver slices of about 2-3 mm in thickness were cut out. They were fixed in 10% formaldehyde for 24 hrs and then 75% ethanol until sections were embedded in wax by standard procedures. The remaining part of the liver was stored at -80°C for further analysis.

### 3.3.3 Progression (Experiment 2):

This experiment was designed to investigate the effect of AND at the progression stage of rat hepatocarcinogenesis. Fifteen Spraque Dawley rats were equally divided into negative control, positive control and AND-treated groups. The intraperitoneal treatments for all the groups were the same as those in experiment I. Oral treatment with corn oil (1 ml/kg of body weight) or AND (10 mg/kg of body weight) was not given to the groups until the 32$^{nd}$ week of the experiment. At the end of the 56$^{th}$ week, rats were weighed and killed by nitrogen gas. Blood samples were collected for further analysis. Liver samples were perfused and stored as described in experiment I.

Figure 3.3.2 Experimental protocol for rat treatments in Experiment 1

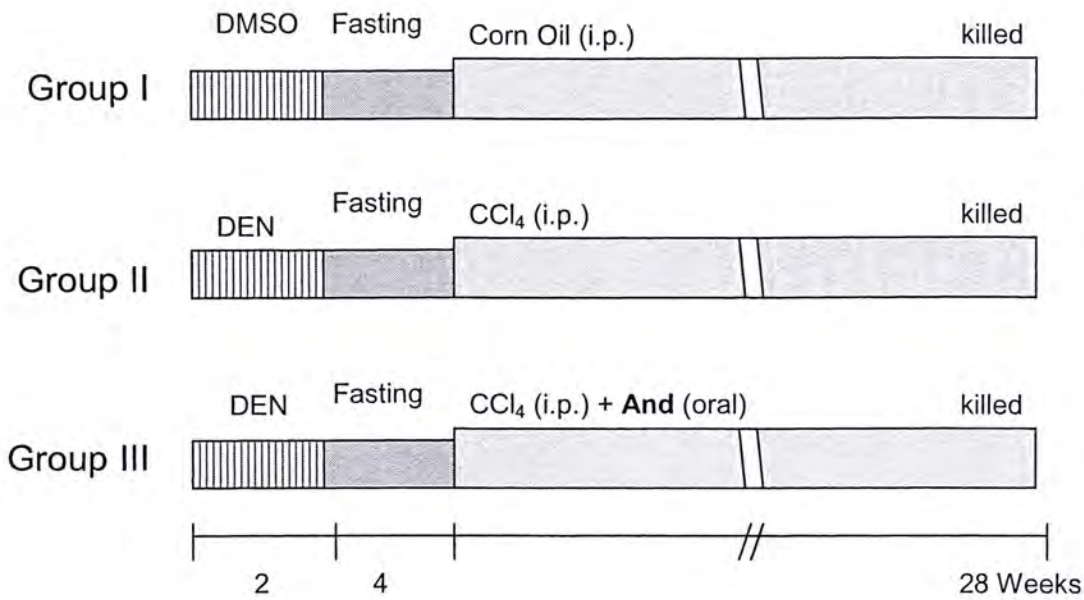


**Figure 3.3.2** Treatment schedule of the rat in the promotion stage of hepatocarcinogenesis. Group I represents the negative control rats which did not receive any toxicants. Group II is the positive control rats which were exposed to DEN and $CCl_4$. Group III represents the AND-treated group which was not given treatment until the $5^{th}$ week of the experimental schedule.

Figure 3.3.3 Experimental protocol for rat treatments in Experiment II

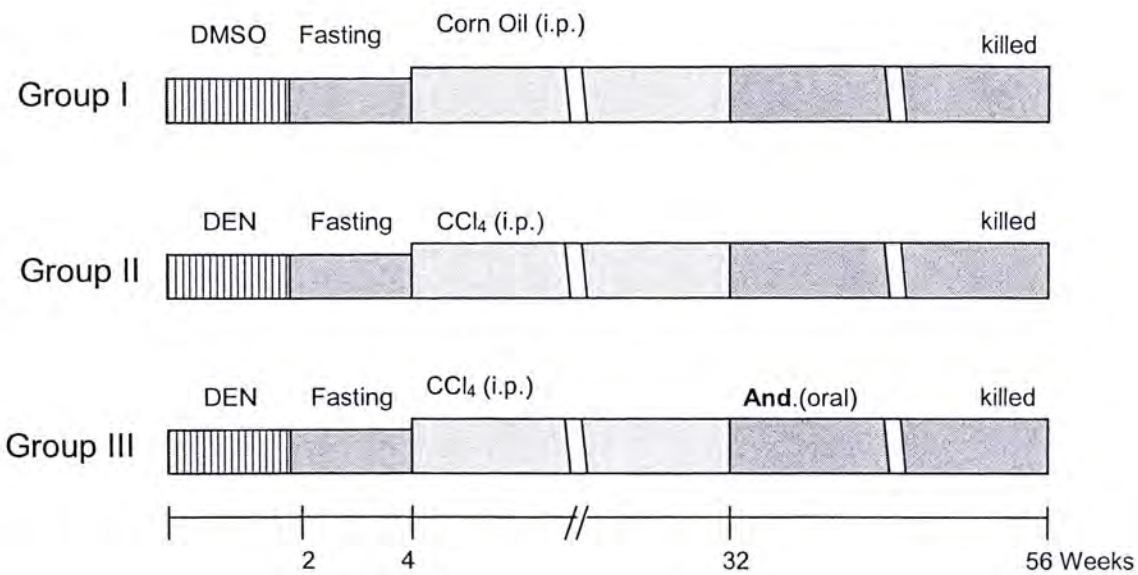


**Figure 3.3.3** The schedule of the rat treatments in the progression stage of hepatocarcinogenesis. Group I represents the negative control rats which did not receive any toxicants. Group II is the positive control rats which were exposed to DEN and $CCl_4$. Group III represents the AND-treated group. Oral treatments for the three groups were not given until the 32$^{nd}$ week of the experimental schedule.

## Measurement of serum ALT and AST

### 3.3.4 Extraction of blood serum

Blood samples collected from rats were transferred to Vacutainers and were allowed to sit on ice for 10 min. After that, samples were centrifugated for 15 min at 4,000 rpm. Serum was extracted and was put on ice for ALT and AST analysis.

### 3.3.5 Measurement of absorbance

Activities of ALT and AST in rat serum were measured using Stanbio GP- and GO- Transminase Kits. The ALT kit (Procedure No. 0930) contained 13 mmol/L of a-ketoglutarate and 0.4 mol/L of DL-alanine. The AST kit (Procedure No. 0920) contained 12 mmol/L of 2-oxoglutarate and 0.2 mol/L of L-aspartic acid. The reagent was reconstituted with 15 ml of $dH_2O$ and 1 ml of reconstituted reagent was added to cuvet and pre-warmed to 37°C for 3 min. Serum (0.1 ml) was added to the cuvet and was mixed gently by pipetting up and down several times. The content was warmed at 37°C for exactly 1 min. After the incubation, cuvet was placed into a spectrophotometer and was blanked at time zero. The absorbance was measured at 340 nm and readings were recorded at 30-second interval for 3 min. The amounts of ALT and AST were calculated as follows:

$$U/L = \frac{\Delta A / Min}{Absorptivity} \times \frac{Total\ volume}{Sample\ volume}$$

$$U/L = \Delta A / Min \times 1768$$

## Histological Analysis: H&E and immunohistochemical stainings

### 3.3.6 Tissue processing

Liver slices that were fixed in 75% ethanol were embedded in wax by tissue processor according to standard procedures. The waxed tissue samples were trimmed until the whole surface of sample was exposed. Samples were cut on a microtome at 5 um thick and were put into a 40°C water bath for a few minutes. Then two to three sections of each sample were mounted on glass slides for hematoxylin and eosin (H&E) staining and on superfrost plus microscope slides for immunohistochemical staining, respectively.

Slides, each containing two to three liver sections, were placed in a slide holder and warmed to 48°C in oven for 10 minutes. Sections were then dewaxed and rehydrated with xylene (5 min x 3), 100% ethanol (5 min x 3), 95% ethanol (1 min), 80% ethanol (1 min), 70% ethanol (1 min) and water (5 min).

### 3.3.7 Hematoxylin and Eosin (H&E) Staining (Nucleus & Cytoplasm)

Glass slides containing liver samples were stained in hematoxylin for 3 min. They were rinsed with tap water and allowed stain to develop for 5 min. After that they were destained with acid alcohol for 3 sec, followed by rinsing with tap water. Sections were placed in Scott tap for 1 min and then rinsed briefly in tap water. Then, slides were stained in eosin for 4 to 5 min, followed by rinsing with tap water. Sections were dehydrated briefly in 70% and 80% ethanol, and then 95% ethanol for 1 min, 100% ethanol for 5 min for 3 times, and lastly xylene for 5 min for 3 times. Finally slides were mounted with coverslip and Permount.

### 3.3.8 Immunohistochemical staining of GST-P

Superfrost plus microscope slides containing two to three sections of liver samples were dewaxed and rehydrated as described previously. Endogenous peroxidase activities of liver samples were blocked in 1% $H_2O_2$ for 5 min at room temperature. Sections were washed in tap water for 5 min, followed by antigen retrieval in 300 ml of citric acid buffer. The case and the buffer were first pre-warmed in microwave for 5 min. After the slides were placed in the buffer, sections were further heated for another 5 min on a hot plate. Sections were washed in tap water for 5 min and excess water was wiped off gently around each section. About 150-200 µl of diluted NS was added to each section to block the unspecific antigens and sections were allowed to incubate for 1 hr at room temperature. After the excess NS was drained off from the slides, sections were covered with 150-200 µl of anti-GST-P polyclonal antibody in 1:10 ratio and incubated overnight at 4°C inside moist chamber. After binding with primary antibody, sections were washed in PBS three times for 5 min each. About 200 µl of biotinylated goat anti-rabbit IgG diluted in 1:200 was added to each section and incubated for 30 min at room temperature. The slides were washed with PBS for three changes, each for 5 min, and then covered with 200 µl of freshly prepared ABC for 30 min at room temperature. After washing with PBS with three changes for 5 min each, sections were immersed in DAB solution for approximately 3 min, and positive areas could be visualized under microscope. Sections were washed with tap water for 5 min, followed by counterstaining in hematoxylin for 2 min. Then the slides were washed with tap water, and were briefly destained with acid alcohol for 2 sec. Slides were rinsed with tap water, then immersed in Scott tap for about 30 sec, and again rinsed with tap water. The slides were briefly dehydrated in 70% and 80% ethanol, and

then 95% ethanol for 1 min, 100% ethanol for 5 min for 3 times, and lastly xylene for 5 min for 3 times. Finally, slides were mounted with coverslip and Permount.

### 3.3.9 Examination of liver sections

Liver sections were examined using an Axiophot-2 Universal microscope (Zeiss) coupled with Spot 32 image analysis system. Sections were viewed under 5x, 10x, 20x and 40x magnifications and were analyzed using Image J program.

## Chapter 4. Effects of Andrographolide on the expressions of Mdm2, p53, PCNA, Bax, Bcl-2 and p21

*mRNA & protein extraction from liver, RT-PCR, SDS-PAGE & Western blots*

*4.1 Materials and Solutions*

| | |
|---|---|
| Agarose, TEMED, HEPES, diethyl pyrocarbonate (DEPC), ammonium persulfate (APS), acrylamide/bis, MOPS, glycerol, bromophenol blue, sodium dodecyl sulfate (SDS), 5X M-MLV reaction buffer, M-MLV reverse transcriptase | USB |
| Chloroform, EDTA, isopropanol, formaldehyde, tris, magnesium chloride ($MgCl_2$), dithiothreitol (DTT), phenylmethylsulfonyl fluoride (PMSF), triethanolamine-HCl, beta-mercaptoethanol, deionized formamide, triton x-100, ethidium bromide (EB) | Sigma |
| Oligo dT primer, 10 mM dNTP mix, Taq polymerase, β-actin primer mix | Invitrogen |
| Trizol reagent, PCR buffer | Gibco BRL |
| Target gene primers | Tech Dragon Ltd |
| Complete 20 tablets (protease inhibitors) | Roche |
| Millipore Immobilon 26.5x375 cm Roll | Bio-Gene tech. Ltd |
| 3MM Filter paper | Whatman |
| Tween-20 | Pharmacia Biotech |

| | |
|---|---|
| Primary antibodies: anti-β-actin, anti-mdm2 (SMP14), anti-p53 (Pab246 & 421), anti-Bcl-2 (c-2), anti-Bax (5B7), anti-PCNA (pc10) and anti-p21 mouse monoclonal<br>Secondary antibody: goat anti-mouse HRP labeled antibody | Santa-Cruz Biotech Inc |
| Methanol (MeOH), ethanol (EtOH) | BDH |
| Protein A sepharose CL-4B, ECL-Western Blotting detection reagent | Amersham |
| Fuji Super RX Film | Fuji Photo Products Co. Ltd |

*4.2 Preparation of solutions*

25 mM $MgCl_2$: It was prepared by dissolving 0.119 g of $MgCl_2$ in 50 ml of d $H_2O$.

Solution A for nuclear protein extraction: The solution contained buffer A and 1 mM of PMSF.

Buffer A: It was prepared by dissolving 438.3 mg of NaCl, 119.15 mg of HEPES, 18.61 mg of EDTA $Na_2$ $2H_2O$, and 0.3 g of Triton X-100 in 40 ml of water. The pH was adjusted to 7.9 with 1 M NaOH. The solution was made up to 50 ml of water, and then stored at 4°C.

PMSF solution (200mM): It was prepared by dissolving 348.4 mg of PMSF in 10 ml of isopropanol, and it was stored at -20°C.

Solution B for nuclear protein extraction: The solution contained 50 ml of Buffer B, 250 µl of PMSF, 50 µl of DTT and one complete tablet.

Buffer B: It was prepared by dissolving 238.3 mg of HEPES, 1227.2 mg of NaCl, 5.712

mg of MgCl2, 3.722 mg of EDTA $Na_2$ $2H_2O$, in 35 ml of water. The pH was adjusted to 7.9 with NaOH, and then 12.5 ml of glycerol was added. The solution was made up to a final volume of 50 ml with $dH_2O$ and stored at 4°C.

1 M DTT stock solution: DTT (1.5424 g) was dissolved in 10 ml of water and stored at -20°C.

Solution C for whole cell lysate: It contained 50 ml of solution C, 250 µl PMSF, 62.5 µl DTT and one complete tablet.

Buffer C: It was prepared by dissolving 238.3 g of HEPES, 1227.2 mg of NaCl, 5.712 mg of $MgCl_2$, 3.722 mg of EDTA $Na_2$ $2H_2O$ in 35 ml of water. The pH was adjusted to 7.9 with NaOH. Then 0.3 g of Triton X-100 and 12.5 ml of glycerol were added. The solution was made up to 50 ml of water and stored at 4°C.

Immunoprecipitation (IP) buffer: It contained 20 mM triethanolamine-HCl, 0.7 M NaCl, 0.5% (v/v) Nonidet P-40, 4.6 mM sodium deoxycholate, 1 mM PMSF, and one complete protease inhibitor tablet. The buffer was adjusted to 7.8 with HCl.

Borate buffer: It contained 0.1 M boric acid, 0.1% (v/v) Nonidet P-40, 3.1 mM sodium azide. The pH was adjusted to8.0 with NaOH.

2 X SDS sample loading buffer: The buffer contained 2.5 ml of Tris HCl (1M, pH 6.8), 10 ml of 10% SDS, 0.00625 g of bromophenol blue, 5 ml of glycerol and 2.5 ml of beta-mercaptoethanol (14.4 M) in $dH_2O$ to a final volume of 25 ml.

1 M Tris-HCl (pH 8.8): It contained 12.114 g of Tris in 80 ml of $dH_2O$. The pH was adjusted to 8.8 with HCl. The solution was made up to 100 ml with $dH_2O$.

1.5 M Tris-HCl (6.8): It was prepared by dissolving 18.171 g of Tris in 60 ml of $dH_2O$, and pH was adjusted to 6.8 with HCl. The solution was made up to 100 ml with $dH_2O$.

10% SDS: It contained 10 g of SDS in 100 ml of $dH_2O$.

30% Acrylamide/Bis: It was prepared by mixing 29 g of acrylamide and 1 g of bis-acrylamide in 100 ml of $dH_2O$.

10% ammonium persulfate: It contained 0.1 g of ammonium persulfate in 1 ml of $dH_2O$.

1 X running buffer: The buffer contained 3.02 g of Tris-base, 18.8 g of glycine and 10 ml of 10% SDS in 990 ml of $dH_2O$.

Transfer buffer: It contained 200 ml of MeOH, 2.93 g of glycine, 5.82 g of Tris and 3.75 ml of 10% SDS in 796.25 ml of $dH_2O$.

Tris-buffered saline/Tween (TBST) buffer: It was made up of 10 mmol of Tris-HCl (pH 7.5), 150 mmol NaCl and 0.1% Tween-20.

Blocking solution (5%): The blocking solution was prepared by dissolving 0.2 g of non-fat milk in 4 ml 1X TBST.

*4.3 Procedures*

## Semi-Quantitative RT-PCR Analysis of mRNA expression

### 4.3.1 Total mRNA extraction from liver

The liver tissue (25 to 50 mg) was homogenized with 0.5 ml of Trizol reagent. The extraction of mRNA was performed as described in sections 2.3.2 to 2.3.4.

### 4.3.2 Reverse transcription of mRNA to cDNA

It was done by mixing 3 µg of RNA, 0.4 µl of oligo dT primer and autoclaved $dH_2O$ to a final volume of 14 µl. Then the solution was incubated at 70°C for 10 min.

After that, 1 µl of dNTP, 4 µl of M-MLV reaction buffer and 1 µl of M-MLV reverse transcriptase were added to the solution to make a final volume of 20 µl. The reverse transcription was carried out at 42°C for 50 min in a Perkin-Elmer GeneAmp® PCR system 9700. Samples were denatured for 15 min at 70°C and then cooled on ice.

### 4.3.3 Protocol for polymerase chain reaction (PCR)

The PCR reactions were performed in a final volume of 20 µl in a GeneAmp® PCR system 9700. Each PCR reaction contained 1 µl of cDNA (synthesized from 4.3.2), 2 µl of PCR buffer, 1.2 µl of $MgCl_2$, 1 µl of primer mix, 0.2 µl of Taq polymerase, 0.4 µl dNTP and 14.2 µl autoclaved $dH_2O$ to a final volume of 20 µl. The PCR mixture was incubated at 94°C for 5 min followed by 30 to 35 cycles of amplification. The number of cycles of each gene was determined from a series of PCR reactions with different cycle numbers. For β-actin and mdm2, each of the 30 cycles consisted of 45 sec of denaturation at 94°C, 45 sec of annealing at 55°C and 30 sec of extension at 72°C. For p53, 35 cycles were performed and each cycle consisted of 45 sec of denaturation at 94°C, 45 sec of annealing at 58°C and 90 sec of extension at 72°C. When all cycles had been completed, a final extension step of 72°C for 10 min was performed.

Table 4.3.3 Primer Sequences for RT-PCR

| Primer Name | Orientation | 5' Primer sequence 3' |
|---|---|---|
| p53-F | Forward | GTGG ATCC TGAA GACT GGAT AACT GTC |
| p53-R | Reverse | AGTC GACA GGAT GCAG AGGC TG |

| | | |
|---|---|---|
| Mdm2-F | Forward | GTCT CTGG ACTC GGAA GATT AC |
| Mdm2-R | Reverse | AAAC AATG CTGC TGGA AGTC G |
| β-actin-F | Forward | ACA CCT CAA ACC ACT CCC AG |
| β-actin-R | Reverse | AAC TCC TAA GGG GAG GAT GG |

### 4.3.4 DNA Gel Electrophoresis

The PCR products were ready for gel electrophoresis which was performed as described in section 1.3.5.

## Analysis of Protein expressions

### 4.3.5 Nuclear protein extraction

The nuclear protein extraction was performed by homogenizing 300 mg of liver tissue in 0.9 ml of solution A (buffer A and 125 µl of 200 mM PMSF stock solution) on ice. The mixture was subsequently transferred to a microcentrifuge tube and centrifuged for 30 sec at 2,000 rpm at 4°C to get rid of any unbroken tissue. After that, the supernatant was incubated for 5 min on ice and centrifuged for 5 min at 5,000 rpm at 4°C. The supernatant was discarded and the pellet was resuspended in solution B and incubated on ice for 20 min for high-salt extraction. The lysed nuclei were transferred to a new microcentrifuge tube and centrifuged at 12,000 rpm for 30 sec to pellet the cellular debris. The supernatant was transferred to another microcentrifuge tube and was stored at -20°C for the detection of p53 and mdm2.

### 4.3.6 Cytosolic protein extraction

A 300 mg of liver samples were homogenized on ice in 0.9 ml of solution C and then centrifuged at 13,000 rpm for 5 min at 4°C. The supernatant was stored at -20°C for the detection of expression of Bax, Bcl-2, p21 and PCNA.

### 4.3.7 Determination of protein concentration

The protein concentration was determined by spectrophotometry at 280 nm. After correcting the protein concentration with the dilution factor, 2 X SDS-PAGE sample loading buffer was added to adjust the protein concentration to 100 mg/ml. Samples were boiled for 5 minutes, mixed by vortexing and spinned down.

### 4.3.8 Immunoprecipitation of p53 from liver nuclear protein

For immunoprecipitation, the protein A-sepharose beads were first activated by suspending 1 g of dry beads in 4 ml of borate buffer and mixing for 1 hr. The borate buffer was centrifuged for 15 sec at 15,000 g and it was removed. The beads were resuspended in borate buffer to obtain 50% (v/v) suspension, and stored at 4 °C.

The wild type anti-p53 (Pab 246) monoclonal antibody (2 μg), $dH_2O$ (100 μl), nuclear protein (200 μg), and 2 X IP buffer (100 μl) were added to a microcentrifuge tube and incubated for 1 hr with agitation at 4°C. The goat anti-mouse IgG antibody (5 μg) was added and the solution was further incubated for another 30 min. Then, 50% protein A-sepharose beads (50 μl) were added and incubated for 30 min at 4°C with agitation. The protein A-sepharose beads were recovered by centrifugatioin (15 sec at 15,000 g) and washed with IP buffer by centrifugation (15 sec at 15, 000 g) and resuspended in 400 μl of

IP buffer. The pellet was resuspended in 30 µl of 2 X SDS-PAGE sample loading buffer and was loaded onto an SDS-PAGE gel for electrophoresis separation after boiling.

### 4.3.9 Protein gel electrophoresis by SDS-PAGE

The electrophoresis system, Mini-PROTEAN® II cell from Bio-Rad, was used for sodium dodecyl sulfate-polyacrylamide gel electrophoresis (SDS-PAGE). A gel casting mould was assembled and tested with $dH_2O$ for leakage. The resolving gel solution (10%) was set and poured into the gel casting form. The top of the gel was layered with $dH_2O$ and the gel was allowed to polymerize for about 30 min. Water was discarded and stacking gel solution (4%) was poured on top of the resolving gel. A 10-tooth comb was inserted and the gel was allowed to polymerize for another 30 min. Samples mixed with 2 X sample loading dye were boiled at 95°C for 5 min. After samples were loaded into the wells, the gel was run at constant voltage at 150 V for 1 hr in 1 X running buffer.

Table 4.3.9 Components of resolving and stacking gels in SDS-PAGE

| | **Resolving gel 10% (1 gel)** | **Stacking gel 3% (1 gel)** |
|---|---|---|
| $dH_2O$ | 3.6 ml | 2.55 ml |
| Tris | 2.25 ml (1 M, pH 8.8) | 0.48 ml (1.5 M, pH 6.8) |
| 30% Acrylamide/Bis | 2.96 ml | 0.68 ml |
| 10% SDS | 75 µl | 37.5 µl |
| 10% (w/v) AP | 75 µl | 37.5 µl |
| TEMED | 3.5 µl | 3.75 µl |

### 4.3.10 Western blotting

After SDS-PAGE was completed, the gel was removed and immersed into transfer buffer. Whatman 3 MM paper (6 pieces per gel) and PVDF membrane were cut into the same dimension as the resolving gel. Before transfer, the PVDF membrane was rinsed briefly with 100% MeOH for around 1 min and then immersed into transfer buffer. The 6 pieces of Whatman papers were also soaked into transfer buffer before use. Semi-dry Trans-Blot electroblotter (Bio-Rad) was used for the protein transfer. A gel sandwich was assembled with the PVDF membrane and the resolving gel layered between two stacks of 3 Whatman papers. Proteins were transferred to the membrane at constant voltage at 10 V for 1.5 hr.

When the transfer was completed, the sandwich was disassembled and the membrane was rinsed briefly with TBST buffer. The membrane was immersed into blocking solution with primary antibody for 16 hr at 4°C with continuous agitation. The primary antibody used was mouse monoclonal anti-p53 (1:1,000), anti-mdm2 (1:500), anti-p21 (1:500), anti-Bcl-2 (1:500), anti-Bax (1:500) and anti-β-actin (1:5,000). The unbound primary antibody was washed away with TBST for 15 min. After three washings, the membrane was immersed into secondary antibody for 1 hr at room temperature with slow agitation. The secondary antibody used was goat anti-mouse HRP labeled antibody and was diluted in 1:10,000 with blocking solution. The excess antibody was washed away with TBST three times (15 min each). ECL-Western Blotting detection reagents (0.5 ml of each reagent) were mixed together and were applied to the membrane for 3 to 5 min. After removing excess reagent, protein bands on the membrane were visualized and

recorded on a Super RX film (Fuji). Intensities of the bands were analyzed using Image J program.

## Results – *In vitro*

### Chapter 1: Effects of andrographolide on Cell Viability and Cell Cycle

The effect of andrographolide on cell cycle was investigated. Neutral red assays were performed to obtain the $IC_{50}$ of cells treated with different concentrations of AND for 24, 48 and 72 hrs. Treatment of HepG2, the human liver cancer cells, with different concentrations of AND (0 to 100 μM) showed that AND could inhibit cell viability by 50% with concentrations 17.5, 16 and 17 μM with respect to 24, 48 and 72 hrs of incubation (Fig. 1.1). The effect of AND on normal liver cells was also investigated. WRL 68, the human normal liver cell line, was found to be inhibited by 50% with 57, 30 and 35 μM of AND incubated for 24, 48 and 72 hrs respectively (Fig. 1.2). The $IC_{50}$ for Clone 9, the rat normal liver cells, was 22 at 24 hrs, 18 at 48 hrs and 18 μM at 72 hrs of incubation (Fig. 1.3). The $IC_{50}$ determined for HepG2 cells for all three time periods were significantly lower than those determined for WRL 68 cells ($P < 0.05$).

Flow cytometry was performed to study the cell cycle of HepG2 upon treatment of AND. The DNA profiles of HepG2 cells treated with 1% DMSO as the control and 20 and 25 μM AND for 24 hrs were shown in Fig. 1.4. The number of cells counted was 10,000 and the population of cells suspended in each phase of the cell cycle was shown in percentage (Fig. 1.5). Upon treatment of AND, more cells were suspended in sub $G_1$ phase than those treated with DMSO only. There were no significant changes in the population of cells suspended in $G_0/G_1$, S and $G_2/M$ phases between AND-treated cells and control cells ($P > 0.05$). The DNA profiles obtained from PI staining of HepG2 cells treated with 1% DMSO and 12.5 and 25 μM of AND for 48 hrs were shown in Fig. 1.6.

Treatment of AND significantly induced the accumulation of cells in the sub $G_1$ and $G_0/G_1$ phases of the cell cycle when compared with the control cells (Fig. 1.7). The populations of cells suspended in S and $G_2/M$ phases were also significantly decreased when compared with those in the control group ($P < 0.05$). The results suggest that AND-treated cells were unable to progress from the $G_0/G_1$ phase to the S phase. They arrested cell cycle progression in the $G_0/G_1$ phase, causing cell death through apoptosis.

A hallmark feature of apoptosis was the observation that nuclear DNA extracted from apoptotic cells was often degraded (86). Therefore, to further confirm the mechanism through which AND caused cell death, DNA was extracted from HepG2 cells treated with 12.5, 20, 25 and 50 μM AND for 72 hrs. DNA was analyzed using agarose gel electrophoresis and fragmentation at around 200 bp was detected in cells treated with 50 μM of AND (Fig. 1.8). Therefore, it demonstrated that AND caused cell death through apoptosis.

**Figure 1.1 Cell viability of HepG2 treated with AND for 24, 48 & 72 hrs.**

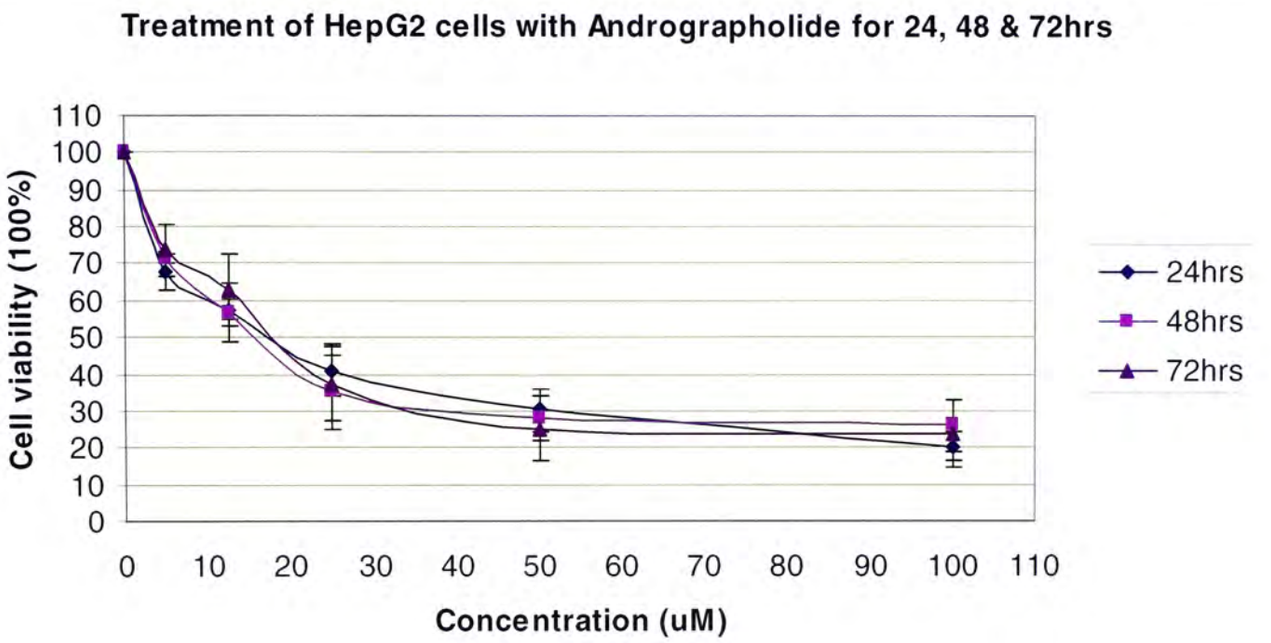


| Time (hrs) | 24 | 48 | 72 |
|---|---|---|---|
| $IC_{50}$ (μM) | 17.5 | 16 | 17 |

**Figure 1.1** HepG2 cells treated with different concentrations of AND were incubated for 24, 48 and 72 hrs. Neutral red assays were performed and absorbance was read at OD 540 nm. $IC_{50}$, the concentration of AND that reduced the cell viability by 50%, was recorded at different incubation time periods.

**Figure 1.2 Cell viability of WRL 68 treated with AND for 24, 48 & 72 hrs.**

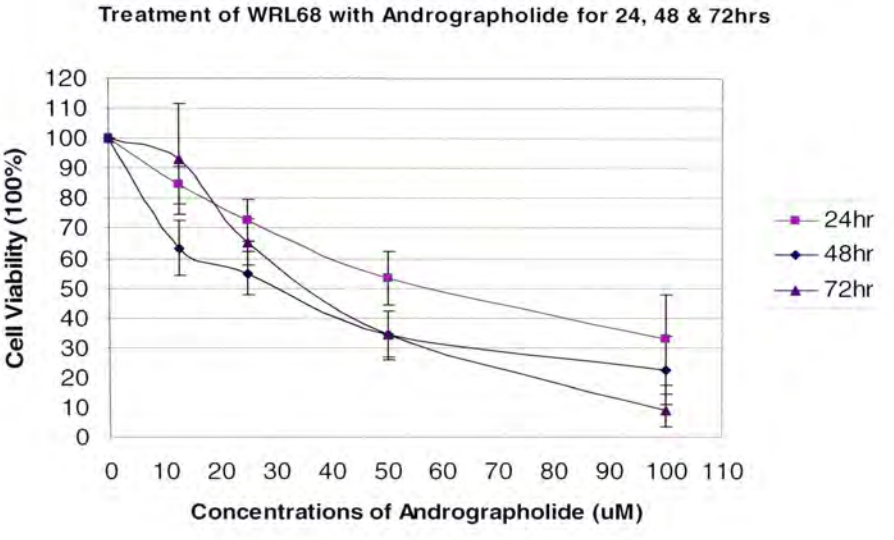


| Time (hrs) | 24 | 48 | 72 |
|---|---|---|---|
| $IC_{50}$ (μM) | 57 | 30 | 35 |

**Figure 1.2** The same treatments as shown in Fig. 1.1 were performed with WRL 68, the human normal liver embryo cells. Neutral red assays were performed and $IC_{50}$ was determined for each incubation time period.

**Figure 1.3 Cell viability of Clone 9 treated with AND for 24, 48 & 72 hrs.**

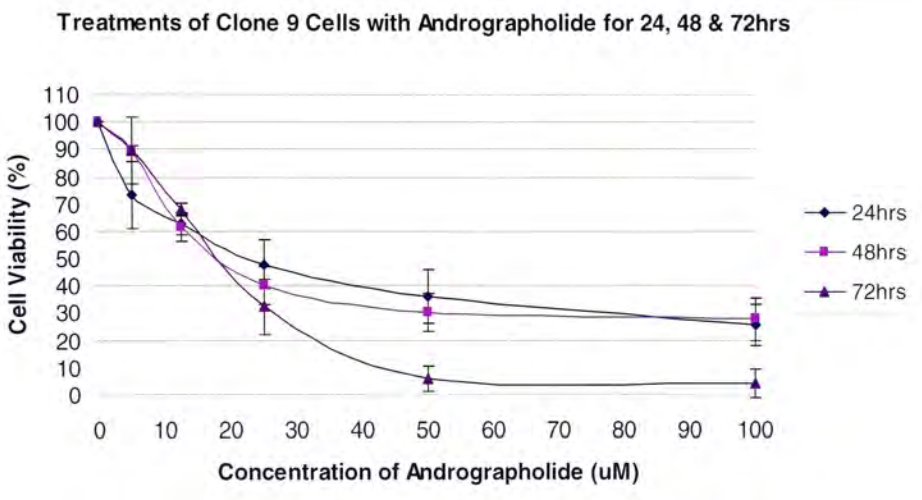


| Time (hrs) | 24 | 48 | 72 |
|---|---|---|---|
| $IC_{50}$ (μM) | 22 | 18 | 18 |

**Figure 1.3** Similar treatments were performed with Clone 9, the rat normal liver cells. Neutral red assays were performed and $IC_{50}$ was recorded for each incubation time period.

**Figure 1.4 DNA profiles of HepG2 cells treated with DMSO and AND for 24 hrs**

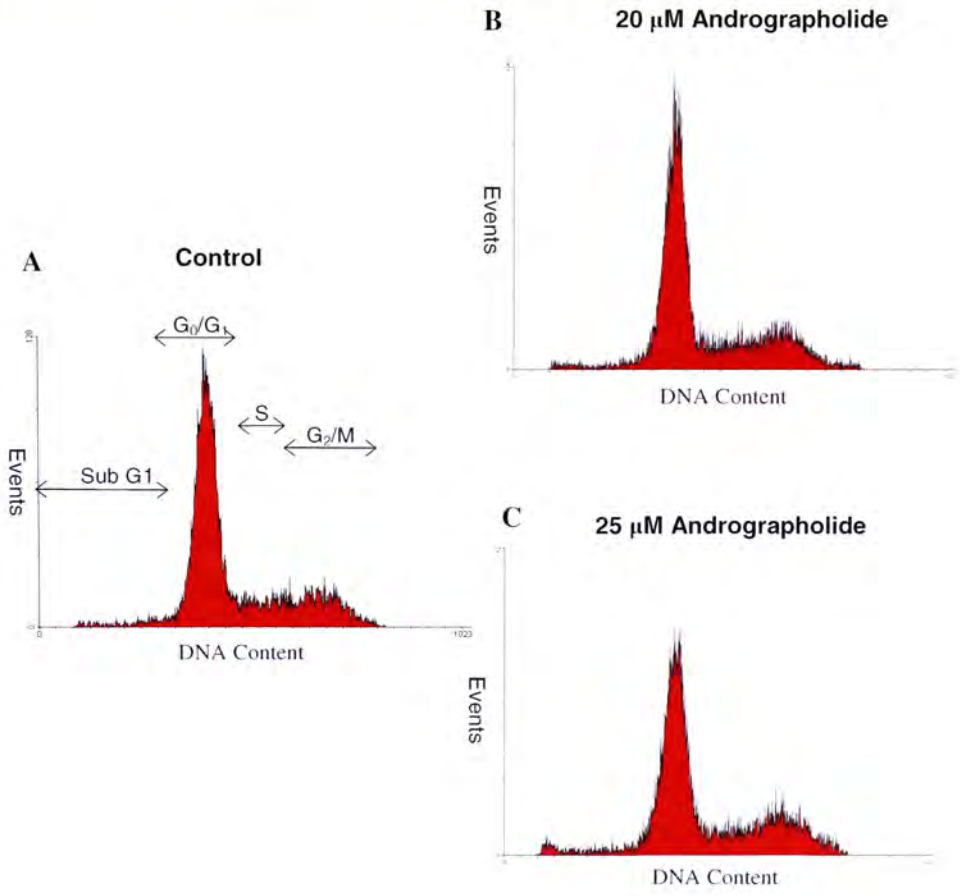


**Figure 1.4** DNA profiles of HepG2 cells treated with DMSO and AND for 24 hrs. HepG2 cells incubated with A) 1% DMSO, B) 20 μM and C) 25 μM of AND for 24 hrs were stained with PI. The DNA profiles were obtained using FACScan flow cytometer and analyzed using FCS Express (V2) software. The area of the profile (in red) represents the total number of cells counted.

**Figure 1.5 Analysis of the cell cycle upon treatment of HepG2 with DMSO and AND for 24 hrs**

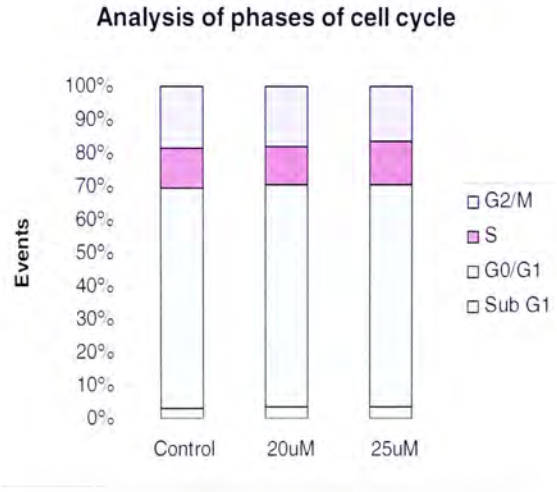


| Sample | Sub $G_1$ | $G_0/G_1$ | S | $G_2/M$ |
|---|---|---|---|---|
| Control | 2.9% ± 0.3 | 66.7% ± 1.7 | 12.3% ± 1.5 | 18.4% ± 1.4 |
| 20 μM | 3.3% ± 0.4 | 67.4% ± 1.3 | 11.3% ± 0.8 | 18.3% ± 1.1 |
| 25 μM | 3.4% ± 0.2 | 66.3% ± 1.6 | 14.0% ± 0.6 | 16.7% ± 1.0 |

**Figure 1.5** After PI staining, 10,000 HepG2 cells were counted on FACScan flow cytometer and the number of cells suspended in each phase of the cell cycle (sub $G_1$, $G_0/G_1$, S and $G_2/M$) was represented in percentage. The data represent mean ± SD ($n = 2$).

**Figure 1.6 DNA profiles of HepG2 cells treated with DMSO and AND for 48 hrs**

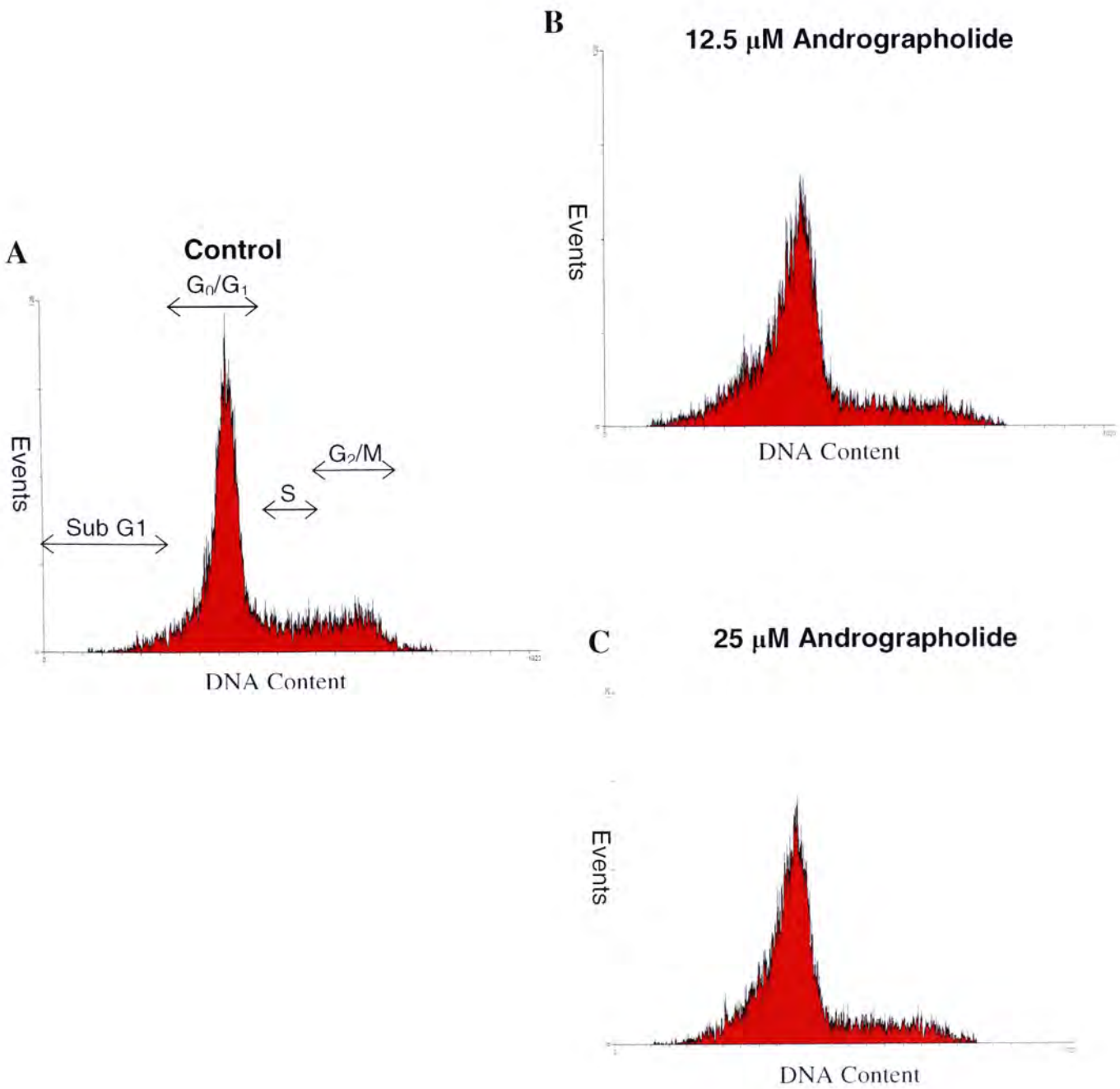


**Figure 1.6** After PI staining, the DNA profiles of HepG2 cells incubated with A) 1% DMSO, B) 12.5 μM and C) 25 μM of AND for 48 hrs were obtained using FACScan flow cytometer and analyzed using FCS Express (V2) software.

**Figure 1.7 Analysis of the cell cycle upon treatment of HepG2 with DMSO and AND for 48 hrs**

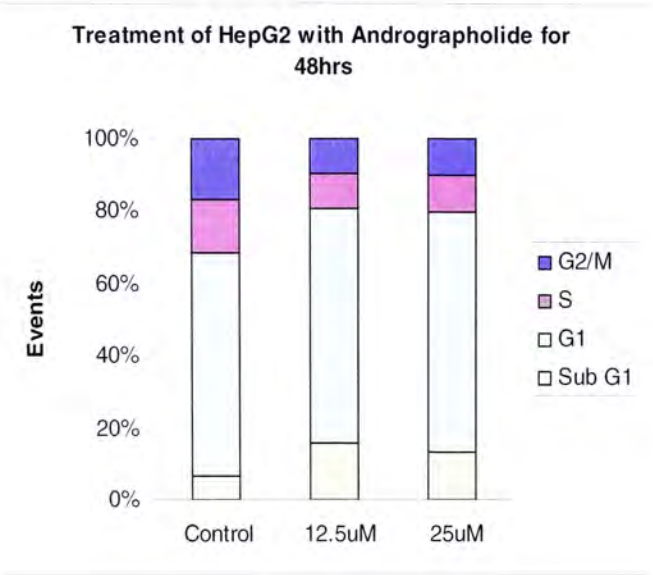


| Sample | Sub $G_1$ | $G_0/G_1$ | S | $G_2/M$ |
|---|---|---|---|---|
| Control | 6.1% ± 0.5 | 62.1% ± 0.8 | 15.1% ± 0.8 | 16.7% ± 1.5 |
| 12.5 μM | 14.5% ± 0.8 | 65.4% ± 0.6 | 9.7% ± 0.5 | 9.8% ± 1.1 |
| 25 μM | 13.1% ± 0.6 | 67.1% ± 0.8 | 9.7% ± 0.7 | 10.4% ± 0.7 |

**Figure 1.7** Analysis of cell cycle upon treatment of DMSO and AND for 48 hrs. HepG2 cells (10,000) were counted on FACScan flow cytometer after PI staining. The number of cells suspended in sub $G_1$, $G_0/G_1$, S and $G_2/M$ was recorded and represented in percentage. All data are expressed as mean ± SD ($n = 2$). Significance was found between control and the cells treated with 12.5 or 25 μM AND in all phases of cell cycle ($p < 0.05$).

**Figure 1.8 Fragmentation of DNA in HepG2 cells after AND treatment**

| Lane | |
|---|---|
| 1 | DNA marker |
| 2 | Control (DMSO) |
| 3 | 12.5 μM |
| 4 | 20 μM |
| 5 | 25 μM |
| 6 | 50 μM |

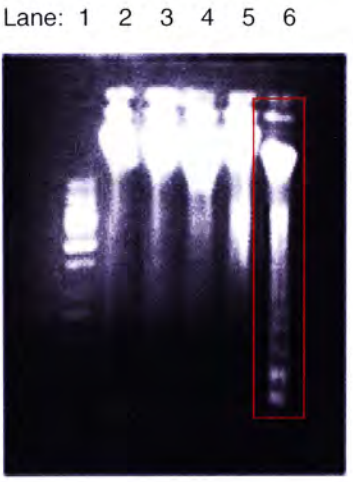


**Figure 1.8** At 72 hrs after treatment of HepG2 cells with DMSO or 12.5, 20, 25 and 50 μM of AND, DNA was extracted. Fragmented DNA was observed in cells incubated with 50 μM of AND.

## Chapter 2: Effects of Andrographolide on gene expressions

In an attempt to evaluate the toxicological aspect of AND, cDNA microarray analysis associated with human toxicology and drug metabolism was performed. This microarray generated the expression profiles of 263 genes related to the metabolic processes of cell stress, cell toxicity, drug resistance, and drug metabolism.

A scatter plot was generated from the arrays of the control and AND-treated groups (Fig. 2.1). The up-regulated genes included those whose expression level is critical in drug metabolism such as NAD(P)H dehydrogenase quinone 1 (NQO1), superoxide dismutase 1 (SOD1), thymidylate synthetase (TYMS) and xanthine dehydrogenase (XDH). Other up-regulated genes also included those that are involved in cell cycle regulation such as RB1.

The down-regulated genes included a number of apoptotic and cell cycle regulators such as BCL2, BCL2L2, and CHEK2. Many genes whose expression level is important to drug metabolism such as CYP 2D6 and CYP 2A6 were also down-regulated. Some genes related to cell growth, proliferation and differentiation were under-expressed. They included IL1B and NFKB2 (Fig. 2.2).

**Figure 2.1 The scatter plot of gene expressions from HepG2 cells treated with DMSO and AND**

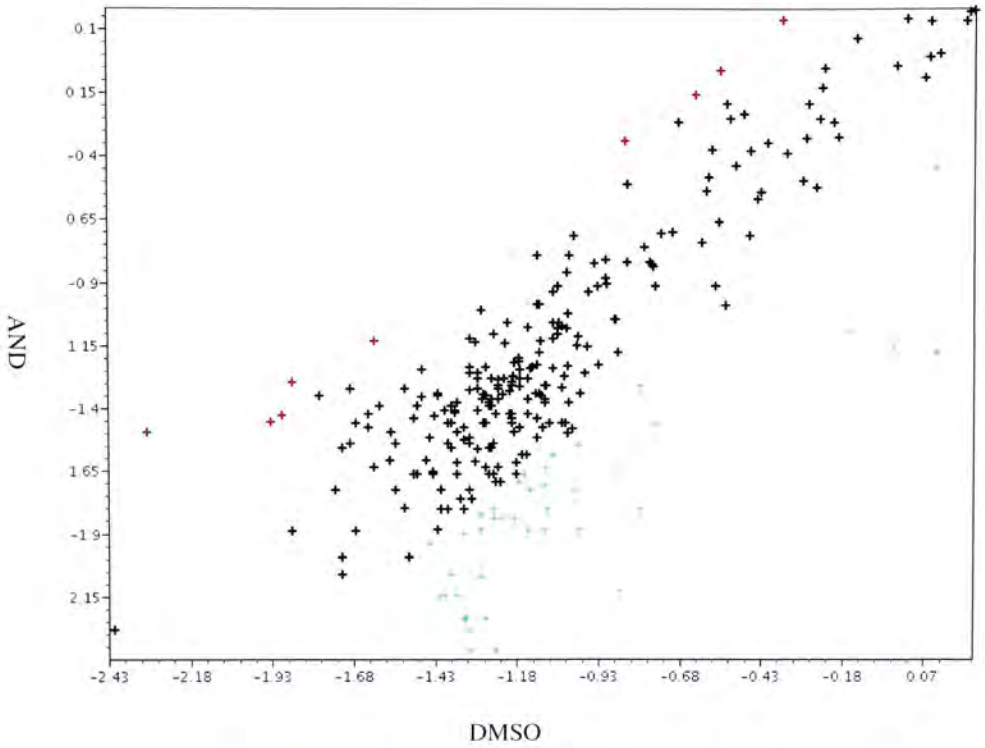


**Figure 2.1** The scatter plot of gene expressions of HepG2 cells treated with DMSO and AND. Each symbol represented one gene. The center line indicates no changes in gene expression. Parallel lines represent the boundary which was set to be 3. The black symbols indicate the genes of which expression changes were less than the boundary. Red symbols indicate an increase in gene expression from X axis to Y axis greater than the boundary. Green symbols indicate a decrease in gene expression from X axis to Y axis greater than the boundary.

**Figure 2.2 cDNA microarray analysis**

A

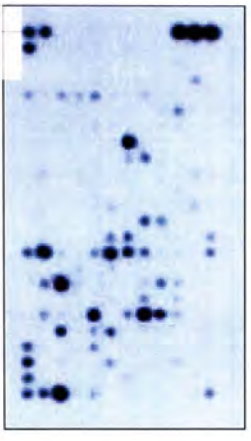

B

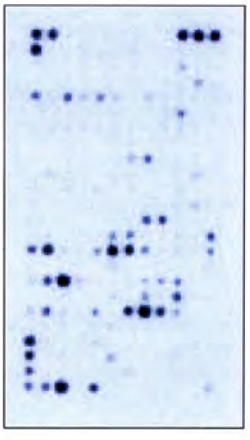

C

| Symbol | Gene name | Fold changes |
|---|---|---|
| BCL2 | Bcl-2 | -4.9 |
| BCL2L2 | Bcl-w | -3.2 |
| CCND1 | Cyclin D1 | -3.6 |
| CHEK2 | CHK2 | -4.3 |
| MDM2 | Mdm2 | -3.4 |
| NF-κB2 | NF-κB2 | -3.1 |
| RB1 | Rb | +3.2 |
| SOD1 | Cu/ZnSOD | +3.1 |

**Figure 2.2** cDNA microaray analysis of A) DMSO control and B) AND-treated cells. C) Upon treatment of 16 μM of AND for 48 hrs, six genes were up-regulated 3-folds or more than the control; forty-two genes were down-regulated 3-folds or more and some of them were listed above.

## Results – *In vivo*

### Chapter 3: Effects of Andrographolide on hepatocarcinogenesis in rats

In this part of the experiment, the promotion and progression stages of hepatocarcinogenesis were investigated. The combined effects of DEN and $CCl_4$ was observed after 5 months of treatment. Gross examination of the liver showed that the liver had expanded from the right to the left side of the rat's abdomen (Fig. 3.1A). A closer look of the liver showed that there had been a change in morphology and nodules were observed across the liver surface (Fig. 3.1B). In the promotion experiment, the livers of the negative control group generally had a smooth surface and neither nodules nor lipids could be observed on the surface. On the other hand, the positive control livers had a thickened border and the surface was rough with lipid droplets distributing throughout the whole surface. The AND-treated livers had a smooth surface and generally resembled the negative control livers (Fig. 3.2). In the progression experiment, no abnormal appearance of the rat liver was found in negative control group. However, it was observed that rat livers were hardened and nodules or lumps were present in positive control group. There were also some nodules present on the surface of the AND-treated livers, but the structure of the livers generally resembled that of the normal livers (Fig. 3.3).

The relative liver weights of rats from the negative, positive and AND-treated groups in both experiments were compared (Fig. 3.4). There was a significant increase in the relative liver weights in positive control groups as compared with those of rats in negative control groups. A significant reduction in the relative liver weights was found in the AND-treated groups in both experiments. No significant difference was observed in

AND-treated groups when compared with negative control groups in both experiments (Fig. 3.4).

Serum AST and ALT activities were measured to assess liver damage. The percentage changes of serum AST and ALT levels relative to negative control were summarized in Fig. 3.5. In both experiments, values for serum AST and ALT levels in rats of positive control group were elevated as compared with those in negative control group. There was a significant reduction in AST and ALT levels in rats that had treated with AND (Fig. 3.5A for promotion experiment, $p < 0.01$; Fig. 3.5B for progression experiment, $p < 0.05$). These data suggest that AND is effective in decreasing serum AST and ALT levels.

Histological examination of livers from rats in the promotion stage of hepatocarcinogenesis was carried out through Hematoxylin & Eosin (H & E) staining. The nuclei of hepatocytes were stained blue due to the color of hematoxylin and the cytoplasm was stained red due to eosin. The liver section of a negative control rat had a typical histological structure with a characteristic pattern of hexagonal lobules. The central vein was clearly observed and hepatocytes surrounding the central vein were arranged in columns, radiating from it (Fig. 3.6A, B). It was shown that after treatment of carcinogens, normal hepatocyte alignment was disrupted and cytoplasmic vacuolization within hepatocytes could be observed (Fig. 3.6C). The conditions were improved in those livers obtained from AND-treated rats. Liver structure was restored and hepatocyte arrangement was not as distorted as that of the positive control sections. Vacuolization was reduced and distinct cytoplasm was visible (Fig. 3.6D). In the progression experiment, the structural appearance of the negative control section was similar to that in the

promotion group (Fig. 3.7A). The liver section of the rat treated with AND also showed normal alignment of hepatocytes around central vein (Fig. 3.7B). The positive control sections, on the other hand, showed that hepatocytes were arranged randomly across the whole section and distinct cytoplasm could not be observed (Fig. 3.7C, D).

Immunohistochemical staining of GST-P foci was performed to detect the presence of neoplastic cells. Negative control rats in the promotion stages of hepatocarcinogenesis did not develop any GST-P positive liver foci (Fig. 3.8A, B). In carcinogen treated groups, GST-P foci were detected (Fig. 3.8C, D). The expression of GST-P was found in clusters or groups and they could be found across the whole liver section. In the AND-treated liver section, the expression of GST-P was present but the affected area was reduced (Fig. 3.8E, F). In the progression group, GST-P foci could not be detected in the normal rat liver sections (Fig. 3.9A). The rats in the positive control groups showed clusters of GST-P foci (Fig. 3.9B). A closer look at these sections showed cytoplasmic vacuolization and abnormal alignment of hepatocytes (Fig. 3.9C). In some areas of the positive control section where expression of GST-P was not detected, hepatocytes were aligned randomly and no distinct cytoplasm was present (Fig. 3.9D). The AND-treated liver sections were similar to the negative control sections with distinct central vein and normal hepatocyte appearance (Fig. 3.9E, F).

**Figure 3.1 Effects of diethylnitrosamine (DEN) and carbon tetrachloride ($CCl_4$) on rat liver**

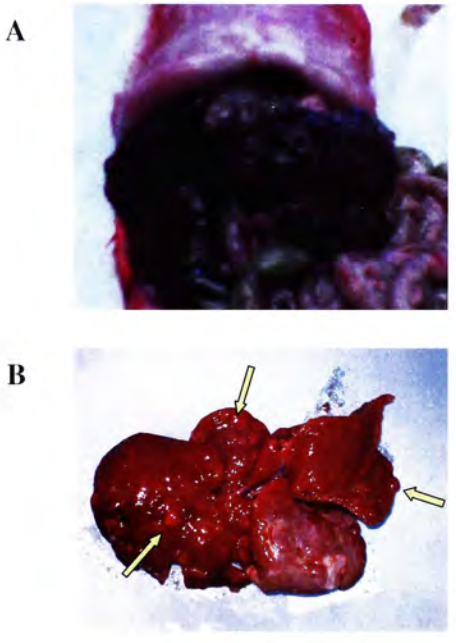


**Figure 3.1** A) The rat was treated with DEN & $CCl_4$ once a week for about 5 months; B) The rat's liver was removed and many nodules as indicated by the arrows was observed across the surface of the liver.

**Figure 3.2 Gross examination of rat livers in the promotion stage of hepatocarcinogenesis**

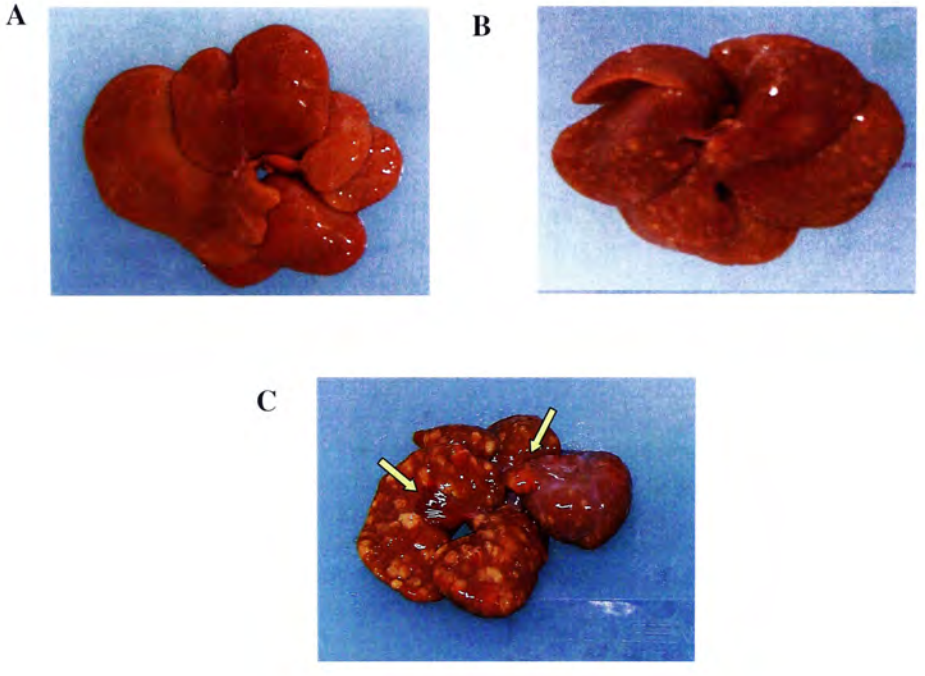


**Figure 3.2** After 28 weeks, rats were killed and their livers were perfused, removed & weighed. Liver removed from A) a normal control rat; B) AND-treated rat and C) positive control rat. Nodules or lumps as indicated by the arrows could be seen across the surface of the positive control liver.

**Figure 3.3 Gross examination of rat livers in the progression stage of hepatocarcinogenesis**

A

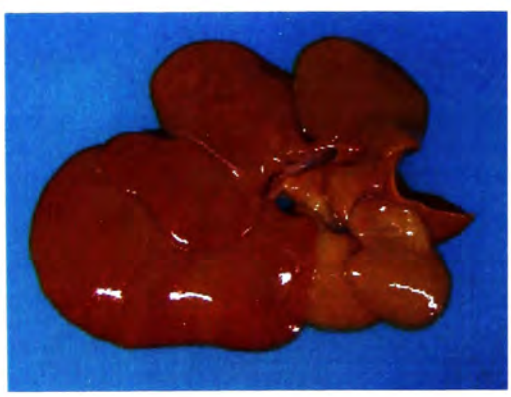

B

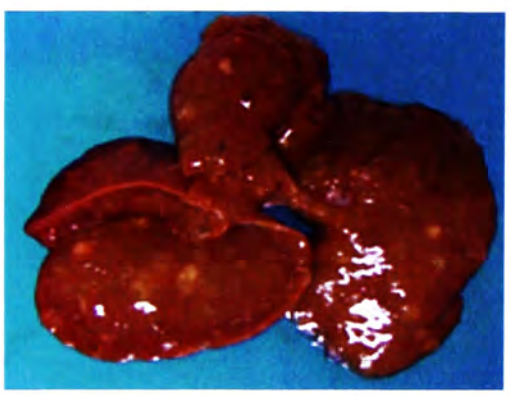

C

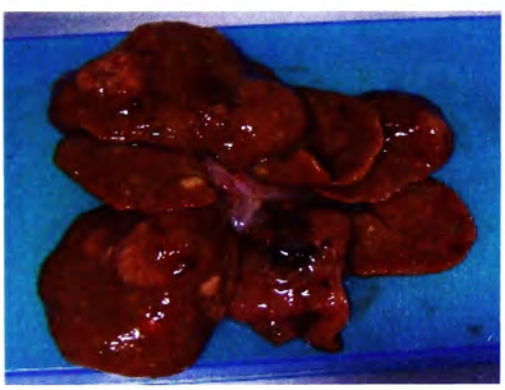

**Figure 3.3** At the end of 56$^{th}$ week, rats were killed and their livers were examined. A) Negative control liver; B) AND-treated liver and C) positive control liver.

**Figure 3.4 Effects of AND on the liver weight of rats in promotion and progression groups**

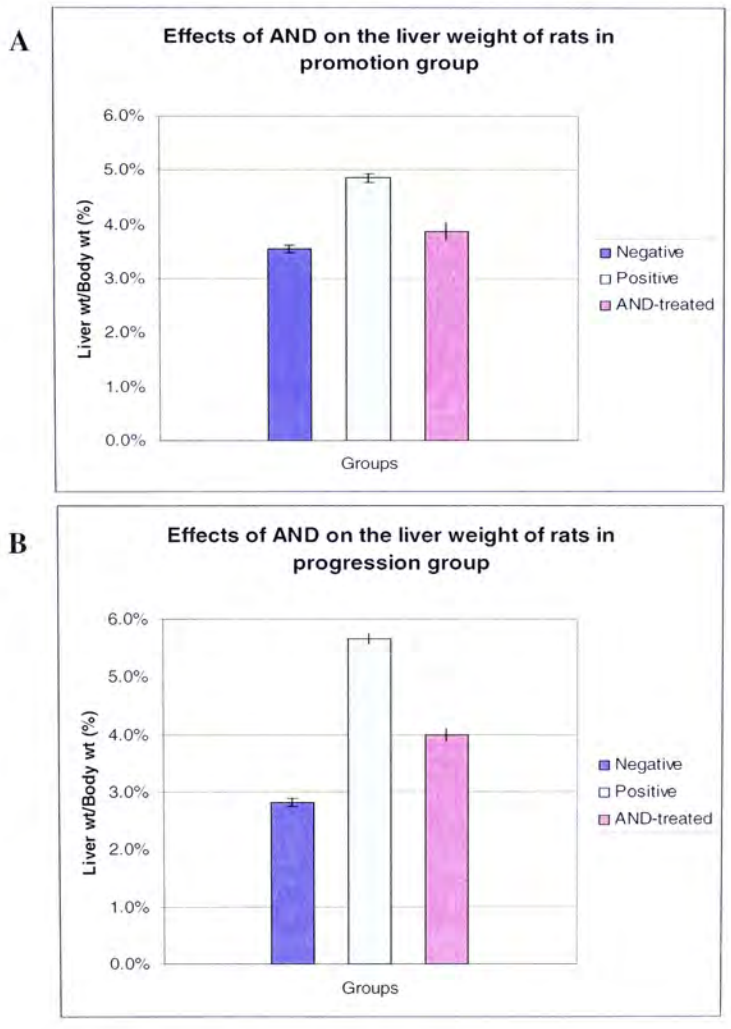


**Figure 3.4** The relative liver weight was expressed as percentage (liver weight/ body weight). The data represent the mean of 5 rats. There was a significant difference between positive control and the AND-treated groups in both the promotion and progression ($P < 0.05$).

**Figure 3.5 AST and ALT assays for the promotion and progression groups of rats**

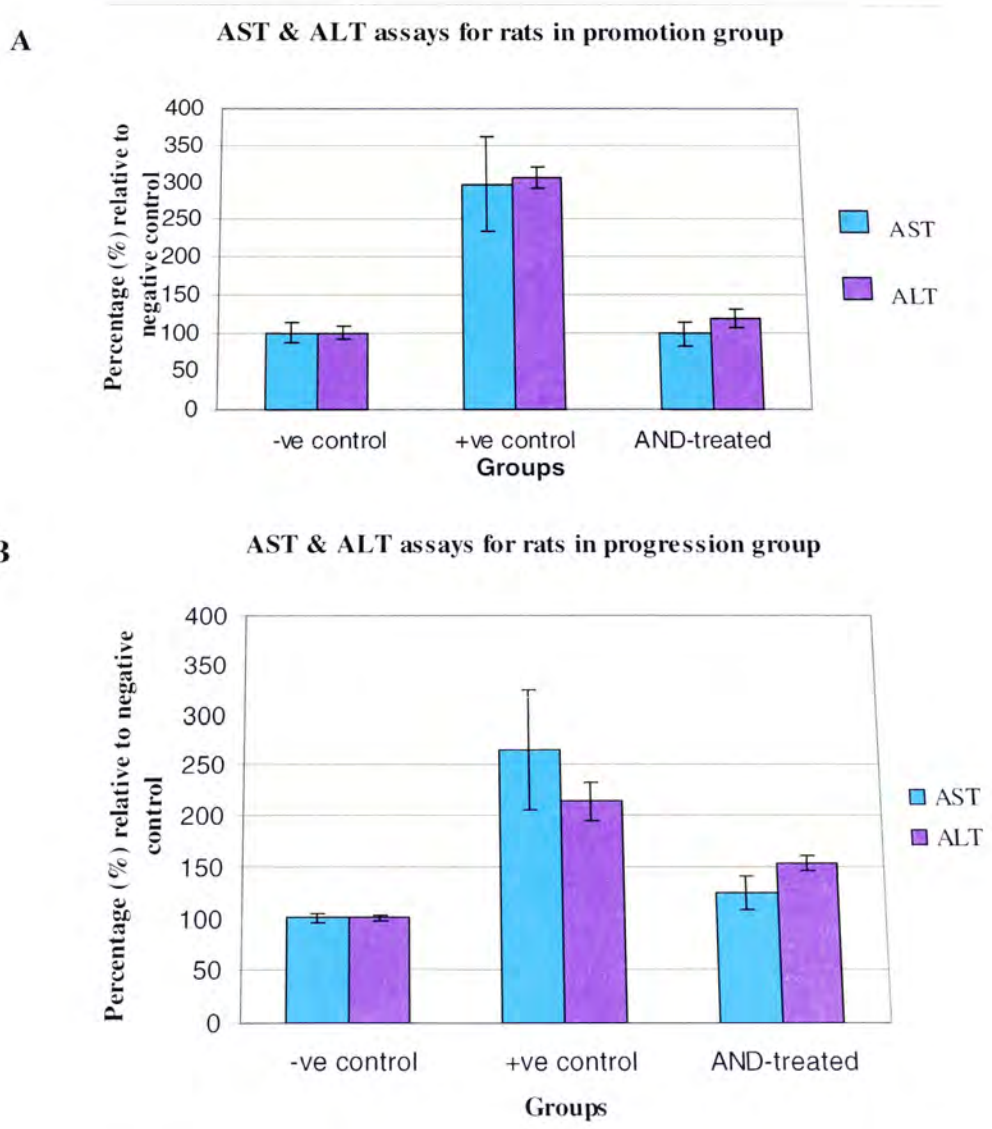


**Figure 3.5** AST and ALT assays for the A) promotion and B) progression groups of rats. The amount of AST and ALT in blood serum was measured and represent the percentage compared with the negative control. Significance was found between the positive control and AND-treated rats in both the promotion and progression groups ($P < 0.05$).

**Figure 3.6 Hematoxylin & Eosin (H&E) staining of rat livers in the promotion stage of hepatocarcinogenesis**

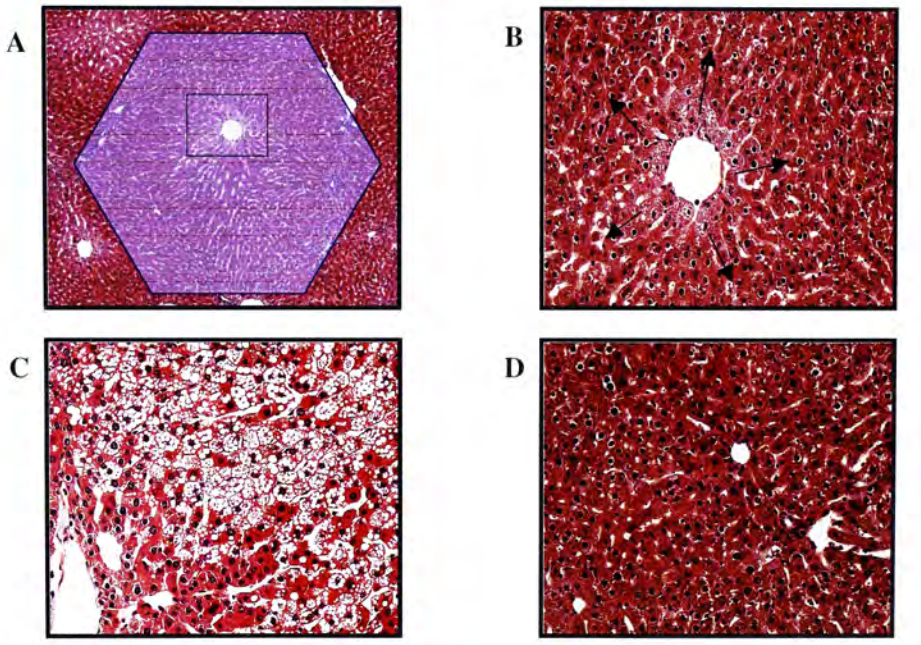


**Figure 3.6** The nuclei of the hepatocytes were stained blue and the cytoplasm was stained red. A) The liver section (10X) of a negative control rat. B) Magnification of the square area in section A (20X). C) Positive control liver sections (20X) and D) AND-treated liver section (20X).

**Figure 3.7 Hematoxylin & Eosin (H&E) staining of rat livers in the progression stage of hepatocarcinogenesis**

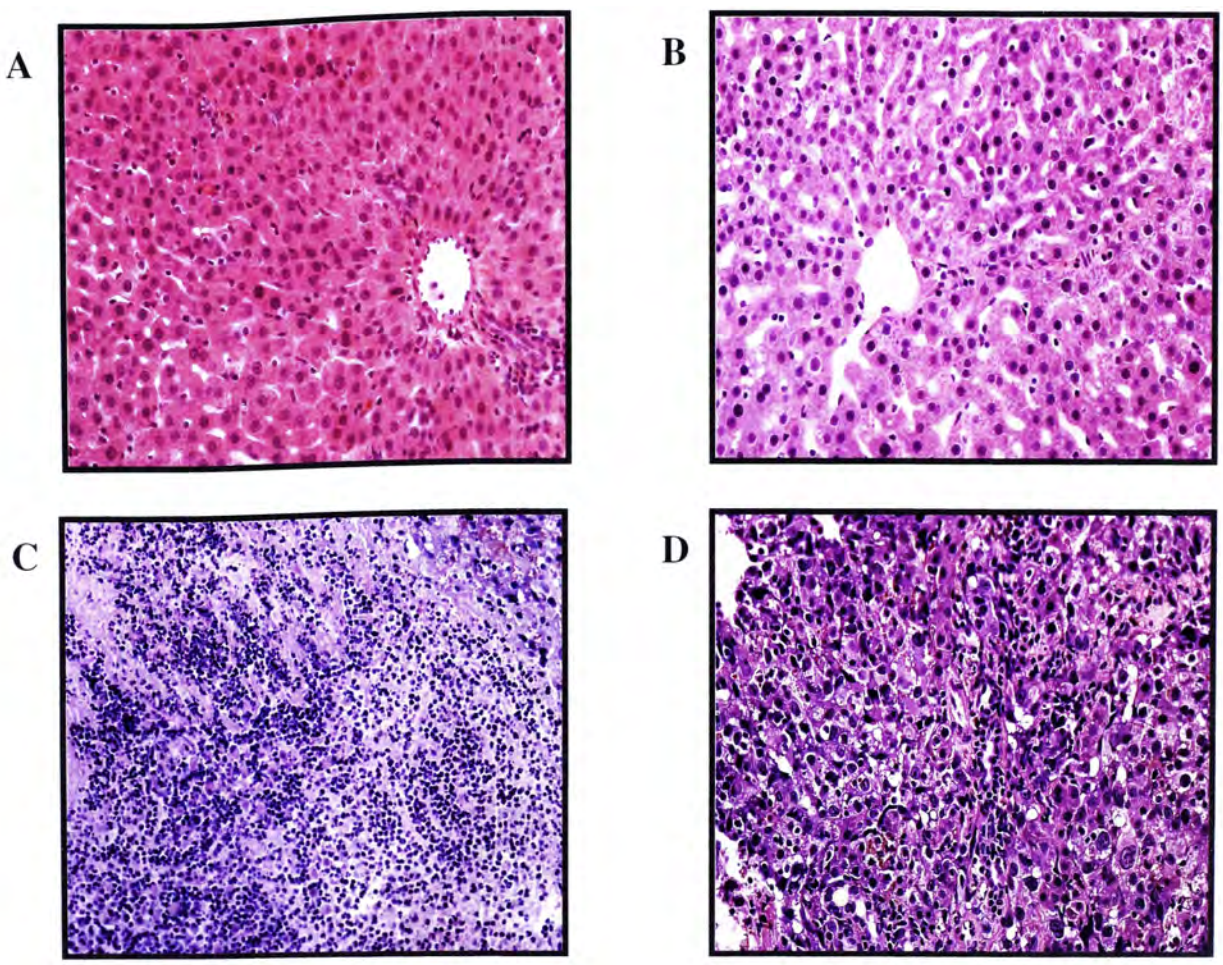


**Figure 3.7** A) The liver section of a negative control rat (20X). B) The liver section of a rat treated with AND (20X). C) Positive control sections with no distinct cytoplasm (10X) and D) hepatocytes were arranged randomly across the whole section (20X).

**Figure 3.8 Immunostaining of GST-P of rat liver sections in the promotion group**

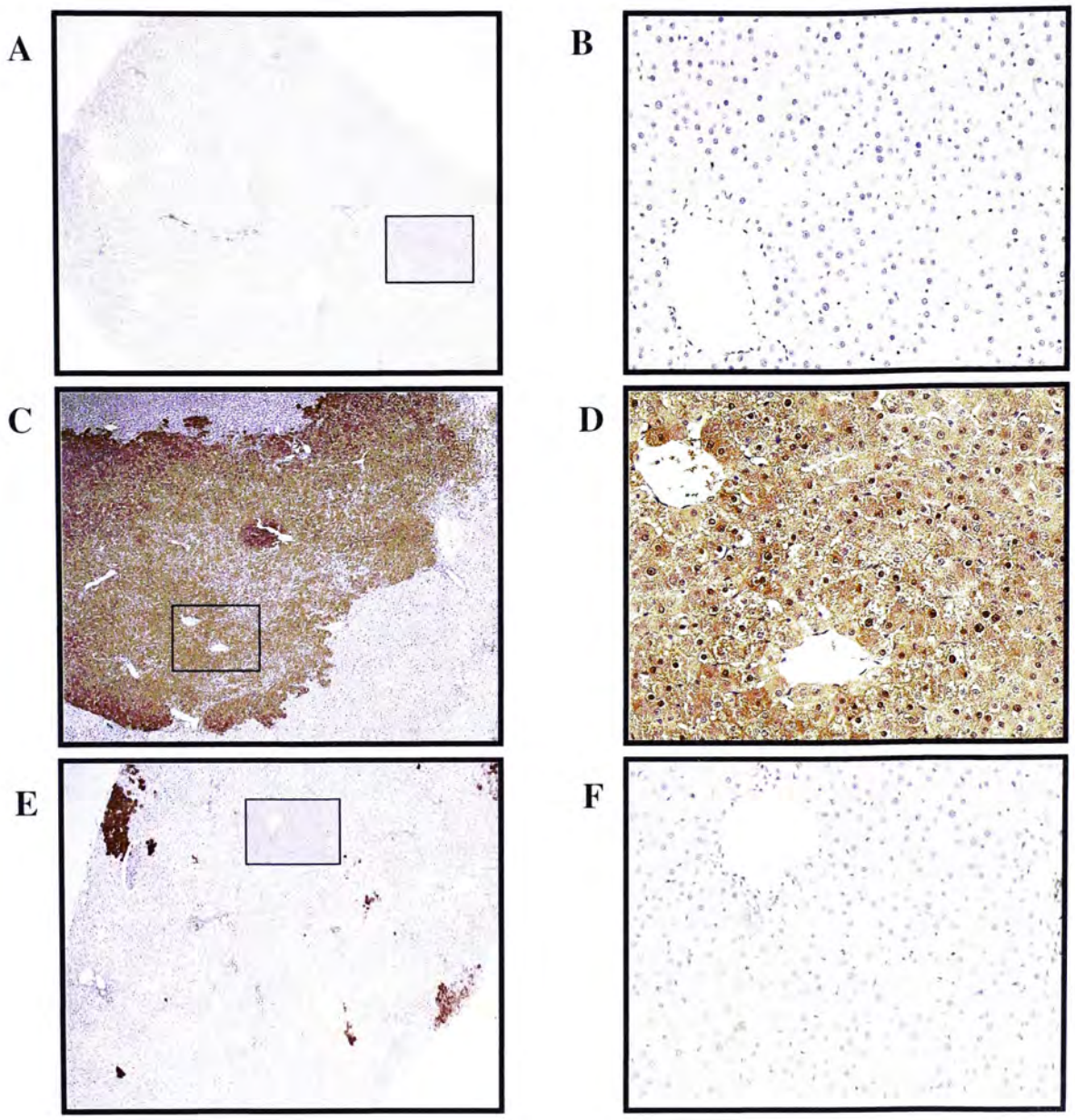


**Figure 3.8** The nuclei of the hepatocytes were stained blue and the areas with GST-P expression were stained brown. A) Negative control section showed no expression of GST-P (10X). B) Magnification of the section in A (20X). C) Liver section from a positive control rat (10X). D) Magnification of the section in C (20X). E) Liver section obtained from AND-treated liver (10X) and F) the magnified area from section E (20X).

**Figure 3.9 Immunostaining of GST-P of rat liver sections in the progression group**

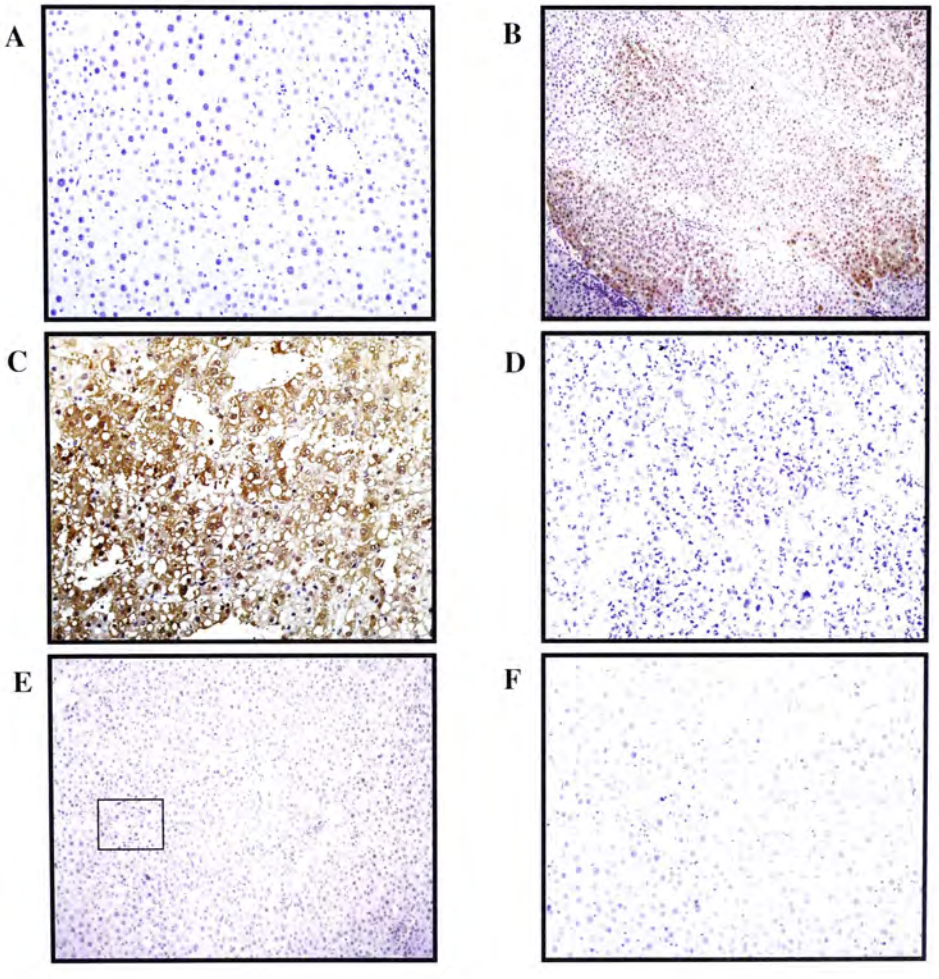


**Figure 3.9** A) The negative control sections with distinct central vein (20X). B) Positive control section showed expressions of GST-P in groups (10X). C) Positive control section showed the appearance of hepatocytes (20X). D) Positive control section with no GST-P expression (20X). E) The AND-treated liver sections (10X). F) The magnified area in section E (20X).

## Chapter 4. Effects of Andrographolide on the expressions of Mdm2, p53, PCNA, Bax, Bcl-2 and p21

To study the effect of AND on the inhibition of hepatocarcinogenesis in both the promotion and progression stages, Western blot of PCNA, a marker of cell proliferation was done (Fig. 4.1). The level of PCNA expression in DEN-$CCl_4$ treated rat was found to be significantly higher than that in the negative control and AND-treated groups in the progression experiment. However, there was no significant difference in the levels of PCNA expression in the AND-treated and positive control groups in the promotion experiment.

To determine the effect of AND on cells associated with apoptosis, the protein expressions of Bax and Bcl-2 were investigated by Western blot analysis (Fig. 4.3). In both experiments, the levels of Bax protein expressed in the liver of rats which received carcinogens were significantly lower than those rats which received vehicle or AND treatment. The levels of Bcl-2 in the liver of carcinogen-treated rats in the positive control groups were higher than that in the control or AND-treated groups. These data suggest that AND had triggered a reduction of Bax expression but an increase in Bcl-2 expression.

The effects of AND on cell cycle regulation were investigated through the Western blot analysis of p21 (Waf1/Cip1/Sdi1), which functions at major transition points in the cell cycle. In both the promotion and progression experiments, the levels of p21 (Waf1/Cip1/Sdi1) in carcinogen-treated groups were lower than those in the negative control and AND-treated groups. However, no significant difference could be observed among the three groups (Fig. 4.4).

The total p53 protein (wild type and mutant) expressions in rat liver nuclei were measured (Fig. 4.5). When compared with the negative control groups, higher levels of total p53 protein expression were found in rats treated with DEN-CCl4 alone in the positive control groups and the AND-treated groups in both the promotion and progression experiments. However, no significant difference was observed among these groups. The wild type p53 functions in cell cycle arrest and in triggering the apoptotic event. The changes in the wild type p53 protein expression were determined through immunoprecipitation and western blot analysis (Fig. 4.6). In the promotion experiment, the level of wild type p53 protein expression was lower than that in the AND-treated and control rats. However, no significant difference was observed in these groups. In the progression experiment, nuclear wild type p53 was significantly reduced in the positive control group as compared to those in the negative or AND-treated groups. The results showed that administration of AND significantly increased the expression of wild type p53 compared with the positive control.

The protein expression of p53 was regulated by Mdm2. In both experiments, there was a significant overexpression of Mdm2 in DEN-$CCl_4$ treatment in positive control groups as compared with those that received the vehicle treatment. A significant decrease in the levels of Mdm2 was observed in AND-treated groups as compared with the positive control groups (Fig. 4.7). The findings suggest that treatment with AND significantly reduced the protein expression of Mdm2.

The effects of AND on the inhibition of hepatocarcinogenesis were further investigated at the transcriptional level of total *p53* and *Mdm2*. The transcripts encoding the mRNA of *p53* and *Mdm2* were normalized with the corresponding *β- actin* mRNA

transcripts and changes in the transcriptional level were expressed in ratio as shown in Fig. 4.7 and Fig. 4.8. In both experiments, it was observed that the mRNA expression of *p53* was low in the vehicle control groups. The treatment of DEN-$CCl_4$ significantly increased the mRNA transcripts of *p53*. Upon treatment of AND, there was a significant reduction in the total *p53* transcription expression which was brought about by the carcinogens. The mRNA expression of *Mdm2* was also low in the vehicle-treated rats as shown in Fig. 4.9. There was a considerate over-expression of *Mdm2* mRNA in carcinogen-treated positive control groups in both experiments. However, the expression of *Mdm2* mRNA was significantly reduced in AND-treated groups when compared with that in the positive control groups.

**Figure 4.1 Western blot analysis of PCNA protein**

A

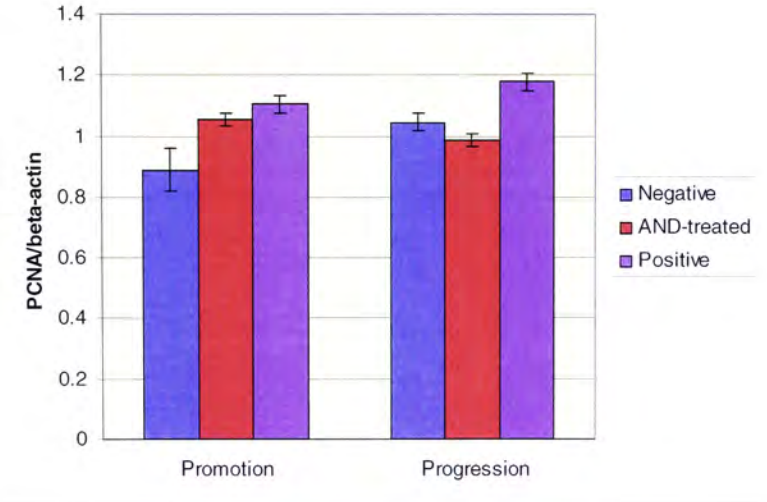


B


**Figure 4.1** The cytosolic proteins in the rat liver were separated by 10% SDS-PAGE and transferred onto PVDF membrane. A) PCNA was detected and expressed in PCNA : β-actin ratio. Significance was found between the AND-treated and positive control groups in the progression experiment ($p < 0.05$). All data were expressed as mean ± SD ($n = 5$). B) PCNA expression. β-actin was the internal standard.

## Figure 4.2 Western blot analysis of Bax protein

A

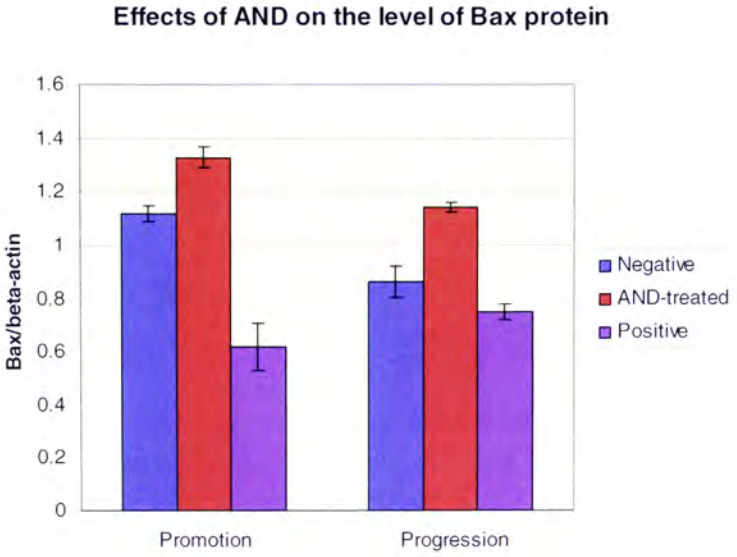


B


**Figure 4.2** The cytosolic protein, Bax, in the rat liver was separated by 10% SDS-PAGE and transferred onto PVDF membrane. It was detected with mouse antibodies against Bax followed by goat anti-mouse-HRP visualization. A) Bax was expressed in Bax : β-actin ratio. Significance was found between the AND-treated and positive control groups in both experiments ($p < 0.05$). All data were expressed as mean ± SD ($n = 5$). B) Bax expression. β-actin was the internal standard.

**Figure 4.3 Western blot analysis of Bcl-2 protein**

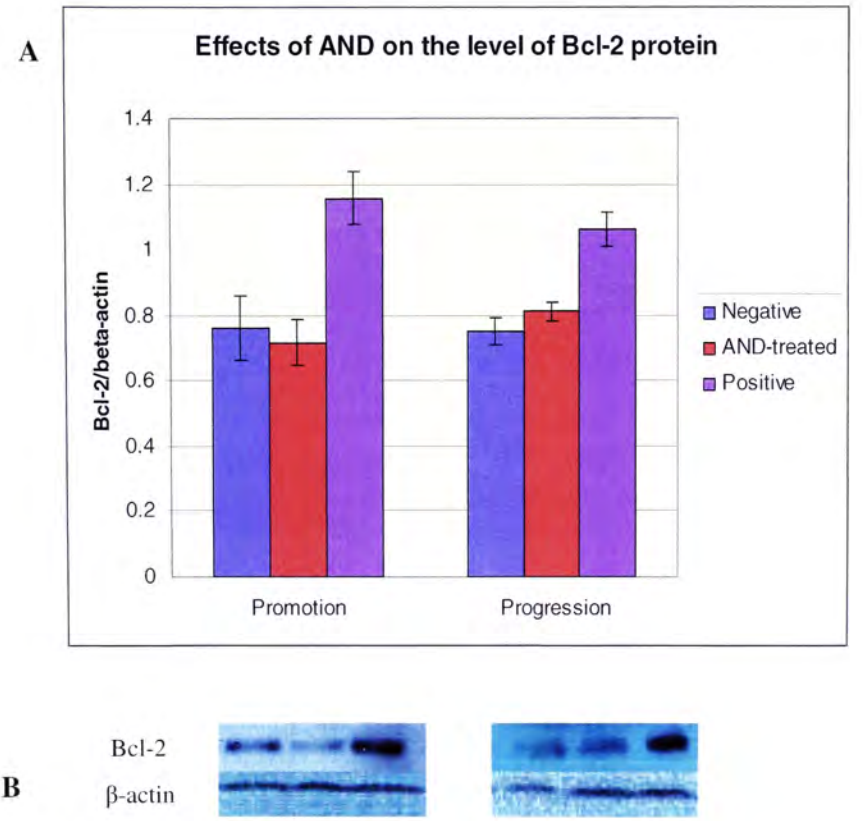


**Figure 4.3** The cytosolic proteins in the rat liver were separated by 10% SDS-PAGE and transferred onto PVDF membrane. Bcl-2 was detected with mouse antibodies against Bcl-2 followed by goat anti-mouse-HRP visualization. A) Bcl-2 was expressed in Bcl-2 : β-actin ratio. Significance was found between the AND-treated and positive control groups in both experiments ($p < 0.05$). All data were expressed as mean ± SD ($n = 5$). B) Bcl-2 expression. β-actin was the internal standard.

**Figure 4.4 Western blot analysis of p21 protein**

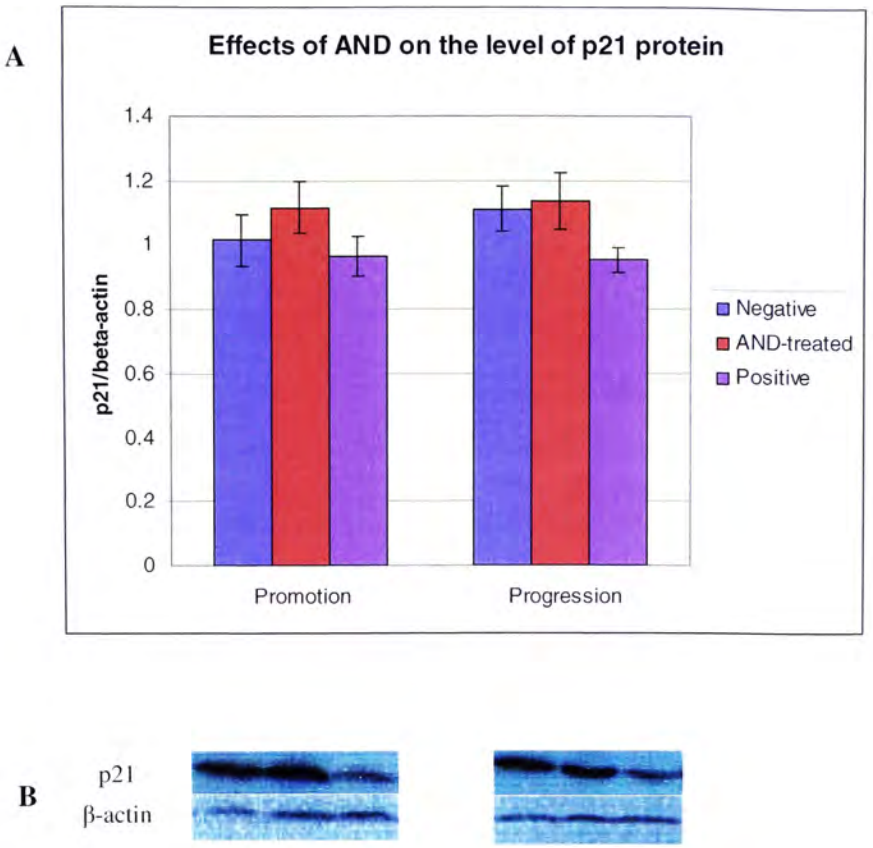


**Figure 4.4** The protein p21 in the rat liver was separated by 10% SDS-PAGE and transferred onto PVDF membrane. It was detected with mouse antibodies against p21 followed by goat anti-mouse-HRP visualization. A) p21 was expressed in p21 : β-actin ratio. Levels of p21 in AND-treated groups were higher than positive control groups, but no significant difference was observed in both experiments. All data were expressed as mean ± SD ($n$ = 5). B) p21 expression. β-actin was the internal standard.

**Figure 4.5 Western blot analysis of total p53 protein**

A

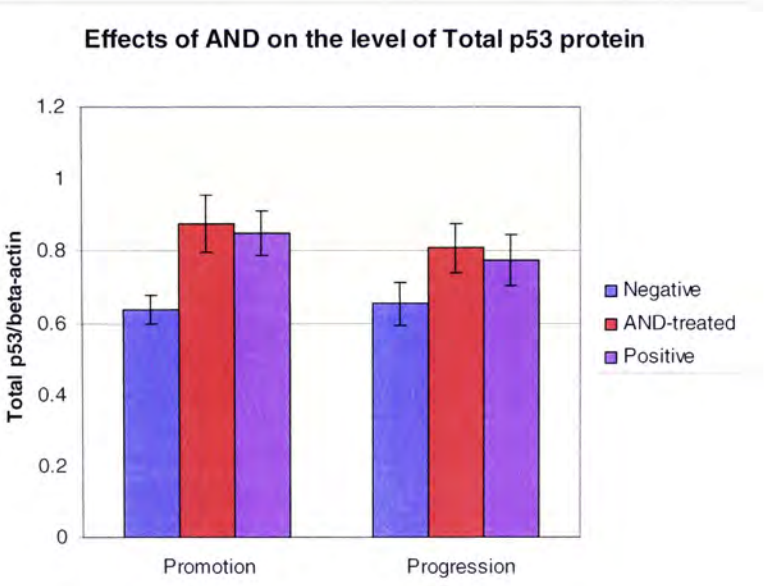


B

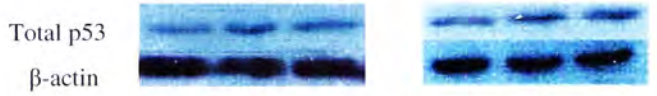


**Figure 4.5** Total p53 was separated by 10% SDS-PAGE and then transferred onto PVDF membrane. The nuclear protein was detected with mouse antibodies against p53 (Pab 421) and goat anti-mouse-HRP. A) Total p53 was expressed in p53 : β-actin ratio. There was no significant difference in the levels of total p53 in AND-treated groups as compared with the positive control groups in both experiments. All data were expressed as mean ± SD ($n$ = 5). B) Total p53 expression. β-actin was the internal standard.

**Figure 4.6 Western blot analysis of wildtype p53 protein**

A

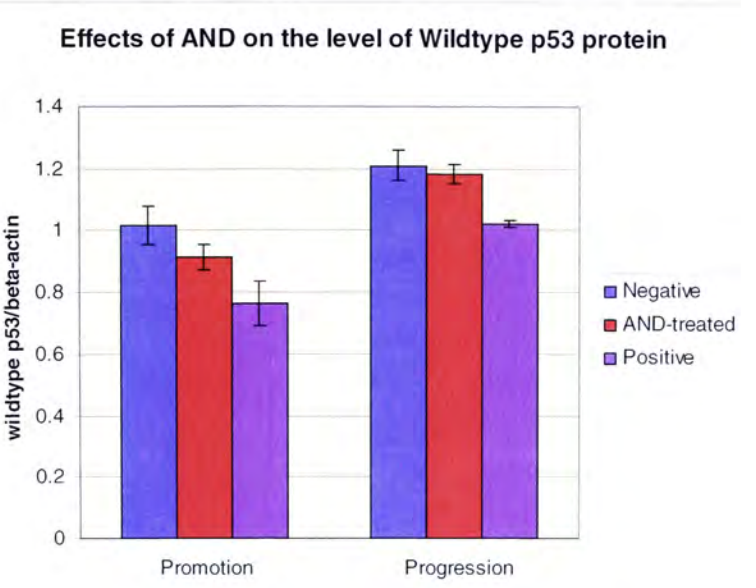


B


**Figure 4.6** Nuclear proteins were immunoprecipitated with mouse monoclonal anti-p53 antibody (Pab 246). The precipitated protein were separated and transferred onto the PVDF membrane. Wildtype p53 was detected with mouse antibodies against wt p53 (Pab 421) and goat anti-mouse-HRP. A) Wt p53 was expressed in wt. p53 : β-actin ratio. There was no significant difference in the levels of wt. p53 in AND-treated group as compared with that in the positive control group in the promotion experiment. In the progression experiment, however, a significant increase in the level of wt. p53 in AND-treated group was observed when compared with that in the positive control group ($p < 0.05$). All data were expressed as mean ± SD ($n = 5$). B) Wt. p53 expression. β-actin was the internal standard.

## Figure 4.7 Western blot analysis of Mdm2 protein

A

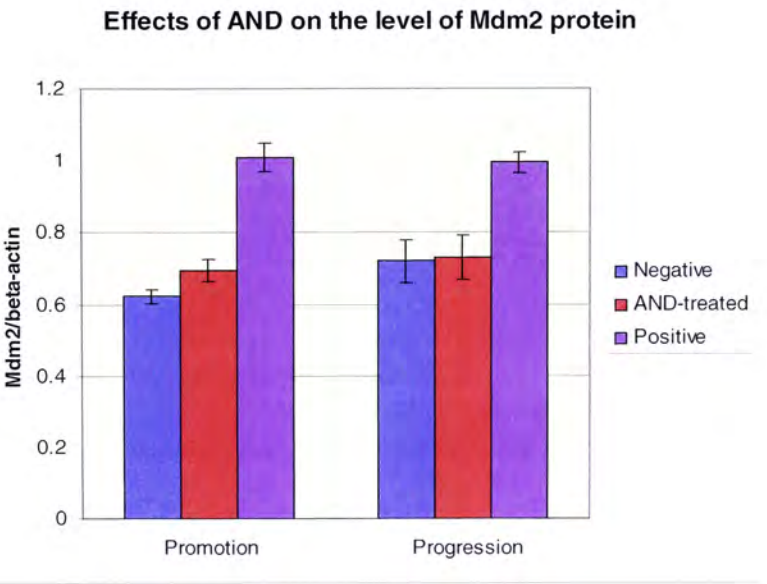


B


**Figure 4.7** The nuclear proteins in the rat liver were separated by 10% SDS-PAGE and transferred onto PVDF membrane. Mdm2 was detected with mouse antibodies against Mdm2 and goat anti-mouse-HRP. A) Mdm2 was expressed in Mdm2 : β-actin ratio. There was a significant decrease in the levels of Mdm2 in AND-treated groups as compared with the positive control groups in both experiments ($p < 0.05$). All data were expressed as mean ± SD ($n = 5$). B) Mdm2 expression. β-actin was the internal standard.

**Figure 4.8 Effects of AND on the expression of *p53* mRNA**

A

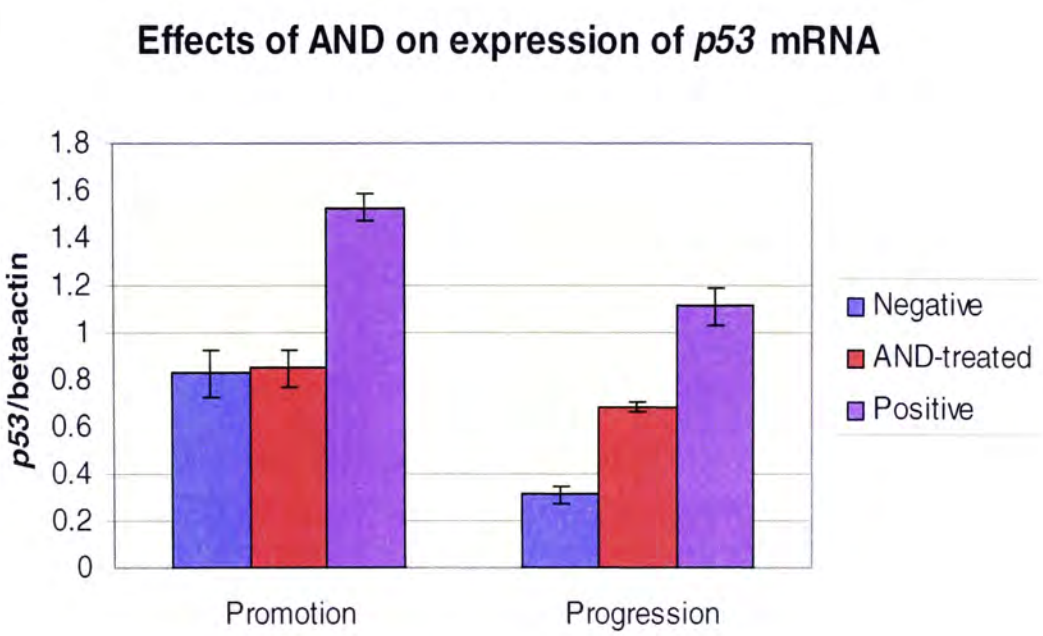


B


**Figure 4.8** A) *p53* expression was measured as the ratio of *p53* : *β-actin*. There was a significant reduction in the expression in the AND-treated group when compared to that in the positive control group in both experiments ($p < 0.05$). All data were expressed as mean ± SD ($n = 5$). B) *p53* mRNA expression. β-actin was the internal standard.

## Figure 4.9 Effects of AND on the expression of *Mdm2* mRNA

A

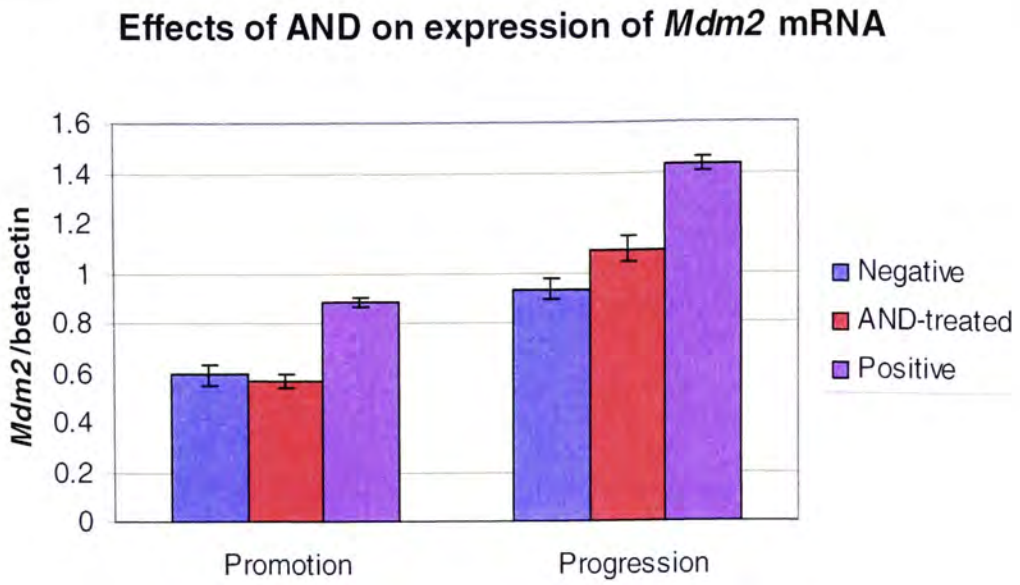


B


**Figure 4.9** A) *Mdm2* expression was measured as the ratio of *Mdm2* : *β-actin*. There was a significant reduction in the expression in the AND-treated group when compared to that in the positive control group in both experiments ($p < 0.05$). All data were expressed as mean ± SD ($n = 5$). B) *Mdm2* mRNA expression. β-actin was the internal standard.

## Discussion

Andrographolide (AND), the active component extracted from Andrographis Paniculata (AP), was reported to possess pharmacological properties. These include protozoacidal, anti-mutagenic and anti-carcinogenic activities (82-85). The beneficial effects of AND on liver, however, are not fully understood. Therefore, the present study was aimed at investigating the biological activities of AND on the liver through *in vitro* and *in vivo* studies.

*AND causes inhibition of cell growth*

Cell cycle is an ordered set of events in a eukaryotic cell from one cell division to the next. It is initiated in the presence of mitogenic stimulus and is normally regulated by cyclins and cyclin-dependent kinases (87). However, this regulation of the cell cycle is lost in cancer cells and they continue to divide in the presence or absence of a mitogenic stimulus (88). Many anti-cancer agents are known to possess the ability to block the cell cycle at different stages. This includes doxorubicin, an anti-cancer agent that blocks cell cycle at G2 phase (89).

In the present study, AND displayed a significantly inhibitory effect on the proliferation of human liver cancer cell line, HepG2 (Fig. 1.1). On the other hand, the normal liver cells, WRL 68 and Clone 9, were less sensitive to AND, although significant cytotoxicity was also detectable at a concentration of 18 μM (Fig. 1.2 & 1.3). The results imply that AND could have therapeutic potential in treatment of cancer when lower doses are administered to rats.

In addition, FACS analysis demonstrated that the HepG2 cells treated with AND (25 μM) for 48 hrs exhibited a dramatic accumulation (67.1%) of cells in $G_0/G_1$ phase of the cell cycle (Fig. 1.7). The increase in the population of cells suspended in $G_0/G_1$ phase is regulated by many cell cycle proteins. The most critical determinant of the $G_1$ arrest is p21 (Waf1/Cip1/Sdi1) which interacts with cyclins D and E during the early $G_1$ phase of the cell cycle, inhibiting the activity of cyclin D/ CDK complex (42). The inactive cyclin D/CDK complex leads to the inactivation of kinases which subsequently activates the tumor suppressor, retinoblastoma (Rb), and that inhibits cell cycle progression through the $G_1$ to S phase. Besides the important role of p21, the expression of level cyclin D1 has also been shown to be rate-limiting in cellular proliferation (90). Consistent with its role in cell cycle progression, increased expression of cyclin D1 has been detected in breast cancer cells (91) and colorectal carcinogenesis (92). The tumor suppressor, Rb, functions as an active repressor of the transcription of E2F-responsive genes that are required for the initiation of DNA synthesis (93). Mutations of its DNA sequence or defect in gene transcription can result in Rb inactivation which occurs in all retinoblastomas (94). Therefore, p21, cyclin D1 and Rb are important elements in governing cell cycle progression at $G_1$-S-phase transition. In the present study, although no significant difference was observed, a higher expression of p21 was detected *in vivo* by Western blots in livers from negative control and AND-treated rats than that from the positive control rats. Microarray analysis further revealed that expression of *CCND1*, whose protein product is cyclin D1, was down-regulated whereas *RB1*, whose protein product is Rb, was up-regulated upon treatment of AND. Another cell cycle control gene, *CHEK-2*, whose expression level is critical to cell cycle checkpoint regulation and putative tumor

suppression, was also found to be down-regulated. The findings show that AND can cause an arrest in the cell cycle at $G_1$-S phase transition in liver cells.

*AND causes apoptotic cell death*

Apoptosis is a genetically encoded form of cell suicide central to the development and homeostasis of multicellular organisms. Cells undergoing apoptosis display a characteristic pattern of structural changes in the nucleus and cytoplasm, including nuclear disintegration (95). The cleavage of DNA into oligonucleosomal-length fragments is a late event in apoptosis and it was detected *in vitro* in the cell cycle analysis. The treatment of HepG2 cells with AND (25 μM) resulted in a significant increase in the percentage of cells (13.1%) suspended in the Sub G1 phase of the cell cycle (Fig. 1.7). DNA fragmentation in HepG2 cells was further confirmed with 50 μM of AND incubated for 72 hrs (Fig. 1.8).

Mitochondria have been shown to play a central role in the apoptotic process, because both the intrinsic pathway and the extrinsic pathway converge at the mitochondrial level and trigger mitochondrial membrane permeabilization (96). After apoptotic-stimulated mitochondrial membrane permeabilization, cytochrome *c* and other proapoptotic proteins release into the cytosol. Released cytochrome *c* subsequently triggers the activation of caspases, substrate cleavage, and cell death (97). Bcl-2, and Bax are the two members of the Bcl-2 family that have been implicated as major regulators in the control of mitochondrial cytochrome *c* release (97). Bcl-2 is an anti-apoptotic factor that binds to the outer membrane of mitochondria and blocks cytochrome *c* efflux. Conversely, upon apoptosis induction, Bax translocates from the cytosol to the

mitochondria where it enhances cytochrome *c* release through the outer membrane of mitochondria. Many anticancer agents or apoptotic stimuli can trigger cytochrome *c* release through either down-regulation of Bcl-2 and/or up-regulation of Bax such as Doxorubicin (98). In the present study, Bcl-2 protein expressions were significantly lower in both the negative and AND-treated rats than that in the positive control rats (Fig. 4.3). The protein levels of Bax were also significantly increased in the negative control and AND-treated groups than that in the positive control group (Fig. 4.2). Moreover, the microarray analysis revealed that *Bcl-2* and *Bcl-w*, an anti-apoptotic gene, were down-regulated in HepG2 cells treated with 16 μM of AND for 48 hrs (Fig. 2.2). The data indicate that the anti-HCC effect of AND is associated with Bcl-2, Bcl-w and Bax proteins that trigger apoptosis.

*AND increases the stability of wild-type p53*

The tumor suppressor gene p53 is regarded as a key regulator in maintaining a balance between cell growth and cell death and it plays an important role in tumor growth inhibition and induction of apoptosis (99). The wild-type p53 mediates the expressions of Bax, Bcl-2 and p21 proteins. The results from *in vivo* study showed that wild-type p53 expression was decreased in the liver of DEN-$CCl_4$ treated rats, while total p53 (wild-type and mutant) expression was increased. It implies that the expression of mutant p53 was increased in the DEN-$CCl_4$ treated rats. The major regulator of p53 turnover, Mdm2, was found to be over-expressed at the transcriptional level in the livers of these rats (Fig. 4.7). This is due to the fact that Mdm2 expression is also induced by p53 through a binding site

of the *Mdm2* gene. Since mutant p53 cannot be degraded by Mdm2, the over-expression of Mdm2 leads to an increase of wild-type p53 degradation.

The present data demonstrate a significant increase in the expression of p53 mRNA in the positive control rats, resulting in an increase in the total p53 protein level in both the promotion and progression stages of carcinogenesis. On the other hand, the p53 mRNA expression was found to decrease in the AND-treated group, and yet the total p53 protein was increased. Since wild-type p53 protein expression was significantly increased in the AND-treated rats and there was a significant decrease in the expression of Mdm2 simultaneously, the results suggest that AND down-regulates the expression of Mdm2, leading to an increased level of wild-type p53. It is confirmed with the microarray analysis, which showed a 3.4-fold changes in the down-regulation of *Mdm2* expression in HepG2 cells treated with AND (16 μM) for 48 hrs (Fig. 2.2C). The under-regulated *Mdm2* gene expression reduces the protein level of Mdm2 to degrade wild-type p53, suggesting an increase in the stability of p53. Subsequently, the wild-type p53 can regulate the expressions of Bax, Bcl-2 and p21, resulting in cell cycle arrest and apoptosis in tumor cells.

*AND reduces liver damage caused by DEN and $CCl_4$*

Spraque Dawley rats were treated according to established protocols in order to investigate the effects of AND on the promotion and progression stages of hepatocarcinogenesis. The initial stage of HCC can be developed in rat liver by the administration of diethylnitrosamine (DEN), an indirect initiator that produces DNA adducts. Within a few weeks, populations of initiated cells called the enzyme-altered foci

can be detected (100). With the administration of a promoter like $CCl_4$, the growth of the initiated preneoplastic cells is enhanced. Furthermore, the two periods of fasting in the treatment schedule were believed to reduce the latency period for the incidence of early lesion during chemical carcinogenesis in rat liver (101).

In generating a chemical carcinogenesis model in rat liver, liver cell proliferation plays a very important role in the whole process (102). It specifically exerts a critical effect in the promotion of carcinogen-initiated cells (103). Proliferating cell nuclear antigen (PCNA) is a co-factor for DNA polymerase δ and is synthesized in early $G_1$ and S phases of the cell cycle. It serves as a significant marker for proliferating cells and hence clinical malignancy. In the present study, livers from rats treated with DEN-$CCl_4$ alone in both the promotion and progression experiments had a significantly higher expression of PCNA than those treated with vehicle. After AND treatment, the PCNA expression was reduced in both experiments, suggesting that liver cell proliferation was regulated upon AND treatment.

AST and ALT are normally located in liver cells. When liver cells are injured, these two enzymes will leak out into the general circulation and cause an elevated level in blood serum. Hence, AST and ALT are often used as an indicator to evaluate the degree of liver damage. In the promotion and progression experiments, the serum levels of AST and ALT in AND-treated rats were significantly lower than those in the positive control rats (Fig. 3.5). The findings, therefore, suggest that liver damage was significantly reduced in rats that had been treated with AND in both the promotion and progression stages of hepatocarcinogenesis.

*AND reduces the expression of GST-P foci*

Immunohistochemical identification of GST-P has been used widely for the detection of preneoplastic lesion in rat hepatocarcinogenesis (104). GST-P is normally absent in rat hepatocytes but it can be induced by various xenobiotics. It has been shown that GST-P mRNA is induced by lead nitrate, aflatoxin metabolites or phenobarbital (105, 106). Several studies also reported that GST-P can be induced by epidermal growth factor (EGF) or insulin (107). In the present study, no GST-P foci could be detected in the negative control liver sections but clusters or groups of GST-P foci were extensively observed in the positive control sections (Fig. 3.8 & 3.9). The expression of GST-P foci in the DEN-$CCl_4$ treated livers indicates the induction of preneoplastic lesions in both promotion and progression stages of carcinogenesis. Upon treatment of AND at a dose of 10 mg/kg for 24 and 52 weeks, a decrease in the number and area of GST-P positive foci was detected at these two stages (Fig. 3.8 & 3.9). The results demonstrate that AND can reduce the expression of GST-P and thus the number of preneoplastic foci that were induced by DEN-$CCl_4$.

*AND restores the morphology of normal liver*

Gross examination of the rat liver that had been treated with DEN-$CCl_4$ showed the presence of lipid droplets, nodules and eventually tumors across the surface of the liver. There was also a significant increase in the relative liver weights in these rats as compared with those in the vehicle-treated rats. This phenomenon is typical in the treatment of $CCl_4$ to rats. The carcinogen induces CYP 2E1 which activates oxygen via an NADPH-dependent mechanism (108). Subsequent dissociation of superoxide radicals from the

enzyme-substrate complex generates free radicals that react with microsomal membranes to induce lipid peroxidation that leads to cell membrane damage (109). The chronic administration of certain xenobiotics and the metabolizing enzymes has been reported to induce liver enlargement in rats (110). The increase of the relative liver weight with $CCl_4$ is thought to be due to liver cell proliferation called hyperplasia (111). Consistent with this observation, significant hyperplasia could be detected in the livers of rats that had been treated with DEN-$CCl_4$ in both the promotion and progression experiments (Fig. 3.4). This induction of cell proliferation becomes particularly important for tumorigenesis in slowly proliferating tissues such as liver.

In the promotion experiment, the AND-treated livers retained a smooth surface and generally resembled the negative control livers (Fig. 3.6). It was observed that some nodules were present in the livers that had been treated with AND in the progression stage (Fig. 3.7). However, the structure of the liver generally resembled that of the normal livers. The results reflect that AND restores the basic structure of rat livers.

Moreover, histological examination of rat livers revealed that hepatocytes of AND-treated livers adopted the well-defined, cuboidal shape that is characteristic of normal hepatocytes. Swollen hepatocytes and cytoplasmic vacuolization, which are common in $CCl_4$ intoxication, were only observed in positive control sections in both experiments. The findings further indicate that AND can retain the normal hepatic morphology.

## Conclusion

Andrographolide (AND) is an active component isolated from Andrographis Paniculata, a Chinese herbal medicine, which possesses many biological activities (74). However, the beneficial effects of AND on liver have yet to be elucidated. Thus, in the present study, the biological activities of AND on liver was evaluated through *in vitro* and *in vivo* studies.

The effect of AND on the cell cycle was demonstrated. It increased the population of cells suspended in $G_0/G_1$ phase, inhibiting the growth of HepG2 cells at low doses. Apoptotic cell death was also observed as DNA fragmentation was detected in AND-treated cells. The changes in gene expression upon treatment of AND further indicated its effects on the regulation of mRNA expression of genes whose expression levels are critical in cell cycle and apoptosis. These genes included *CCND1, RB1, CHEK-2, BCL2, BCL2L2 and MDM2*.

The effects of AND on hepatocarcinogenesis induced by diethylnitrosamine (DEN) and carbon tetrachloride ($CCl_4$) in Spraque Dawley rats were demonstrated. AND was shown to inhibit the development of HCC in the promotion and progression stages. The liver conditions of rats, as indicated by levels of AST/ALT in serum and PCNA protein expression in liver, were found to be significantly improved. Histological examination of AND-treated liver sections showed normal hepatic morphology. GST-P positive foci were also found to decrease in these sections.

The protein expression of p53 revealed that wild-type p53 was increased and mutant p53 was decreased with treatment of AND. The increased wild-type p53 regulated

the expressions of Bax, Bcl-2 and p21, causing a decrease in Bcl-2 and an increase in Bax and p21. The expression of Mdm2, a protein that controls the expression of p53, was decreased in the AND-treated groups. It indicates the stability of wild-type p53 which regulates the expressions of other cell cycle and apoptotic proteins.

The present study demonstrated the effectiveness of AND in inhibiting the growth of HepG2 cells and reducing HCC in rats. Through the inhibition of the apoptotic events, cancer cells can be killed. The mediation of p53 and other signaling proteins associated with cancer was a result of treatment of cells with AND, leading to an array of pharmacological activity. The results reflect the therapeutic benefits of AND for treatment of liver cancer. In the future, studies can be performed to investigate the detailed mechanism of AND on HCC. Modification of the chemical structure of this compound can be performed in order to enhance its potency and to reduce the cytotoxicity of AND in normal human liver cells.

# References


1. Parkin,D.M., Pisani,P. and Ferlay,J. (1999) Global cancer statistics. *CA Cancer J. Clin.* 49: 33-64.

2. El-Serag, HB, Davila, J.A., Petersen, N.J. and McGlynn K.A. (2003) The continuing increase in the incidence of hepatocellular carcinoma in the United States: an update. *Ann Intern Med.* 139(10): 817-23.

3. Marrero, J.A. (2006) Hepatocellular carcinoma. *Curr. Opin Gastroenterol.* 22(3): 248-53.

4. Kirk, G.D., Lesi, O.A., Mendy, M., Akano, A.O., Sam, O., Goedert, J.J. et al. (2004) The Gambia liver cancer study: Infection with hepatitis B and C and the risk of hepatocellular carcinoma in West Africa. *Hepatology.* 39: 211-219.

5. Wang, X.W., Hussain, S.P., Huo, T.I., et al (2002) Molecular pathogenesis of human hepatocellular carcinoma. *Toxicology.* 181–182: 43-7.

6. Sakamoto, M., Hirohashi, S. and Shimosato, Y. (1991) Early stages of multistep hepatocarcinogenesis: adenomatous hyperplasia and early hepatocellular carcinoma. *Hum Patho.* 22: 172-8.

7. Chao, Y., Li, C.P., Chau, G.Y., et al (2003) Prognostic significance of vascular endothelial growth factor, basic fibroblast growth factor, and angiogenin in patients with resectable hepatocellular carcinoma after surgery. *Ann Surg Oncol.* 10: 355-62.

8. Hirohashi, S. (1991) Pathology and molecular mechanisms of multistage human hepatocarcinogenesis. *Princess Takamatsu Symp* 22: 87-93.

9. Yuspa, S.H. and Poirier, M.C. (1988) Chemical carcinogenesis: from animal models to molecular models in one decade. *Adv Cancer Res.* 50: 25-70.

10. Neumann, H.G. (1988) Role of extent and persistence of DNA modifications in chemical carcinogenesis by aromatic amines. *Recent Results Cancer Res.* 84: 77-89.

11. Pitot, H.C. (1990) Altered hepatic foci: Their role in murine hepatocarcinogenesis. *Annu Rev Pharmacol Toxicol.* 30: 465-500.

12. Bannasch, P., Haertel, T. and Su, Q. (2003) Significance of hepatic preneoplasia in risk identification and early detection of neoplasia. *Toxicol Pathol.* 31: 134-9.

13. Ashendel, C.L. (1985) The phorbol ester receptor: a phospholipids-regulated protein kinase. *Biochem Biophys Acta.* 822: 219-242.

14. Fishbein, L. (1979) Potential halogenated industrial carcinogenic and mutagenic chemicals. II. Halogenated saturated hydrocarbons. *Sci Total Environ.* 11(2): 163-95.

15. Loeb, L.A. and Cheng, K.C. (1990) Errors in DNA synthesis: a source of spontaneous mutations. *Mutat Res.* 238: 297-304.

16. Lengauer, C., Kinzler, K.W. and Vogelstein, B. (1998) Genetic instabilities in human cancers. *Nature.* 396: 643-9.

17. Haber, D. and Harlow, E. (1997) Tumor-suppressor genes: evolving definitions in the genomic age. *Nat. Genet.* 16: 320-2.

18. Kemeny. N, Daly. J, Reichman. B, et al. (1987) Intrahepatic or systemic infusion of fluorodeoxyuridine in patients with liver metastases from colorectal carcinoma. A randomized trial. *Ann Intern Med.* 107: 459-65.

19. Ackerman, N.B. (1974) The blood supply of experimental liver metastases. IV. Changes in vascularity with increasing tumor growth. *Surgery.* 75: 589-96.

20. Ensminger, W.D., Rosowsky, A., Raso, V., et al. (1978) A clinical-pharmacological evaluation of hepatic arterial infusions of 5-fluoro-2'-deoxyuridine and 5-fluorouracil. *Cancer Res.* 38: 3784-92.

21. Allen-Mersh, T.G., Glover, C., Fordy, C., et al. (2000) Randomized trial of regional plus systemic fluorinated pyrimidine compared with systemic fluorinated pyrimidine in treatment of colorectal liver metastases. *Eur J Surg Oncol.* 26: 468-73.

22. Livraghi, T., Goldberg, S.N., Lazzaroni, S., et al. (2000) Hepatocellular carcinoma: Radiofrequency ablation of medium and large lesions. *Radiology.* 214: 761-8.

23. Livraghi, T., Goldberg, S.N., Lazzaroni, S., et al. (1999) Radiofrequency ablation vs. ethanol injection in the treatment of small hepatocellular carcinoma. *Radiology.* 210:655-61.

24. Curley, S.A., Izzo, F., Ellis, L.M., et al. (2000) Radiofrequency ablation of hepatocellular cancer in 110 patients with cirrhosis. *Ann Surg..* 232: 381-91.

25. Sparchez, Z. and Bolog, N. (2003) Ultrasound guided percutaneous ethanol injection of hepatocellular carcinoma. Rom. *J. Gastroenterol* 12: 147-55.

26. Llovet, J.M., Bruix, J., Fuster, J., Castells, A., Garcia-Valdecasas, J.C., Grande, L., et al. (1998) Liver transplantation for small hepatocellular carcinoma: The tumor-node-metastasis classification does not have prognostic power. *Hepatology.* 27: 1572-77.

27. Marsh, J.W., Dvorchik, I., Subotin, M., Balan, V., Rakela, J., Popechitelev, E.P., et al. (1997) The prediction of risk of recurrence and time to recurrence of hepatocellular carcinoma after orthotopic liver transplantation: A pilot study. *Hepatology.* 26: 444-50.

28. Cox, A.D. and Der C.J. (2002) Ras family signaling: therapeutic targeting. *Cancer Biol. Ther.* 1(6): 599-606.

29. Fernandez, P.C., Frank, S.R., Wang, L., Schroeder, M., Liu, S., Greene, J., Cocito, A. and Amati, B. (2003) Genomic targets of the human c-Myc protein. *Genes Dev.* 17(9): 1115-29.

30. Sigal, A. and Rotter, V. (2000) Oncogenic mutations of the p53 tumor suppressor: the demons of the guardian of the genome. *Cancer Res.* 60: 6788-93.

31. El-Shanawani, F.M., Abdel-Hadi, A.A., Abu Zikri, N.B., Ismail, A., El-Ansary, M. and El-Raai, A. (2006) Clinical significance of aflatoxin, mutant P53 gene and sIL-2 receptor in liver cirrhosis and hepatocellular carcinoma. *J. Egy. Soc. Parasitol.* 36(1): 221-39.

32. Lleonart, M.E., Kirk, G.D., Villar, S., Lesi, O.A., Dasgupta, A., Goedert, J.J., Mendy, M., Hollstein, M.C., Montesano, R., Groopman, J.D., Hainaut, P. and Friesen, M.D. (2005) Quantitative analysis of plasma TP53 249-Ser-mutated DNA by electrospray ionization mass spectrometry. *Cancer Epid. Biom. Prev.* 14(12): 2956-62.

33. Jackson, P.E., Kuang, S.Y., Wang, J.B., Strickland, P.T., Munoz, A., Kensler, T.W., Qian, G.S. and Groopman, J.D. (2003) Prospective detection of codon 249 mutations in plasma of hepatocellular carcinoma patients. *Carcinogenesis.* 24(10): 1657-63.

34. Ndububa, D.A., Yakicier, C.M., Ojo, O.S., Adeodu, O.O., Rotimi, O., Ogunbiyi, O. and Ozturk, M. (2001) P53 codon 249 mutation in hepatocellular carcinomas from Nigeria. *Afr. J. Med. Med. Sci.* 30(1-2): 125-7.

35. Turner, P.C., Sylla, A., Kuang, S.Y., Marchant, C.L., Diallo, M.S., Hall, A.J., Groopman, J.D. and Wild, C.P. (2005) Absence of TP53 codon 249 mutations in young Guinean children with high aflatoxin exposure. *Cancer Epid. Biom. Prev.* 14(8): 2053-5.

36. El-Kafrawy, S.A., Abdel-Hamid, M., El-Daly, M., Nada, O., Ismail, A., Ezzat, S., Abdel-Latif, S., Abdel-Hamid, A., Shields, P.G. and Loffredo, C. (2005) P53 mutations in hepatocellular carcinoma patients in Egypt. *Int. J. Hyg. Environ. Health.* 208(4): 263-70.

37. Kuang, S.Y., Lekawanvijit, S., Maneekarn, N., Thongsawat, S., Brodovicz, K., Nelson, K. and Groopman, J.D. (2005) Hepatitis B 1762T/1764A mutations, hepatitis C infection, and codon 249 p53 mutations in hepatocellular carcinomas from Thailand. *Cancer Epid. Biom. Prev.* 14(2): 380-4.

38. Cadwell, C. and Zambetti, G.P. (2001) The effects of wild-type p53 tumor suppressor activity and mutant p53 gain-of-function on cell growth. *Gene* 277: 15-30.

39. Linda, J.K. and Prives, C. (1996) p53: puzzle and paradigm. *Genes & Dev.* 10: 1054-72.

40. Ashcroft, M. and Vousden, K.H. (1999) Regulation of p53 stability. *Oncogene.* 18: 7637-43.

41. Chen, J., Jackson, P. K., Kirschner, M.W. and Dutta, A. (1995) Separate domains of p21 involved in the inhibition of Cdk kinase and PCNA. *Nature.* 374:386-8.

42. Harper, J.W., Adami, G.R., Wei, N., Keyomarsi, K. and Elledge, S.J. (1993) The p21 Cdk-interacting protein Cip1 is a potent inhibitor of G1 cyclin-dependent kinases. *Cell.* 75: 805-816.

43. Flores-Rozas, H., Kelman, Z., Dean F.B., Pan, Z.Q., Harper, J.W., Elledge, S.J., O'Donnell, M. and Hurwitz, J. (1994) *Proc Natl Acad Sci USA.* 91(18): 8655-9.

44. Takahashi, T., et al. (1997) Detection of proliferating cell nuclear antigen (PCNA) in peripheral blood mononuclear cells and sera of patients with malignant lymphoma. *Leuk Lymphoma.* 28(1-2): 113-25.

45. Kawahira, K. (1999) Immunohistochemical staining of proliferating cell nuclear antigen (PCNA) in malignant and nonmalignant skin diseases. *Arch Dermatol Res.* 291(7-8): 413-8.

46. Ioachim, E., et al. (1999) Altered patterns of retinoblastoma gene product expression in benign, premalignant and malignant epithelium of the larynx: an immunohistochemical study including correlation with p53, bcl-2 and proliferating indices. *Anticancer Res.* 19(1A):541-5

47. Horiguchi, J., et al. (1998) Long-term prognostic value of PCNA labeling index in primary operable breast cancer. *Oncol Rep.* 5(3):641-4.

48. Danial, N. N. and Korsmeyer, S. J. (2004) Cell death: critical control points. *Cell.* 116: 205–219.

49. Fridman, J. S. and Lowe, S. W. (2003) Control of apoptosis by p53. *Oncogene* 22: 9030–40.

50. Zamzami, N., Brenner, C., Marzo, I., Susin, S.A. and Kroemer, G. (1998) Subcellular and submitochondrial mode of action of Bcl-2-like oncoproteins. *Oncogene.* 16: 2265-82.

51. Bakhshi, A. et al. (1985) Cloning the chromosomal breakpoint of t(14;18) human lymphomas: clustering around JH on chromosome 14 and near a transcriptional unit on 18. *Cell.* 41: 899-906.

52. Yunis, J.J., Oken, M., Kaplan, M.E., et al. (1982) Distinctive chromosomal abnormalities in histology, subtypes of non-Hodgkin's lymphomas. *N. Engl. J. Med.* 307: 1231–6.

53. Tsujimoto, Y. and Croce C.M. (1986) Analysis of the structure, transcripts, and protein products of bcl-2, the gene involved in human follicular lymphoma. *Proc. Natl. Acad. Sci. USA.* 83: 5214-5218.

54. Yang, J., Liu, X., Bhalla, K., Kim, C.N., Ibrado, A.M., Cai, J., Peng, T.I., Jones, D.P. and Wang, X. (1997) Prevention of apoptosis by Bcl-2: Release of cytochrome c from mitochondria blocked. *Science.* 275: 1129-32.

55. Hockenberry, D., Nunez, G., Milliman, C., Schreiber, R. D. and Korsmeyer, S. J. (1990) Bcl-2 is an inner mitochondrial membrane protein that blocks programmed cell death. *Nature*. 348: 334-336.

56. Desoize, B. (1994) Anticancer drug resistance and inhibition of apoptosis. *Anticancer Res.* 14: 2291-2294.

57. Zamzani, N., Brenner, C., Marzo, I., Susan, S.A. and Kroemer, G. (1998) Subcellular and submitochondrial mode of action of Bcl-2-like oncoproteins. *Oncogene*. 16: 2265-82.

58. Miyashita, T. and Reed, J.C. (1995) Tumor suppressor p53 is a direct transcriptional activator of the human bax gene. *Cell*. 80: 293-299.

59. Miyashita, T., Krajewski, S., Krajewska, M., Wang, H. G., Lin, H. K., Liebermann, D. A., Hoffman, B. and Reed, J. C. (1994) Tumor suppressor p53 is a regulator of bcl-2 and bax gene expression in vitro and in vivo. *Oncogene.* 9: 1799-1805.

60. Ludwig, R.L., Bates, S. and Vousden, K.H. (1996) Differential activation of target cellular promoters by p53 mutants with impaired apoptotic function. *Mol. Cell Biol.* 16(9): 4952-60.

61. Wolter, K.G., Hsu, Y.T., Smith, C.L., Nechushtan, A., Xi, X.G. and Youle, R.J. (1997) Movement of Bax from the cytosol to mitochondria during apoptosis. *J. Cell Biol.* 139(5): 1281-92.

62. Vousden, K.H. (2000) p53: death star. *Cell.* 103:691-4.

63. Maki, C. G., Huibregtse, J. M. and Howley, P. M. (1996) In vivo ubiquitination and proteasome-mediated degradation of p53. *Cancer Res.* 56: 2649-54.

64. Honda, R., Tanaka, H. and Yasuda, H. (1997) Oncoprotein MDM2 is a ubiquitin ligase E3 for tumor suppressor p53. *FEBS Lett.* 420: 25-27.

65. Tao, W. and Levine, A.L. (1999) Nucleocytoplasmic shuttling of oncoprotein Hdm2 is required for Hdm2-mediated degradation of p53. *Proc. Natl. Acad. Sci. USA* 96: 3077-80.

66. Jones, S.N., Roe, A.E., Donehower, L.A. and Bradley, A. (1995) Rescue of embryonic lethality in Mdm2-deficient mice by absence of p53. *Nature* 378: 206-8.

67. Fang, S., Jensen, J. P., Ludwig, R. L., Vousden, K. H. and Weissman, A. M. (2000) Mdm2 is a RING finger-dependent ubiquitin protein ligase for itself and p53. *J. Biol. Chem.* 275: 8945–51.

68. Zhang, Z., Wang, H., Li, M., Agrawal, S., Chen, X. and Zhang, R. (2004) Mdm2 is a Negative Regulator of $p21^{WAF1/CIP1}$, independent of p53. *J.Biol. Chem.* 279(16): 16000-6.

69. Power, C., Sinha, S., Webber, C., Manson, M.M. and Neal, G.E. (1987) Transformation related to expression of glutathione S-transferase P in rat liver cells. *Carcinogenesis* 8:797.

70. Maugart-Loubootin, C., Charrier, J., Sagin, C., Cuilliere, P., Martin, S., Menegalli, D., Lajat, Y., Resche, F. and Ali-Osman, F. (1996) Correlation between glutathione S-transferases (GST) Pi expression in human astrocytomas determined by RT-PCR and histological grade. *Proc Annu Meet Am Assoc Cancer Res.* 37: A2305.

71. Sato, K., Satoh, K., Tsuchida, S., Hatayama, I., Shen, H., Yokoyama, Y., Yamada, Y. and Tamai, K. (1992) Specific expression of glutathione S-transferase Pi forms in (Pre)neoplastic tissues – their properties and functions. *Tohoku J Exp Med.* 168: 97-103.

72. LaDue, J.S. and Wroblewski, F. (1956) Serum glutamic pyruvic transaminase SGP-T in hepatic disease: a preliminary report. *Ann Intern Med.* 45(5): 801-11.

73. Wiart, C., Kumar, K., Yusof, M.Y., Hamimah, H., Fauzi, Z.M. and Sulaiman, M. (2005) Antiviral properties of ent-labdene diterpenes of Andrographis paniculata nees, inhibitors of herpes simplex virus type 1. *Phytother Res.* 19(12): 1069-70.

74. Reyes, B.A., Bautista, N.D., Tanquilut, N.C., Anunciado, R.V., Leung, A.B., Sanchez, G.C., Magtoto, R.L., Castronuevo, P., Tsukamura, H. and Maeda, K.I. (2006) Anti-diabetic potentials of Momordica charantia and Andrographis paniculata and their effects on estrous cyclicity of alloxan-induced diabetic rats. *J. Ethnopharmacol.* 105(1-2): 196-200.

75. Kumar, R.A., Sridevi, K., Kumar, N.V., Nanduri, S. and Rajagopal, S. (2004) Anticancer and immunostimulatory compounds from Andrographis paniculata. *J. Ethnopharmacol.* 92(2-3): 291-5.

76. Panossian, A., Hovhannisyan, A., Mamikonyan, G., Abrahamian, H., Hambardzumyan, E., Gabrielian, E., Goukasova, G., Wikman, G. and Wagner, H. (2000) Pharmacokinetic and oral availability of andrographolide from Andrographis paniculata fixed combination Kan Jang in rats and human. *Phytomed.* 7(5): 351-64.

77. Rajagopal, S., Kumar, R.A., Deevi, D.S., Satyanarayana, C. and Rajapopalan R. (2003) Andrographolide, a potential cancer therapeutic agent isolated from Andrographis paniculata. *J. Exp. Ther. Oncol.* 3(3): 147-58.

78. Shen, Y.C., Chen, C.F. and Chiou W.F. (2002) Andrographolide prevents oxygen radical production by human neutrophils: possible mechanism(s) involved in its anti-inflammatory effect. *Br. J. Pharmacol.* 135(2): 399-406.

79. Visen, P.K., Shukla, B., Patnaik, G.K. and Dhawan, B.N. (1993) Andrographolide protects rat hepatocytes against paracetamol-induced damage. *J. Ethnopharmacol.* 40(2): 131-6.

80. Iruretagoyena, M.I., Hermoso, M., Sepulveda, S.E., Lezana, J.P., Bronfman, M., Gutierrez, M.A., Jacobelli, S.H. and Kalergis, A.M. (2006) Inhibition of nuclear factor-

kappa B enhances the capacity of immature dendritic cells to induce antigen-specific tolerance in experimental autoimmune encephalomyelitis. *J. Pharmacol. Exp. Ther.* 318: 59-67.

81. Tsai, H.R., Yang, L.M., Tsai, W.J. and Chiou, W.F. (2004) Andrographolide acts through inhibition of ERK1/2 and Akt phosphorylation to suppress chemotactic migration. *Eur. J. Pharmacol.* 498(1-3): 45-52.

82. Qin, L.H., Kong, L., Shi, G.J., Wang, Z.T. and Ge, B.X. (2006) Andrographolide inhibits the production of TNF-alpha and interleukin-12 in lipopolysaccharide-stimulated macrophages: role of mitogen-activated protein kinases. *Biol. Pharm. Bull.* 29(2): 220-4.

83. Madav, H.C., Tripathi, T. and Mishra, S.K. (1995) Analgesic, antipyretic, and antiulcerogenic effects of andrographolide. *Indian J. Pharm. Sci.* 57(3): 121-25.

84. Matsuda, T., Kuroyanagi, M., Sugiyama, S., Umehara, K., Ueno, A. and Nishi, K. (1994) Cell differentiation-inducing diterpenes from Andrographis paniculata nees. *Chem Pharm Bull* 42(6): 1216-25.

85. Kapil, A., Koul, I.B., Banerjee, S.K. and Gupta, B.D. (1993) Antihepatotoxic effects of major diterpenoid constituents of Andrographis paniculata. *Biochem. Pharmacol.* 46(1): 182-5.

86. Wyllie, A.H. (1980) Glucocorticoid-induced thymocyte apoptosis is associated with endogenous endonuclease activation. *Nature.* 284: 555-6.

87. Norbury, C. and Nurse, P. (1992) Animal cell cycles and their control. *Ann. Rev. of Biochem.* 61: 441-70.

88. Fearon, E.R. (1997) Human cancer syndromes: Clues to the origin and nature of cancer. *Science.* 278: 1043-50.

89. Rao, P.N. (1980) The molecular basis of drug-induced G2 arrest in mammalian cells. *Mol. Cell Biochem.* 29(1): 47-57.

90. Quelle, D.E., Ashmun, R.A., Shurtleff, S.A., Kato, J.Y., Bar-Sagi, D., Roussel, M.F., and Sherr, C.J. (1993). Overexpression of mouse D-type cyclins accelerates G1 phase in rodent fibrolasts. *Genes Dev.* 7: 1559-1571.

91. Lee, R.J., Albanese, C., Stenger, R.J., Watanabe, G., Inghirami, G., Haines, G.K., Webster, M., Muller, W.J., Brugge, J.S., Davis, R.J. and Pestell, R.G. (1999). 60(v-src) induction of cyclin D1 requires collaborative interactions between the extracellular signal-regulated kinase, p38, and Jun kinase pathways. A role for cAMP response element-binding protein and activating transcription factor-2 in pp60(v-src) signaling in breast cancer cells. *J. Biol. Chem.* 274: 7341-50.

92. Arber, N., Hibshoosh, H., Moss, S.F., Sutter, T., Zhang, Y., Begg, M., Wang, S., Weinstein, I.B. and Holt, P.R. (1996). Increased expression of cyclin D1 is an early event in multistage colorectal carcinogenesis. *Gastroenterology* 110: 669-74.

93. Dyson, N. (1998) The regulation of E2F by pRB-family proteins. *Genes Dev.* 12: 2245-62.

94. Clarke, A. R., Maandag, E.R., Van Roon, M., Van der Lugt, N.M.T., Van der Valk, M., Hooper, M.L., Berns, A., Te, H. and Riele. (1992) Requirement for a functional Rb-1 gene in murine development. *Nature (London)* 359: 328-30.

95. Wyllie, A.H. (1992) Apoptosis and the regulation of cell numbers in normal and neoplastic tissues: an overview. *Cancer Metastasis Rev.* 11: 95-103.

96. Jin, Z. and El-Deiry, W.S. (2005) Overview of cell death signaling pathways. *Cancer Biol. Ther.* 4(2): 139-63.

97. Cho, S.G. and Choi, E.J. (2002) Apoptotic signaling pathways: caspases and stress-activated protein kinases. *J. Biochem. Mol. Biol.* 35(1): 24-7.

98. Panaretakis, P., Pokrovskaja, K., Shoshan, M.C. and Grander, D. (2002) Activation of Bak, Bax and BH3-only Proteins in the Apoptotic Response to Doxorubicin. *J. Biol. Chem.* 277(46): 44317-26.

99. Agarwal, M.L., Taylor, W.R., Chernov, M.V., Chernova, O.B. and Stark, G.R. (1998) The p53 network. *J Biol Chem.* 273: 1-4.

100. Schwarz, M., Buchmann, A. and Bock, K.W. (1995) Role of cell proliferation at early stages of hepatocarcinogenesis. *Toxicol. Lett.* 82-83.

101. Tomasi, C., Laconi, E., Laconi, S., Greco, M., Sarma, D.S. and Pani, P. (1999) Effect of fasting/refeeding on the incidence of chemically induced hepatocellular carcinoma in the rat. *Carcinogenesis* 20: 1979-83.

102. Farber, E. and Sarma, D.S.R. (1987) Hepatocarcinogenesis: a dynamic cellular perspective. *Lab. Inves.* 56: 4-21.

103. Columbano, A., Ledda-Columbano, G.M., Curto, M., Ennas, G.M. Coni, P., Sarma, D.S.R. and Pani, P. (1990) Cell proliferation and promotion of rat liver carcinogenesis: different effect of hepatic regeneration and mitogen-induced hyperplasia on the development of enzyme altered foci. *Carcinogenesis.* 11: 771-776.

104. Ogawa, K., Solt, D.B., Farber, E. (1980) Phenotypic diversity as an early property of putative preneoplastic hepatocyte populations in liver carcinogenesis. *Cancer Res.* 40: 725-33.

105. Roomi, M. W., Columbano, A., Ledda-Columbano, G. M., and Sarma, D. S. R. (1986) Lead nitrate induces certain biochemical properties characteristic of hepatocyte nodules. *Carcinogenesis.* 7: 1643-6.

106. Power, C., Sinha, S., Webber, C., Manson, M.M. and Neal, G.E. (1987) Transformation related to expression of glutathione S-transferase P in rat liver cells. *Carcinogenesis.* 8: 797.

107. Vadenberghe, Y., Morel, F., Foriers, A., Ketterer, B., Vercruysee, A., Guillonzo, A. and Rogiers, V. (1989) Effect of Phenobarbital on the expression of glutathione S-transferase isozyme in cultured rat hepatocytes. *FEBS Lett.* 251: 59.

108. Clawson, G.A. (1989) Mechanisms of carbon tetrachloride hepatoxicity. *Path. Immunopathol. Res.* 8: 104-12.

109. Recknagel, R.O., Glende, E.A., Dolak, J.A. and Waller, R.L. (1989) Mechanisms of carbon tetrachloride toxicity. *Pharmacol. Ther.* 43: 139-54.

110. Schulte-Hermann, R. (1979). Adaptive liver growth induced by xenobiotic compounds: Its nature and mechanism. *Archives of Toxicology* 2: 113-24.

111. McGhee, J.O'D. and Patrick, R.S. (1969) The synthesis of sulphated mucopolysaccharide in mouse liver following carbon tetrachloride injury. I. Autoradiographic studies. *Br. J. Exp. Pathol.* 50: 521-26.